Investigation on soil carbon loss mitigation through organic fertilizer application and enhanced rock weathering

（有機肥料投入と風化促進技術による土壌炭素損失緩和策に関する研究）

Hokkaido University

Graduate School of Agriculture

Frontiers in Environmental Sciences

Doctor Course

YANG Yilin

Acknowledgements

I would like to express my deepest gratitude to my supervisor, Professor Yo Toma, for his invaluable guidance, support, and encouragement throughout my doctoral studies. From the initial stages of my research plan to the final writing of my dissertation, his advice and insights have been essential to my academic journey. I am profoundly grateful for his unwavering support. I would also like to extend my sincere appreciation to Professor Ryusuke Hatano, who deepened my understanding of soil science during my master's studies and provided me with the inspiration for the "organic fertilizer" component of my doctoral research. His continued guidance throughout my doctoral studies has been invaluable, and I am truly thankful for his advice and mentorship.

Many people and institutions supported me during my research, particularly in the fieldwork and sampling processes. Regarding the "organic fertilizer" study, I am deeply thankful to Professor Masahito Kawai and the staff at the Shizunai Research Field for their generous assistance, which began during my master's studies. I greatly appreciate their help with soil and compost sampling and their invaluable insights during the planning stages of this research. I would also like to extend my heartfelt thanks to Mr. Norikazu Yamaki and Mr. Katsuro Taira from the Experimental Farm of Hokkaido University for their assistance in collecting methane fermentation liquid and digestate. The knowledge and experience I gained through their support were crucial for completing this research. I am sincerely grateful to everyone who contributed to this part of my study on organic fertilizers.

For my research on ERW, I received considerable support from various organizations and researchers. This study was funded by the New Energy and Industrial Technology Development Organization (NEDO). I would like to express my deepest gratitude to

Professor Takao Nakagaki, the project leader, and Professor Atsushi Nakao from the Agriculture Group for their support and guidance. I would also like to thank Professor Takuro Shinano, Professor Toshihiro Watanabe, Professor Hayato Maruyama, Mr. Hiroshi Uchibayashi, and Ms. Ayaka Wakao from the Crop Nutrition Laboratory for their assistance in managing soybean cultivation and for providing valuable advice on plant cultivation. The experience I gained will be beneficial in my future research endeavors. I am sincerely grateful to Professor Shoichiro Hamamoto and Ms. Yan Zhu from the Soil Conservation Laboratory for their help in setting up field sensors and measuring soil physical properties. Additionally, I would like to thank Mr. Shinya Iwasaki and many other researchers from various institutions for their valuable suggestions during the fieldwork on Ishigaki Island. A special thanks goes to Mr. Gen Kosaka from the Soil Science Laboratory, who has been a crucial part of my research journey for the past two years. From planning experiments to fieldwork, data collection, and analysis, he has been a constant support, and I am truly grateful for the memories we shared during this period.

I would also like to thank Sensei Kanta Kuramochi for his advice and assistance in sample collection and laboratory procedures. My heartfelt thanks go to my fellow students, seniors, and juniors who have accompanied me throughout my master's and doctoral studies. In particular, I am deeply grateful to my doctoral cohort—Ms. Hirori Namie, Mr. Hiroshi Uchibayashi, and Mr. Motohiro Yoshimura—as well as Mr. Kohei Kurokawa from Kyoto Prefectural University, Mrs. Chiho Sugiyama and Mr. Hiromichi who worked alongside me during our arduous field surveys in Shizunai during my master's program, and Mrs. Jiayue Zhan and Mr. Shilei Peng who provided tremendous support in my daily life. Together, we overcame countless challenges and made my final years as a student an unforgettable and fulfilling experience. Your support and encouragement were essential for me to persevere through these challenging five years.

To everyone mentioned here and to those who have supported me in various ways but whose names are not listed, I extend my most sincere thanks and appreciation.

Finally, I would like to take this opportunity to express my deepest gratitude to my parents, who have supported me throughout my entire academic journey of more than 20 years. Without their unwavering love and support, I would not have come this far. Thank you very much from the bottom of my heart.

謝辞

本論文の執筆にあたり、博士課程を通じて常にご指導、ご助言、そして励ましをくださった当真要先生に、心より感謝申し上げます。研究計画の立案から論文の執筆に至るまで、数々の貴重なご指導を賜りましたこと、誠にありがとうございました。修士課程において、土壌学の基礎から応用までの知見を深める機会を与えてくださり、さらに本論文の研究テーマの一つである「有機肥料」の着想を得るきっかけをくださった波多野隆介先生にも、心より感謝申し上げます。博士課程においても、度重なる貴重なご助言をいただきましたこと、深く御礼申し上げます。

本研究の実施に際し、多くの方々から施設の利用や調査へのご協力を賜りました。「有機肥料」に関する研究においては、静内研究牧場の河合正人先生および牧場スタッフの皆様に、修士課程の頃より多大なるご協力をいただきましたこと、深く感謝いたします。土壌採取や堆肥サンプリングの際のご助力にも心より御礼申し上げます。また、研究の立案段階でも多くの貴重なご意見を賜りましたこと、重ねて感謝いたします。北海道大学生物生産研究農場の八巻憲和様、平克郎様には、メタン発酵液および消化液の採取の際に多大なご支援をいただき、貴重な経験を得ることができました。これらの「有機肥料」に関する研究をサポートしてくださった皆様に、深く感謝申し上げます。

次に、ERW に関する研究についても、多くの方々や組織からご協力をいただきました。本研究は、New Energy and Industrial Technology Development Organization（NEDO）

の資金支援を受けて実施されました。プロジェクト総責任者の中垣隆雄先生、農学班の中尾淳先生に心より感謝申し上げます。また、大豆の栽培管理に際し、作物栄養学研究室の信濃卓郎先生、渡部敏裕先生、丸山隼人先生、内林太志さん、若尾彩果さんには、植物栽培に関する多くの知識と経験を共有していただき、今後の研究活動にも大いに役立てていきたいと思います。

さらに、土壌保全学研究室の濱本昌一郎先生、朱顔さんには、圃場でのセンサー設置や土壌物理性の測定管理において多大なるご助力を賜りましたこと、心より感謝申し上げます。また、石垣島での調査にご同行いただいた岩崎真也さんをはじめ、他機関の多くの研究者の皆様からも貴重なご意見をいただきましたこと、深く御礼申し上げます。特に、土壌学研究室の小坂弦君には、2 年にわたり、研究計画の策定、実験の遂行、データの保存・分析に至るまで、常に共に歩んでいただきました。このような貴重な経験を共にできたことを、大変ありがたく思います。

また、土壌学研究室での学びと生活の中で、多くの先生方や同級生、先輩、後輩の皆様にもお世話になりました。倉持寛太先生には、サンプリングや実験操作の際に貴重なアドバイスをいただき、深く感謝申し上げます。修士課程から博士課程までの間、共に学び、励まし合い、支え合ってくださった皆様にも、心より感謝いたします。特に、博士課程の同期の浪江日和さん、内林太志さん、吉村基博さん、および京都府立大学の黒川耕平さん、修士時代に静内での調査で共に汗を流した杉山千穂さんと高橋大道さん、

そして日常生活の中で多大なるご支援をいただいた詹佳月さんと彭石磊さんには、共に努力し、数々の困難を乗り越え、学生生活最後の日々を最高の思い出にしてくださったことに、深く感謝申し上げます。皆様の存在がなければ、この波乱に満ちた 5 年間を乗り越えることはできなかったでしょう。

本論文に関わってくださった全ての皆様、またここにお名前を挙げることができなかった方々にも、改めて心より御礼申し上げます。

最後になりますが、長きにわたり私の学生生活を支えてくれた両親へ、この場をお借りして、最も深い感謝の意を表したいと思います。お二人の支えなくして、ここまで歩んでくることはできませんでした。本当にありがとうございました。

Contents

List of Tables

List of Figures

1. General Introduction

Since the Industrial Revolution, the global climate system has undergone significant changes. According to the latest scientific evidence from the Sixth Assessment Report (AR6) of the Intergovernmental Panel on Climate Change (IPCC, 2023), the global mean surface temperature during 2011–2020 was approximately 1.09°C higher than that of 1850–1900 (Fig 1.1). This warming trend has been particularly pronounced in recent decades, especially since the 1970s, with a further acceleration in the rate of global temperature increase, reaching approximately 0.2°C per decade. Along with rising temperatures, a series of climate system-related changes have emerged, including but not limited to sea-level rise, increased frequency of extreme weather events, and the loss of soil carbon sinks, marking the transition of global warming from a theoretical concept to a tangible challenge.

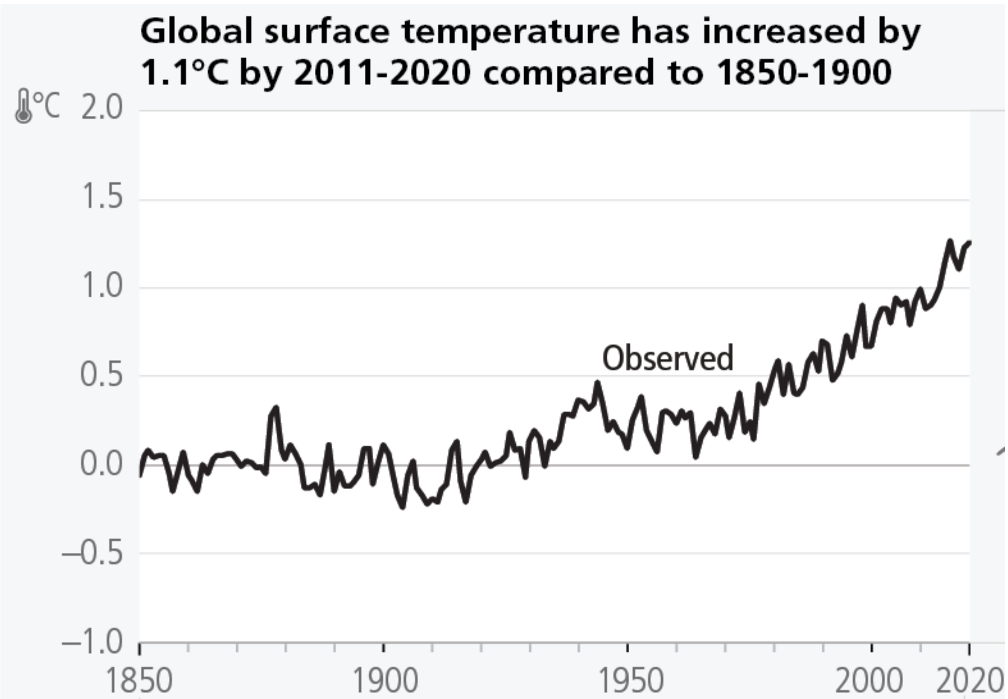

Fig. 1.1. Global surface temperature change from 1850 to 2020 (IPCC, 2023).

The drivers of these climatic changes can be broadly categorized into natural and anthropogenic factors. Natural factors include volcanic eruptions that release substantial amounts of volcanic ash and variations in solar radiation (Cole-Dai, 2010; Lean, 2010). Although natural factors have played a significant role in historical climate changes, their influence on recent global warming has been relatively minor. IPCC (2023)analyses indicate that since the Industrial Revolution, changes in solar radiation have contributed to less than 0.1°C of temperature variation. In contrast, anthropogenic greenhouse gas emissions have been the dominant contributors to global warming (Fig 1.2). Since the Industrial Revolution, extensive combustion of fossil fuels (e.g., coal, oil, and natural gas) has led to a marked increase in atmospheric carbon dioxide (CO_2) concentrations. (Revelle and Suess, 1957) were the first to propose that fossil fuel combustion had caused CO_2 levels to rise beyond the natural absorption capacity, laying the foundation for modern climate change research. Through carbon isotope analysis, (Graven et al., 2020) revealed significant changes in the proportions of ^{12}C and ^{13}C released into the atmosphere due to fossil fuel combustion since the industrial era, further confirming that human activities are the primary drivers of rising CO_2 concentrations. Moreover, historical data from (Andres et al., 1999) documented CO_2 emissions from fossil fuel combustion between 1751 and 1950, providing additional support for this conclusion.

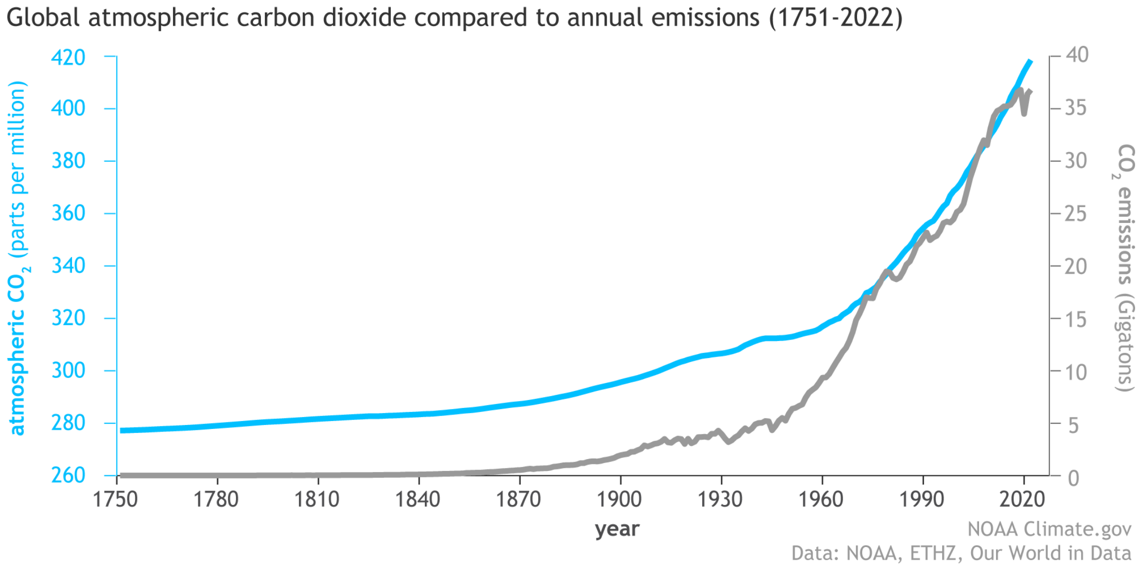

Fig. 1.2. Global atmospheric CO_2 change compared to annual emissions (NOAA, 2024).

As anthropogenic greenhouse gas emissions have been identified as the primary driver of global warming, particularly the persistent increase in atmospheric CO_2 concentrations, solely relying on reducing fossil fuel combustion is insufficient to rapidly mitigate the ongoing warming trend. The IPCC reports emphasize that even under stringent emission reduction scenarios, the CO_2 already accumulated in the atmosphere will continue to exert a lasting influence on the climate system (IPCC, 2023). Therefore, to limit global warming to within the 1.5°C or 2°C targets set by the Paris Agreement, in addition to significantly reducing greenhouse gas emissions, proactive carbon dioxide removal (CDR) strategies are essential to lower atmospheric CO_2 concentrations. The concept of CDR was first introduced in the 2005 IPCC Special Report on *Carbon Dioxide Capture and Storage (CCS)* (IPCC, 2005) and was further clarified and reinforced in the 2018 IPCC Special Report on *Global Warming of 1.5°C* (IPCC, 2018).

CDR strategies encompass a variety of approaches across different sectors, demonstrating significant potential in energy, industry, ocean systems, and technological innovations. In the energy sector, Direct Air Capture (DAC) and Bioenergy with Carbon Capture and Storage (BECCS) are considered critical methods for achieving net-zero emissions, effectively removing carbon dioxide from the atmosphere (Dowell et al., 2022). In the industrial sector, carbon capture and mineralization technologies are being increasingly applied to high-emission industries such as cement and steel production, aiming to reduce carbon emissions generated during manufacturing processes (Parson and Buck, 2020). Furthermore, ocean-based carbon removal technologies, including ocean alkalinization and deep-sea carbon sequestration, are actively under investigation, exploring the potential of utilizing ocean systems to absorb more atmospheric CO_2 (Brad and Schneider, 2023).

In recent years, agricultural CDR has garnered significant attention, as soil organic carbon (SOC) accounts for approximately one-third of the global carbon stock, with total SOC content within the top 1-m soil depth estimated at 1500–2000 Pg (Stockmann et al., 2013). This makes soil a critical reservoir in the global carbon cycle. However, due to unsustainable land use and agricultural management practices, soil carbon stocks are under severe threat and are experiencing significant losses. SOC depletion primarily results from excessive tillage, vegetation destruction, and overuse of chemical fertilizers, all of which disrupt the natural carbon storage mechanisms in soil, promoting the decomposition of organic carbon and release CO_2 (Lal, 2004). For instance, prolonged mechanical tillage increases soil exposure to air, accelerating microbial decomposition of organic carbon and leading to substantial carbon emissions (Paustian et al., 2016). Additionally, soil degradation and land-use changes, such as the conversion of forests to agricultural land, have significantly reduced the soil's capacity to store SOC (Smith et al., 2010). Even a mere 10% loss of SOC could have irreversible impacts on atmospheric

CO_2 concentrations, as once released, this carbon enters the atmosphere as greenhouse gases, further exacerbating global warming (Kirschbaum, 2000). Therefore, mitigating soil carbon loss to achieve CDR has become a vital strategy in addressing global climate change.

Methods to mitigate soil carbon loss can generally be categorized into two approaches (Fig 1.3). The first involves increasing soil carbon sinks through the carbon application, such as the application of organic fertilizers, cover crops, crop rotation, and biochar. These practices not only significantly enhance SOC content but also improve soil structure, nutrient availability, and water retention capacity, thereby boosting agricultural productivity (Abbas et al., 2020; Paustian et al., 2016). For instance, applying organic fertilizers provides a rich carbon source for soil microbes, promoting the accumulation of organic carbon (Freibauer et al., 2004). Biochar technology, which introduces pyrolyzed biomass into the soil, allows for stable carbon sequestration over centuries (Lehmann et al., 2006). However, such methods are not without challenges. The production and transportation of organic fertilizers and biochar may generate additional carbon emissions, and large-scale implementation requires sustained economic and policy support (Cowie et al., 2006). Additionally, although the properties of organic fertilizers vary significantly depending on their sources, studies comparing different types of organic fertilizers remain relatively scarce. The second approach focuses on recapturing CO_2 emitted from the soil and re-sequestering it through various technologies. These include enhanced rock weathering (ERW), direct air capture combined with soil sequestration (DAC + Soil Sequestration), and vegetation restoration to regenerate soil carbon sinks (Smith et al., 2010). The core principle of these technologies is to sequester atmospheric CO_2 back into the soil, reducing overall carbon emissions. However, research remains insufficient regarding the specific amount of CO_2 that can be sequestered by these methods, their long-term stability, and their effectiveness across different soil types (César Izaurralde et al., 2001).

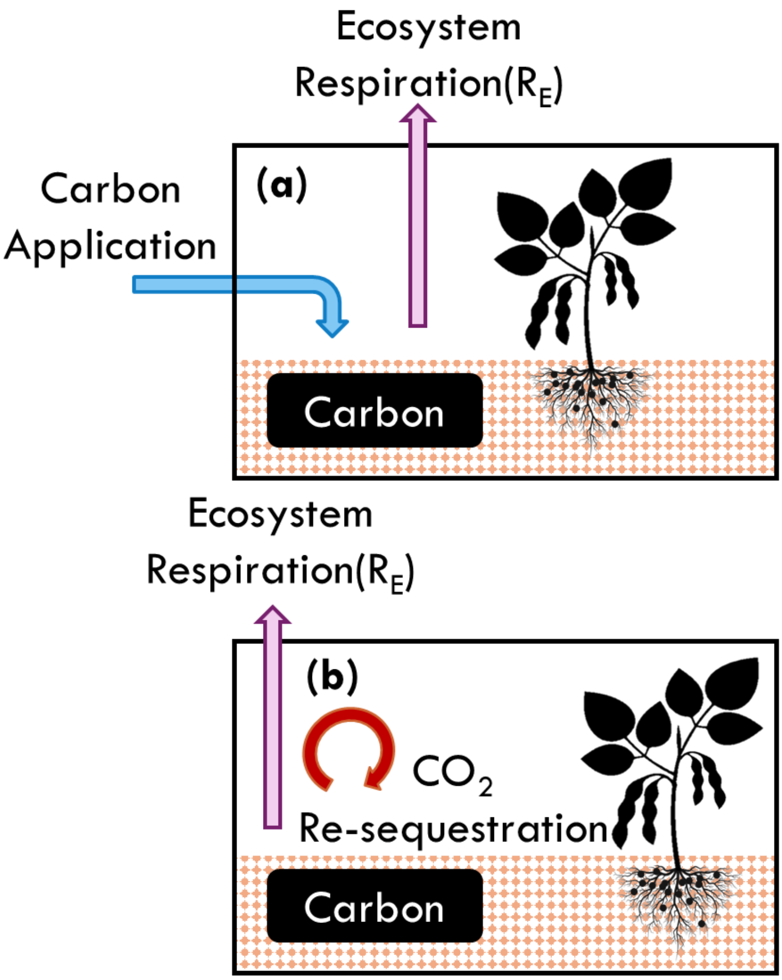

Fig. 1.3. Two kinds of approaches of soil carbon loss mitigation. (a): carbon application; (b): CO_2 re-sequestration.

Based on the above background, this study evaluates two soil carbon loss mitigation strategies—organic fertilizer application and enhanced rock weathering—through laboratory and field experiments. For organic fertilizer application, this study aims to (1) compare the carbon loss mitigation effects among different types of organic fertilizers (compost manure, raw slurry, and digestate) with varying properties; and (2) elucidate the mechanisms underlying these differences by analyzing the relationship between CO_2 emissions ,soil organic carbon pool and soil properties. For ERW, this study aims to: (1) compare the ERW-induced CO_2 removal efficiency between rhizosphere and non-rhizosphere soils to clarify the role of plant root systems in the weathering process; and (2) quantify the field-scale carbon loss mitigation efficiency of ERW through carbon budget assessment. By integrating these two experimental approaches, this study seeks to: compare the carbon loss mitigation potential of these two distinct strategies under a common evaluation framework, thereby elucidating their mechanisms, temporal characteristics, and environmental adaptability to provide scientific guidance for technology selection in agricultural carbon management practices.

This dissertation is divided into seven chapters. The current chapter (Chapter 1) is a general introduction to the study. Chapter 2 provides a review of the relevant literature on the research topic. Chapter 3 describes the general methodology used in the study. Chapter 4 focuses on the carbon loss mitigation potential of different organic fertilizer applications and its effect on soil carbon pool. Chapter 5 focuses on the carbon loss mitigation potential of enhanced rock weathering and its different responses in the rhizosphere and non-rhizosphere soil. Chapter 6 is a general discussion of this study.

2. Literature Reviews

2.1 SOC Loss

The loss of SOC is a critical issue influencing agricultural sustainability and climate change mitigation (Guo et al., 2023a; Keuper et al., 2020; Raza et al., 2020). As a core component of soil health, SOC plays a vital role in maintaining soil fertility, enhancing water retention capacity, and sequestering atmospheric CO_2. However, numerous studies in recent years have shown that changes in land use, improper management practices, and climate change are causing significant SOC losses.

Wiesmeier et al. (2016) utilized the Rothamsted Carbon (RothC) model to simulate SOC dynamics in agricultural and grassland soils in Bavaria, Germany. Their results indicated that climate warming significantly accelerates SOC decomposition, even under a scenario where carbon inputs increase by 20%. Under such conditions, SOC stocks could still decline by 3% to 8%, and under scenarios of unchanged or reduced carbon inputs, SOC losses could reach as high as 16% to 24% (Fig 2.1). The study emphasized that current levels of carbon input are insufficient to counteract the risks of SOC loss associated with rising temperatures, necessitating substantial increases in organic matter inputs to maintain existing SOC stocks. Furthermore, it highlighted that warming accelerates organic matter decomposition at a rate far exceeding the carbon input provided by crop residues, leading to an imbalance in soil carbon equilibrium.

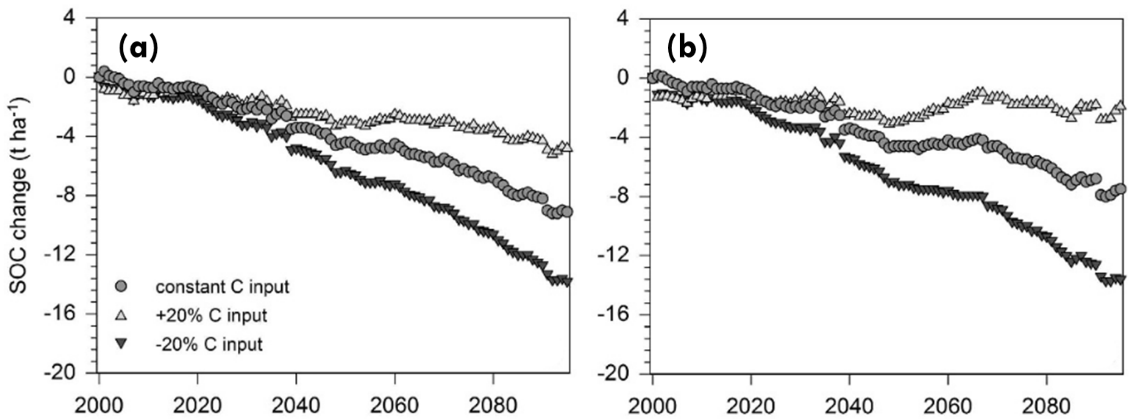

Fig. 2.1. Projected average SOC changes of cropland (a) and grassland (b) between 2000 and 2095 under climate change and different C input scenarios (Wiesmeier et al., 2016).

Tang et al. (2019) conducted a meta-analysis of 81 studies on grassland-to-cropland conversion worldwide, further demonstrating the profound impact of land use changes on SOC. The study found that in the first decade following conversion, SOC loss rates in the 0–30 cm soil layer reached 32%, with significant reductions also observed in the 30–60 cm layer. This change was primarily attributed to reduced vegetation biomass input, alterations in soil physicochemical properties, and shifts in microbial community composition. The research also revealed that SOC losses tend to stabilize approximately 20 years after land conversion, suggesting the formation of a new low-carbon equilibrium (Fig 2.2). However, this equilibrium is established on a significantly reduced SOC stock, posing potential threats to ecosystems and agricultural productivity.

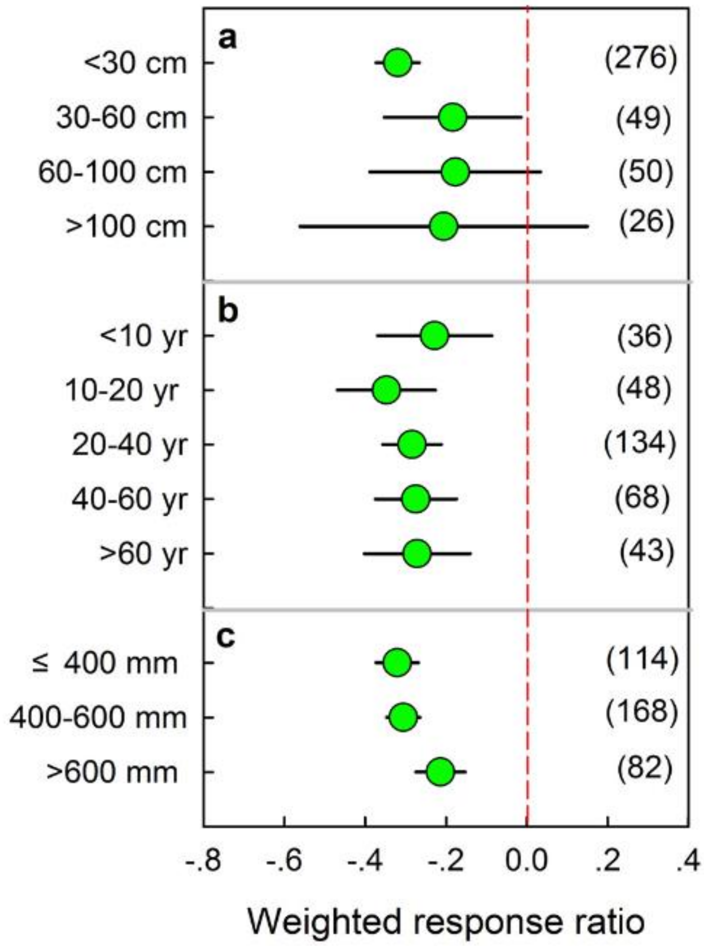

Fig. 2.2. Effects of conversion of grassland to agricultural land on SOC. The data is expressed as the weighted response ratio with 95% confident intervals. The numbers of studies included are indicated in parentheses (Tang et al., 2019).

Keel et al. (2019) examined data from long-term agricultural experiments in Switzerland and revealed that even with the application of organic and mineral fertilizers, SOC losses averaged 0.29 Mg C ha^{-1} y^{-1}. This finding suggests that current organic inputs are insufficient to offset carbon losses from soil organic matter decomposition. Moreover, the study identified initial SOC stocks, soil cover conditions, and levels of organic carbon input as key factors influencing SOC losses, whereas land management practices and tillage types had relatively minor effects. These findings underline the importance of optimizing organic matter management and increasing carbon inputs to mitigate SOC losses.

Overall, SOC loss is driven by multiple factors, including land use changes, management practices, and climatic conditions. Land use changes, such as grassland conversion to cropland, disrupt soil structure, reduce organic carbon inputs, and accelerate soil erosion and organic matter decomposition. Management practices, including crop residue removal, excessive tillage, and insufficient organic fertilizer application, exacerbate carbon losses. Additionally, climate change, particularly rising temperatures, accelerates organic matter decomposition, further widening the soil carbon balance deficit. To mitigate SOC losses, studies suggest increasing organic matter inputs through the application of compost, manure, and biochar; reducing soil disturbances by adopting no-till or reduced-till practices; and maintaining year-round soil cover through cover cropping (Leroux et al., 2022; Yang et al., 2021; Yu et al., 2023). These measures not only enhance SOC stocks but also improve soil quality and increase its resilience to extreme climatic events. Additionally, re-sequestering lost organic carbon back into soil can further help mitigate SOC losses (Harrington et al., 2023).

2.2 Organic Fertilizer Application

Organic fertilizer applications are one of the most common exogenous carbon application methods in agricultural production. It plays a crucial role not only in enhancing soil fertility and promoting healthy crop growth but also in contributing significantly to soil carbon sequestration. Organic fertilizers encompass a wide variety of types, including compost, animal manure, crop residues, and biochar. Their application can significantly improve the physical and chemical properties of the soil. For instance, organic fertilizers enhance soil aeration and water retention, provide abundant nutrients for crops, and stimulate microbial activity, thereby improving soil ecosystems (Chirinda et al., 2010a; Lorenz and Lal, 2016). Studies have shown that long-term compost application in farmland significantly increases soil nutrient supply, resulting in an average crop yield increase of over 20% (Meng et al., 2017).

Organic fertilizer application also plays a pivotal role in the accumulation of SOC. Continuous organic matter input can significantly enhance both the content and stability of SOC. Long-term experiments have demonstrated that the combined application of compost and crop residues not only increases carbon stocks but also reduces the risk of carbon emissions (Wei et al., 2016). In acidic or infertile soils, organic fertilizer application can elevate soil pH, enhance carbon sequestration potential, and provide slow-release nutrients for plants (Lorenz and Lal, 2016). A long-term study conducted in Northeast China showed that organic fertilizer application led to a 30% average increase in SOC stocks and effectively improved soil aggregate structure (Tian et al., 2022). However, research on the short-term effects of organic fertilizers on soil carbon sinks remains limited, as the process of organic fertilizer decomposition and integration into the soil is relatively prolonged, and changes in SOC occur over extended periods (Galamini et al., 2025; Holland et al., 2024). Therefore, evaluating the short-term impacts of organic fertilizers on soil carbon dynamics may require alternative research approaches.

The environmental impacts of organic fertilizer vary greatly depending on their type and management practices. While organic fertilizer application can reduce the use of chemical fertilizers and the associated greenhouse gas emissions during their production and use, improper application may cause a range of environmental issues. For instance, excessive application of animal manure or compost can lead to nitrogen and phosphorus runoff, causing water eutrophication (Meng et al., 2017). Moreover, certain organic fertilizers, such as inadequately treated manure, may introduce risks of soil pathogen transmission and heavy metal accumulation (Verma et al., 2020a).

Generally, while organic fertilizer application offers substantial multifaceted benefits in agricultural production, its optimized management is crucial for achieving sustainable agriculture. Further research on the effects of different organic fertilizers, as well as the mechanisms underlying their impact on soil carbon dynamics and greenhouse gas emissions, can help maximize their contributions to soil health and carbon sequestration while minimizing potential negative environmental impacts.

2.3 Different Organic Fertilizer

As a commonly used soil amendment, different types of organic fertilizers exhibit significant variations in their properties, sources, and effects on soils. Among them, manure, a widely applied organic fertilizer, varies in composition depending on the raw materials and production processes used. These differences not only influence the nutrient supply capacity of manure but also significantly affect greenhouse gas emissions and the dynamics of SOC after application.

The properties of manure are shaped by its raw materials (e.g., crop residues, livestock manure, municipal organic waste) and variations in microbial activity and environmental conditions during composting. For example, soils amended with straw compost presented the highest C mineralized with significantly higher CO_2 emissions throughout the investigation period (Santos et al., 2021). On the other hand, compost derived from livestock manure contains higher nitrogen levels, which can rapidly enhance soil nutrient availability and decrease N_2O emissions compared to inorganic fertilization (Xu et al., 2024). Additionally, compost from chicken manure can significantly improve SOC stock with no significant increase in CO_2 emissions (Han et al., 2017).

The maturity of compost has a pronounced effect on soil carbon dynamics. Mature compost, with its higher proportion of stable organic carbon, contributes more to long-term SOC accumulation, while immature compost may release more soluble organic matter, stimulating microbial activity and leading to soil carbon losses. Studies indicate that long-term compost application increases SOC stocks by over 20%, whereas fields treated with immature compost may experience a 15%–20% increase in short-term CO_2 emissions (Lark and Ferguson, 2004; Wei et al., 2016).

Beyond compost, other types of organic fertilizers, such as liquid residues (Slurry) and digestate (Anerobic Digestion Effluent) from methane fermentation, have gained increasing attention in recent years. These fertilizers, derived as byproducts of anaerobic digestion, are rich in soluble organic carbon and nitrogen, but their impacts on soil and the environment vary depending on composition and application rates. For instance, slurry, which is high in easily degradable organic matter, may increase N_2O and CH_4 emissions in the short term but can rapidly improve soil nutrient availability (Kitamura et al., 2021). By contrast, digestate processed for longer periods exhibit greater stability and exert more significant long-term effects on soil carbon dynamics. Béghin-Tanneau et al. (2019) reported that applying digestate in a one-year experiment increased SOC stocks by 10%–15% while no significant increase in CO_2 emissions.

Emerging organic materials for fertilizers or amendments, such as biochar and organic waste extracts, are also being investigated. For example, biochar, with its high carbon stability, not only significantly increases SOC stocks in acidic soils but also reduces N_2O

emissions by over 50% (Lehmann et al., 2006). Meanwhile, organic waste extracts, rich in active organic matter and microbial stimulants, can enhance microbial activity by approximately 30%, though their long-term effects on SOC dynamics require further study (Brenzinger et al., 2018).

Table 2.1. Comparison of Different Organic Fertilizers

Fertilization	Time	Response	Reference
Manure (Straw)	55 days	Highest CO_2 emissions between 8 types of manure	Santos et al., (2021)
Manure (Pig manure)	8 years	Decreased carbon footprint, increased SOC stock	Xu et al., (2024)
Manure (Chicken manure)	1 year	No significant differences in CO_2 emissions between treatments, increased SOC stock	Han et al., (2017)
Slurry	3 years	Increased GHG emissions, carbon loss mitigation	Kitamura et al., (2021)
Anerobic Degestion Effluent	1 year	Decreased CO_2 emissions with increased SOC stock	Béghin-Tanneau et al., (2019)
Biochar	91 days	Decreased GHG emissions	Sapkota et al., (2024)

These differences indicate that even within the same category of fertilizer, variations in sources and processing methods can significantly alter their effects on soil. Furthermore, distinct organic fertilizer types, such as compost, anaerobic digestates, and biochar, differ substantially in composition, stability, and environmental impacts, requiring careful selection based on specific agricultural scenarios. Therefore, systematic comparisons of different organic fertilizers are crucial for advancing agricultural carbon management and soil health research.

As shown in Table 2.1, while organic fertilizers are widely recognized for improving soil fertility and increasing soil carbon sinks, systematic comparative studies on different types of organic fertilizers remain relatively scarce. Exploring the impacts of various organic fertilizers on soil carbon storage can help scientists and farmers better understand the long-term effects and potential risks associated with exogenous carbon inputs. The decomposition characteristics and nutrient release rates of different fertilizers significantly influence soil carbon cycling, which is critical to the net effects of soil carbon sequestration and greenhouse gas emissions (Han et al., 2013).

Thus, conducting comparative studies on different organic fertilizers not only aids in optimizing fertilization strategies but also provides scientific support for agricultural CDR and sustainable soil management. As agricultural production increasingly shifts toward sustainability and low-carbon practices, balancing carbon sequestration, crop yields, and environmental protection has become a key research direction. Systematic comparisons of various organic fertilizers can elucidate their strengths and limitations in practical applications, laying the foundation for more precise and efficient agricultural carbon management strategies.

2.4 SOC change

The application of organic fertilizers directly improves soil carbon loss through carbon input, and this mitigation effect is ultimately reflected in changes in SOC. Therefore, measuring SOC dynamics is critical for evaluating the efficiency of organic fertilizers. Currently, numerous studies focus on analyzing SOC in soils. For instance, Huang et al. (2019) investigated the effects of organic fertilizer application on SOC dynamics in calcareous Cambisols on the Loess Plateau. Their findings revealed that after 10 years of organic fertilizer application, SOC stocks increased by up to 110%. This increase was not only attributed to exogenous carbon inputs but was also closely related to improved soil aggregate structure and calcium-mediated SOC stabilization. Specifically, organic fertilizers promoted the formation of organic–calcium complexes within microaggregates, enhancing SOC stability. Simultaneously, the specific mineralization rate of SOC significantly decreased under organic fertilizer treatments, particularly in fine soil fractions, indicating strong SOC protection. These results suggest that organic fertilizer application not only significantly enhances SOC stocks but also promotes long-term carbon sequestration efficiency by improving soil aggregate structure and calcium dynamics.

Li et al. (2018) focused on the long-term impacts of organic fertilizer application on SOC and soil microbial properties. Their study showed that the application of organic fertilizers, such as pig manure and crop residue incorporation, significantly increased SOC content. Notably, combined pig manure and crop residue treatments achieved a 54.99% increase in SOC relative to the initial level. In addition, soil total nitrogen (STN) content and the C:N ratio were significantly improved under organic fertilizer treatments, further facilitating SOC stabilization.

From a microbial perspective, organic fertilizer application significantly increased soil microbial biomass carbon, enzyme activities (e.g., urease and sucrase), and soil respiration rates. These indicators were strongly positively correlated with SOC, underscoring the critical role of microbial activity in SOC accumulation. Moreover, the long-term application of organic fertilizers not only enhanced SOC content but also improved the sustainability yield index of crop production, further highlighting the importance of SOC enhancement for agricultural stability.

Notably, the two studies highlighted different factors influencing SOC, focusing on exchangeable calcium ions and microbial mechanisms, respectively. This multidimensional regulation of SOC can be analyzed through long-term field experiments. However, for short-term fertilizer application, such analyses are particularly challenging as SOC changes are often slow (McDaniel and Middleton, 2024; Zhou et al., 2024). Nevertheless, the input of organic fertilizers undoubtedly influences soil carbon, even in the short term.

According to Lazcano et al. (2013), although significant changes in SOC typically require long-term observations, the application of organic fertilizers has an undeniable short-term impact on soil carbon cycling. Their study demonstrated that organic fertilizers, by providing abundant organic carbon, directly stimulated rapid responses in soil microbial activity, particularly promoting the growth of Gram-negative bacteria capable of quickly utilizing soluble organic carbon. This effect resulted in a significant increase in microbial biomass and activity under organic fertilizer treatments, reaching 22.6 μg g^{-1} and 19.4 μg g^{-1}, respectively, compared to 18.5 μg g^{-1} in inorganic fertilizer treatments. Additionally, organic fertilizers significantly increased the activities of soil enzymes, such as β-glucosidase, protease, and phosphomonoesters, which play essential roles in organic matter decomposition and the cycling of carbon, nitrogen, and phosphorus. These findings further confirmed that organic fertilizers not only rapidly enhance soil nutrient supply but also indirectly influence SOC dynamics by boosting soil microbial activity.

In terms of soil carbon content, high-dose vermicompost treatments significantly increased total soil carbon from 33.1 g kg^{-1} (inorganic fertilizer) to 39.3 g kg^{-1}. This effect suggests that organic fertilizers provide not only rapidly available carbon but also more stable forms of complex organic matter, enhancing the potential for carbon storage. Remarkably, these effects were observed within a single growing season (three months), demonstrating that even in the short term, organic fertilizer application can significantly impact SOC by rapidly enhancing microbial activity and organic carbon input.

In summary, organic fertilizers have notable short-term effects on SOC, but measuring SOC alone may not fully capture these changes. Additional evaluation metrics, such as CO_2 emissions and changes in SOC component, may provide more accurate insights into the short-term responses of SOC.

2.5 SOC Components

Labile organic carbon (LOC), as an active fraction of SOC, is widely used in studies on SOC dynamics due to its rapid response to short-term environmental changes. With a short turnover time and high sensitivity to soil management practices and external conditions, LOC is often considered an early indicator of SOC changes.

According to Tirol-Padre and Ladha (2004), LOC was measured using the permanganate oxidation method. Their experiment demonstrated that the application of farmyard manure (FYM) significantly increased LOC concentrations, raising them from 1.2 g kg^{-1} in the control group to 2.3 g kg^{-1} under FYM treatment, an increase in 91%. The study attributed this rise to the abundant supply of decomposable organic matter from FYM and highlighted LOC's ability to quickly reflect SOC dynamics, especially during the initial stages of fertilization or other carbon inputs. Chen et al. (2016) further investigated LOC's response to varying thinning intensities. In Chinese fir plantations, higher thinning intensity (70% tree removal) resulted in a 33.2% increase in LOC concentration compared to the control, while low-intensity thinning (30% tree removal) led to a 21.6% increase. Thinning also significantly influenced the activity of soil enzymes, such as β-glucosidase and cellulase, which play critical roles in the carbon cycle.

For example, β-glucosidase activity increased from 75.3 μg p NP g^{-1} soil h^{-1} in the control to 112.5 μg p NP g^{-1} soil h^{-1} under high-intensity thinning.

Xu et al. (2011) examined the long-term effects of straw return on LOC. Their results showed that a 2-year straw return treatment (50% straw incorporation) increased LOC concentrations from 0.79 g kg^{-1} in the control to 1.12 g kg^{-1}, a 42% rise. After 10 years of straw return, LOC concentrations further increased to 2.09 g kg^{-1}, 2.5 times higher than the control. These findings underscore LOC's sensitivity to exogenous carbon inputs, such as straw return, making it a reliable early indicator of SOC changes. Moreover, LOC changes were strongly correlated with microbial biomass carbon, with a correlation coefficient of 0.894 ($p<0.01$), highlighting the crucial role of microbial activity in LOC dynamics.

In contrast, recalcitrant organic carbon (ROC), as the stable fraction of SOC, is vital for evaluating soil carbon storage and long-term carbon stability. Due to its chemically stable nature and long turnover time, ROC represents the most resistant portion of SOC, persisting in soil for thousands of years or longer.

Shi et al. (2023) revealed ROC's critical role in SOC accumulation and stability through long-term observations of vegetation succession on the Loess Plateau. Over 160 years of succession, the proportion of ROC increased significantly, rising from 62% in the initial farmland stage to 85% in the climax forest stage. This increase reflects not only enhanced soil carbon inputs from vegetation restoration but also ROC's utility as a key indicator of SOC accumulation (Fig 2.3).

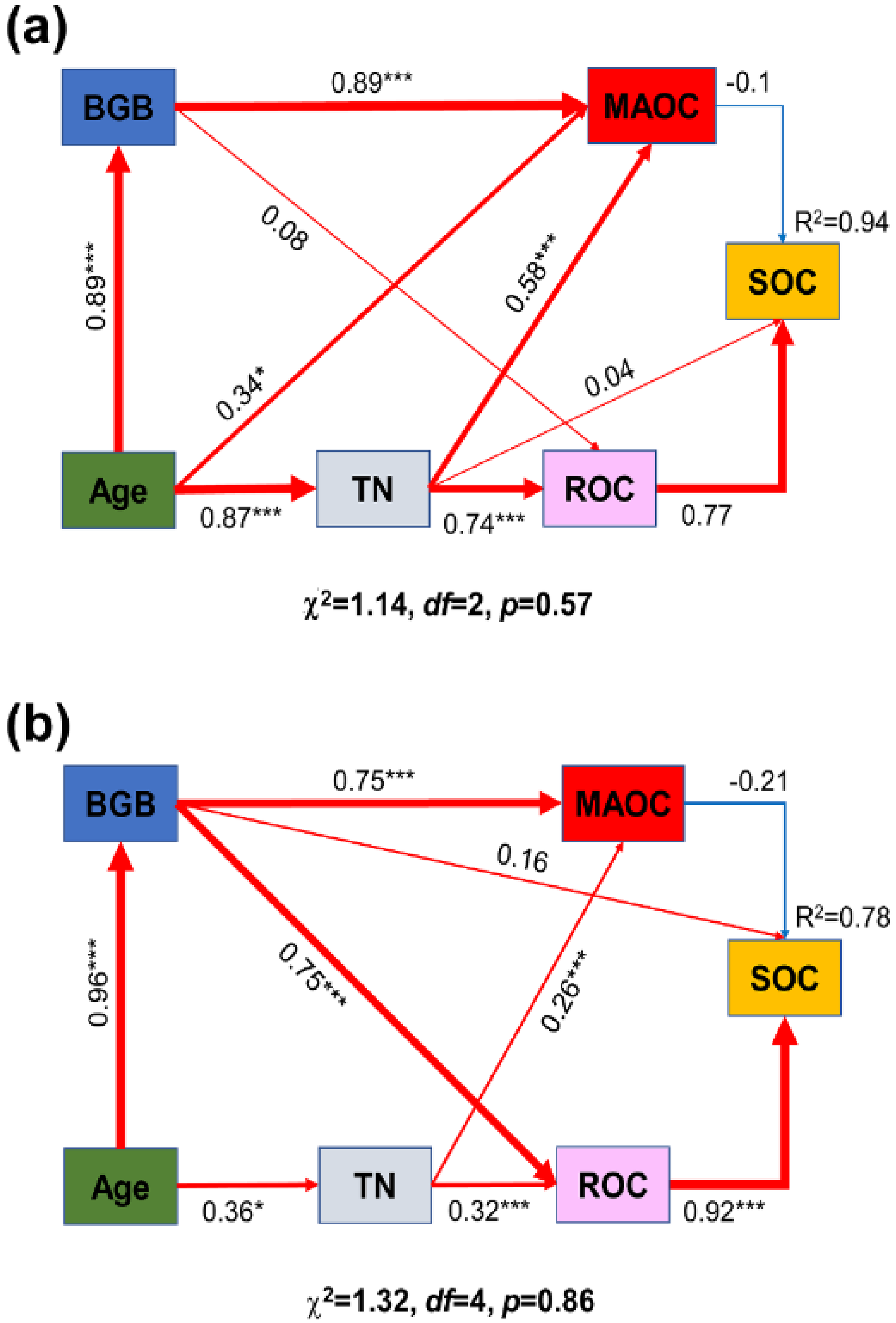

Fig. 2.3. Structural equation model (SEM) analysis of the SOC and its influencing factors at 0–20 (a), 20–40 (b) cm soil depth. The red and blue lines indicate positive coefficients and negative paths, respectively. The numbers on the arrows represent the path coefficients. Line thickness represents the magnitude of the path coefficient. R^2 values represent the proportion of the variance explained for each endogenous variable;

*: $p < 0.05$, ***: $p < 0.001$. Age: succession age, BGB: belowground biomass, TN: total nitrogen, MAOC: mineral associated organic carbon, ROC: recalcitrant organic carbon, SOC: soil organic carbon (Shi et al., 2023).

This study emphasized that ROC distribution is influenced by vegetation type, soil depth, and nitrogen content, with ROC contributing more to SOC in the 20–40 cm layer (67%) compared to the surface layer. Additionally, compared to active carbon fractions such as LOC, ROC exhibited much lower mineralization rates, making it the most stable component of the SOC pool during late succession stages. Kleber (2010) provided a molecular-level analysis of ROC's chemical properties, attributing its recalcitrance to its complex molecular structure, high molecular weight, and strong binding capacity with soil minerals. The study suggested that ROC stability is not solely an inherent property of its molecules but is also influenced by enzymatic reaction kinetics, microbial ecology, and soil physicochemical conditions. For example, lignin and its derivatives, characterized by high aromaticity and low solubility, are considered typical components of ROC. Further analyses using permanganate oxidation and acid hydrolysis revealed ROC's high thermal stability and resistance to external disturbances. Kleber (2010) also noted that ROC stability may be affected by environmental factors such as temperature and moisture, with its sensitivity to global warming potentially underestimated.

In general, LOC provides a critical tool for studying SOC dynamics due to its rapid turnover and sensitivity to environmental changes. Significant LOC changes can quickly reflect the effects of soil management practices, such as fertilization, thinning, or straw return, on carbon inputs. Meanwhile, ROC dynamics serve as an indicator of SOC stability, playing a crucial role in evaluating the long-term carbon sequestration potential of soil management strategies.

2.6 LOC fractions

Due to its rapid response to environmental changes in the short term, LOC is often used as an indicator of SOC dynamics. However, LOC is defined as the fraction of organic carbon that can be oxidized by a specific concentration of potassium permanganate. While this definition partially reflects the decomposable organic matter in soils, it does not fully capture the complexity of microbial survival and activity. To more directly evaluate microbial responses to management practices, subcomponents of LOC, such as dissolved organic carbon (DOC) and microbial biomass carbon (MBC), have recently gained increasing attention.

DOC, as an active component of LOC, is a key indicator of microbial soil due to its solubility and short turnover time. DOC not only serves as a critical substrate for microbial metabolism but also influences soil carbon cycling and nutrient supply through its movement and decomposition in soil solution. Recent studies have shown that DOC concentrations and dynamics are closely related to soil management practices, microbial activity, and environmental conditions. According to Guo et al. (2020), significant differences in DOC concentrations exist across global biomes. In the 0–30 cm soil layer, tundra ecosystems exhibited the highest DOC concentrations, averaging 453 mg kg^{-1}, compared to tropical and temperate forests, which had lower concentrations of 38.2 mg kg^{-1} and 54.5 mg kg^{-1}, respectively. These variations reflect differences in DOC production and decomposition rates across ecosystems and reveal their vertical distribution in soil profiles. More than 50% of total DOC was stored in the 0–30 cm surface soil layer, with concentrations decreasing exponentially with depth. This distribution pattern is primarily controlled by vegetation type, root distribution, and microbial activity.

MBC, on the other hand, directly reflects the abundance and activity of soil microbial communities. It is not only a key indicator of microbial metabolic activity but also a critical regulator of soil carbon cycling and nutrient supply. Deng et al. (2016) investigated soils across different stages of vegetation restoration and found that MBC significantly increased in afforested sites after 15 years of natural vegetation restoration, rising from 221 mg kg^{-1} in cropland to 325 mg kg^{-1}. The proportion of MBC in SOC also increased from 7.1% to 9.5%. Simultaneously, DOC concentrations showed a marked rise, increasing from 30.2 mg kg^{-1} in cropland to 50.1 mg kg^{-1}. These results indicate that vegetation restoration not only promoted SOC accumulation through enhanced organic matter input but also significantly increased microbial activity and the supply of bioavailable carbon sources. This study further emphasized the close relationship between DOC and MBC dynamics. As the soluble fraction of LOC, DOC serves as a primary carbon source for soil microbes. When DOC concentrations increase, microbial metabolic activity is stimulated, leading to a rise in MBC. The experiments revealed a stronger correlation between MBC and SOC in forest soils with higher DOC concentrations, suggesting that microbial activity directly affects soil carbon turnover through DOC consumption.

In summary, DOC, as a key active component of SOC, rapidly responds to soil management practices and environmental changes in the short term. Its dynamic changes provide insights into the state of soil microbial communities and enzyme activities, making it a valuable tool for studying soil carbon cycling. Meanwhile, MBC, by directly reflecting microbial activity and abundance, plays an indispensable role in understanding soil carbon cycling and nutrient supply. Combining the analysis of DOC and MBC offers a more comprehensive understanding of how soil ecosystems respond to management practices and environmental changes.

2.7 Enhanced rock weathering

ERW, an emerging CDR technology, has garnered significant attention in the field of soil carbon loss mitigation. ERW involves the application of finely ground silicate minerals, such as basalt, to soils, promoting mineral weathering reactions that re-fix CO_2 released from the soil as carbonates, thereby mitigating soil carbon loss. The fundamental principle of ERW lies in the reaction of silicate minerals with CO_2 and water in the soil, producing dissolved HCO_3^- and bioavailable mineral nutrients. HCO_3^- is transported via soil water and surface runoff into rivers and eventually to the oceans. During this process, bicarbonate ions react with Ca^{2+} or Mg^{2+} in aquatic systems to form insoluble $CaCO_3$ or $MgCO_3$, which ultimately deposit in riverbeds or seafloors, achieving long-term carbon sequestration (Beerling et al., 2018; Harrington et al., 2023). These sediments can remain stable for thousands or even millions of years, effectively locking atmospheric CO_2 in geological reservoirs and reducing the active carbon content in the global carbon cycle. Additionally, this process contributes to ocean acidification mitigation. As weather products flow into the ocean, the increased alkalinity neutralizes the enhanced acidity caused by excess atmospheric CO_2 absorption. This not only helps stabilize the marine carbonate system but also provides a favorable growth environment for calcifying organisms such as coral reefs and shellfish, promoting the health and stability of marine ecosystems (Bach et al., 2019).

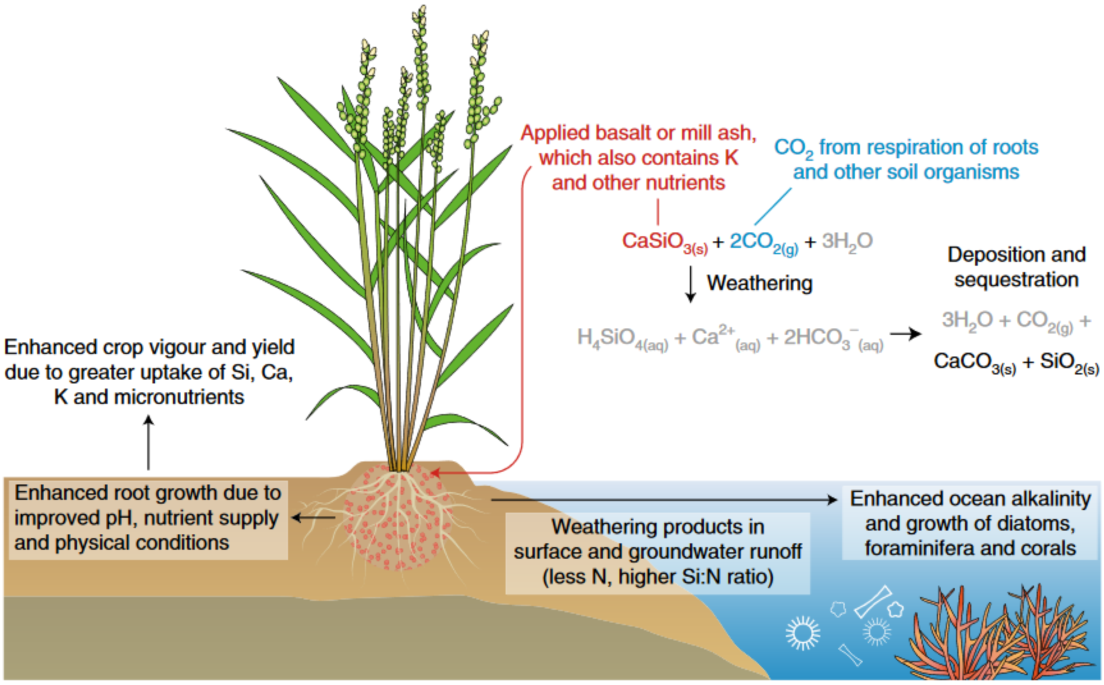

Fig. 2.4. Summary of the potential effects of weathering of crushed basalt or silicate-rich wastes, such as sugarcane mill ash, applied to croplands (Beerling et al., 2018).

According to Beerling et al. (2018), the global implementation of ERW, applying 10 to 30 tons of basalt powder per hectare to 900 million hectares of tropical croplands, could theoretically sequester 1.8 to 14.7 Gt CO_2 by 2100. This carbon capture potential makes ERW a promising candidate for achieving global carbon neutrality. Model analyses by this study further indicated that the effectiveness of ERW is significantly influenced by application rates and regional environmental conditions. Tropical humid climates exhibited the highest weathering rates and CO_2 capture efficiencies. Amann et al. (2022) conducted field experiments using mixtures of basalt and laterite to validate weathering reaction rates and their influencing factors. Their findings showed that under moist soil conditions with higher CO_2 partial pressures, basalt weathering rates increased by over twofold compared to single-material applications. This highlights the importance of designing appropriate materials and optimizing environmental conditions to enhance ERW's carbon capture efficiency. Furthermore, this study emphasized the potential role of microbial activity in weathering processes, as microbial metabolic activities can accelerate mineral dissolution and indirectly promote CO_2 fixation.

In addition to its carbon capture potential, ERW improves soil fertility by releasing mineral nutrients such as Ca, Mg, K, and Si, thereby promoting plant growth. Guo et al. (2023) conducted field trials across multiple climate zones in central China and found that applying 10 kg m^{-2} of silicate rock powder increased crop yields by an average of 7% and biomass by 11%. Notably, in acidic soils, ERW significantly improved soil pH and enhanced nutrient uptake by crops. In regions with low water balances, ERW increased net carbon capture in agricultural systems by 1.6 to 2.4 times, whereas the effect was less pronounced in regions with high water balances. These findings suggest that ERW may be particularly beneficial in water-limited areas while highlighting its variability in agricultural applications.

Research has also demonstrated the impact of soil pH and nutrient availability on changes in crop yields. In low-pH soil, the maximum yield increase reached 31%, indicating the higher effectiveness of alkaline ions and mineral nutrients released by ERW under acidic conditions. These results provide scientific guidance for optimizing ERW application strategies and suggest its potential for enhancing soil fertility and mitigating soil degradation.

However, bicarbonate ions and dissolved alkaline ions generated during the ERW process may influence the carbon cycle in aquatic systems when transported into river networks. Harrington et al. (2023) modeled carbonate precipitation processes in major river basins in the UK to evaluate their impact on ERW's carbon capture efficiency. The results indicated that secondary carbonate precipitation in rivers could lead to the re-release of some captured CO_2, reducing net carbon capture efficiency by 16% to 27%. Moreover, the potential for carbonate precipitation in rivers depended on land use types and hydrological conditions. For instance, basins with higher proportions of agricultural land and lower water flow were more prone to carbonate precipitation, posing challenges for ERW applications in such regions. Nevertheless, the study noted that carbonate precipitation in rivers helps prevent freshwater pH from rising to unsafe levels ($pH > 9$), contributing positively to the stability of river ecosystems.

Once ERW weathering products reach the ocean, they not only facilitate long-term carbon sequestration but also help mitigate ocean acidification by increasing seawater alkalinity. Bach et al. (2019) reported that ERW significantly enhances the buffering capacity of oceans, helping maintain the balance of the marine carbonate system. For example, the release of calcium and magnesium ions promotes carbonate deposition, creating a more stable habitat for calcifying organisms such as corals and shellfish. The study also highlighted that under favorable conditions, silicon released from silicate minerals could enhance phytoplankton productivity, indirectly boosting the ocean's carbon absorption capacity. Furthermore, the study emphasized that ERW's impact on marine systems depends on the type of minerals applied and regional environmental conditions. For instance, silicate weathering may foster a "greener" ocean by promoting the growth of siliceous organisms such as diatoms, while carbonate minerals are more beneficial for supporting calcifying organisms. These findings suggest that tailoring ERW application materials to specific ecosystem needs could achieve multiple ecological benefits.

2.8 Rhizosphere and Non-rhizosphere Soil

Although the CO_2 sequestration efficiency of ERW has been widely studied, its effectiveness varies under different conditions due to the influence of chemical equilibria. Edwards et al. (2017) investigated the weathering potential of ERW in warm and humid tropical regions and found that plant root activity significantly enhanced weathering efficiency. Their experiments demonstrated that CO_2 consumption rates in rhizosphere conditions were 2.5–5 times higher than in non-rhizosphere conditions, primarily due to organic acids secreted by roots and CO_2 released through root respiration. Moreover, the study also highlighted that soil depth significantly impacts weather efficiency. In the surface soil layer (20 cm depth), mineral weathering contributed over 80% of CO_2 capture, whereas in deeper soils (beyond 50 cm), weathering rates dropped to just 20%–30% of those in the surface layer. Furthermore, the root-induced enhancement of weathering rates diminished with decreasing soil cation concentrations (e.g., Ca^{2+}, Mg^{2+}), a limitation particularly evident in older soils (Fig 2.5).

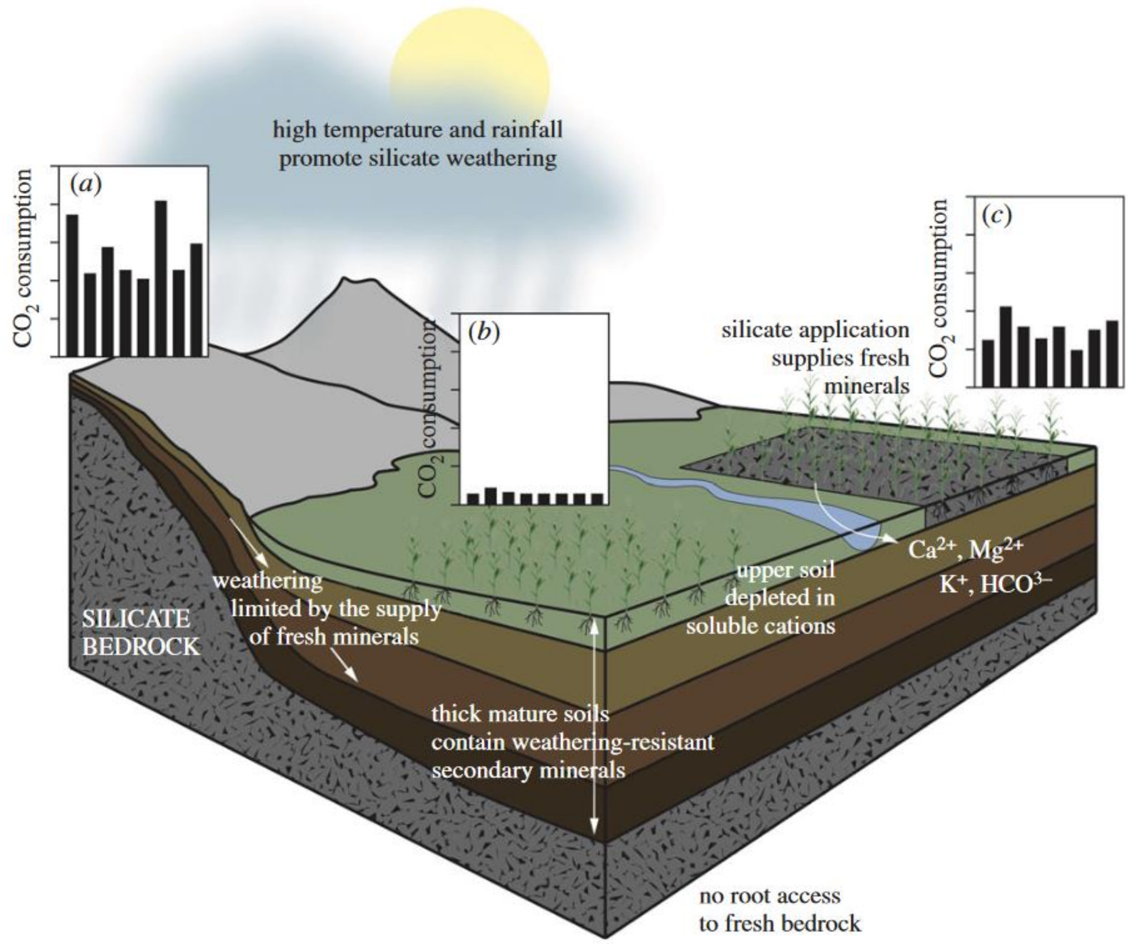

Fig. 2.5. Schematic illustration of enhanced rock weathering for CO_2 removal in the tropics. Relative CO_2 consumption rates are graphed for eight hypothetical tropical rivers draining (a) highlands with limited vegetation and thin/absent soil profiles, (b) lowlands with thick, mature, weathering-resistant soils, and (c)lowlands dressed with reactive ground basalt.

In agricultural systems, soil conditions often include both rhizosphere and non-rhizosphere conditions, such as during fallow periods or intercropping (Gabriel and Quemada, 2011; Rühlemann and Schmidtke, 2015). Recent studies have begun to compare these contrasting conditions. Fu et al. (2022) analyzed microbial community and functional differences between rhizosphere and non-rhizosphere soils in a semi-arid plateau grassland system. Their findings revealed that microbial diversity, as measured by the Shannon index, was significantly higher in rhizosphere soils (3.6) compared to non-rhizosphere soils (2.8; p<0.05). Additionally, rhizosphere soils exhibited 56% higher NO_3^- content and 35% higher NH_4^+ concentration. These results suggest that active microbial communities in rhizosphere soils promote nutrient cycling and organic carbon decomposition, thereby increasing chemical reaction rates essential for mineral weathering.

Kobierski et al. (2018) further compared carbon dynamics between rhizosphere and non-rhizosphere soils, finding significantly higher total organic carbon concentrations in rhizosphere soils (14.3 g kg^{-1}) than in non-rhizosphere soils (10.8 g kg^{-1}; $p<0.01$). DOC concentrations were also 42% higher in rhizosphere soils, reaching 85.4 mg kg^{-1}. The study noted that rhizosphere soils exhibited 23% greater aggregate stability, likely due to the contribution of polysaccharides in root exudates.

Jing et al. (2023) explored the effects of different root diameters on soil enzyme activity and microbial community characteristics. Fine roots (<0.5 mm diameter) significantly increased MBC due to their active secretion processes, with MBC in fine root rhizosphere soils reaching 325 mg kg^{-1} compared to 276 mg kg^{-1} in coarse root (1.0–2.0 mm diameter) rhizosphere soils. Conversely, coarse roots exhibited higher alkaline phosphatase activity under nitrogen deposition conditions, likely due to faster carbon turnover and more efficient nutrient utilization. The study also found that nitrogen deposition significantly affected gas fluxes in the rhizosphere soils. In fine root soils, CO_2 and CH_4 emission rates decreased by 14% and 19%, respectively, whereas no significant changes were observed in coarse root soils.

In summary, rhizosphere and non-rhizosphere soil conditions exert significant influences on CO_2 sequestration efficiency and related soil processes. Rhizosphere soils, with higher microbial activity, nutrient cycling, and organic carbon accumulation, accelerate weathering processes and enhance sequestration efficiency. Conversely, non-rhizosphere soils, with lower microbial activity, may limit ERW effectiveness under fallow and intercropping conditions. Distinguishing the responses of rhizosphere and non-rhizosphere soils to CDR strategies provides a more accurate assessment of CO_2 remove potential and informs the development of optimized implementation strategies.

2.9 Net Biome Productivity

Compared to directly measuring soil carbon changes, Net Biome Productivity (NBP) provides a more comprehensive assessment of ecosystem carbon budget by integrating carbon inputs (e.g., photosynthesis, manure application) and outputs (e.g., harvest, respiration). As a critical indicator for evaluating carbon sequestration capacity, NBP holds significant research value in the context of climate change.

Studies have shown that different land uses and management practices significantly affect NBP. For instance, Shimizu et al. (2015) investigated managed grasslands in Hokkaido and found that plots treated with cattle manure achieved an annual NBP of 4.33 Mg C ha^{-1}, while those treated with chemical fertilizers alone had an NBP of -0.45 Mg C ha^{-1}. This demonstrates that manure application, by increasing organic carbon inputs and promoting mineral nitrogen release, significantly enhances soil carbon sequestration. Seasonal climate variations also influence carbon balance, with the study noting substantial fluctuations in net ecosystem productivity (NEP) across the growing season in manure-treated plots.

Prescher et al. (2010) conducted a comparative study of forests, grasslands, and croplands in eastern Germany. Their results revealed that forests exhibited relatively stable carbon sink characteristics, with annual NBP ranging from -444 to -698 g C m^{-2}. In contrast, grasslands showed considerable variability in NBP, ranging from -28 to 25 g C m^{-2}, depending on mowing frequency. Croplands, strongly influenced by crop type and fertilizer management, had NBP values ranging from -89 to 484 g C m^{-2}. These findings highlight that carbon budgets in croplands and grasslands are not only driven by natural conditions but are also closely linked to human management practices.

At the regional scale, Cervarich et al. (2016) synthesized carbon budget data from several South and Southeast Asian countries, revealing that the region overall acts as a carbon source, with fossil fuel combustion contributing 770 Tg C per year. In comparison, the region's NBP was estimated at 227 ± 279 Tg C yr^{-1}, indicating that its carbon sink capacity is insufficient to offset anthropogenic emissions. The study further noted that Bhutan and Laos, characterized by limited land-use changes and lower emissions, are net carbon sink nations, while other countries primarily act as carbon sources.

These studies suggest that appropriate management practices, such as organic fertilizer application and optimized crop planting, can enhance soil carbon sequestration capacity. However, regional carbon budgets remain significantly constrained by land-use changes and anthropogenic emissions. Future research should focus on further quantifying the contributions of different management strategies to NBP.

3. Materials and Methods

3.1 Study sites information

The study sites are managed grassland located at the Shizunai Experimental Livestock Farm, Field Science Center for Northern Biosphere of Hokkaido University, Shinhidaka, Hokkaido, Japan (42°26′3.3"N, 142°28′55.6"E) and the Experimental Farm of the Field Science Center for Northern Biosphere of Hokkaido University, Sapporo, Hokkaido, Japan (43°04'17.4"N, 141°20'24.6"E).

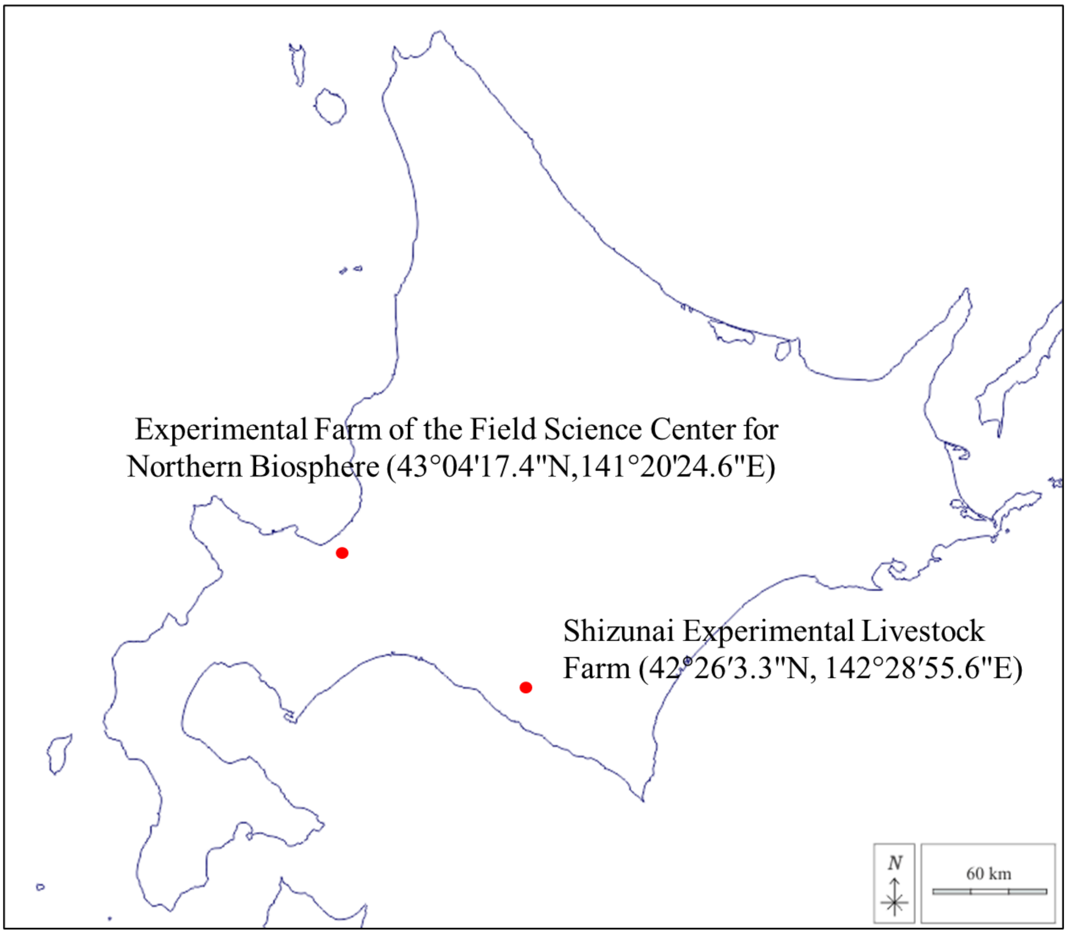

Fig. 3.1. Map of soil sampling site (Shizunai Experimental Livestock Farm) for incubation experiment and research site (Experimental Farm of Field Science Center for Northern Biosphere) for ERW field experiment.

3.1.1 Shizunai Experimental Livestock Farm in Shin-hidaka

3.1.1.1 Climate condition

This experiment site has a cool-temperature climate and is characterized by a humid continental climate with cold winters and warm summers, without apparently wet or dry seasons. According to Automated Meteorological Data Acquisition System (AMeDAS) of the Japan Meteorological Agency, which is located at Shizunaiyamate-cho (42°20.6′N, 142°21.7′E), the mean annual temperature from 2008 to 2018 is 8.3℃, with the monthly mean temperature ranged from -3.6℃ in January and 20.9℃ in August. The annual precipitation from 2008 to 2018 is 1304 mm at AmeDAS located at Shizunai Misono (42°26.0′N, 142°28.9′E). The mean annual sunshine duration was 1881 hours, and the mean annual snowfall was 201 mm. From mid-December to mid-March, the experiment site was covered with snow, and normally soil is frozen in this period.

3.1.1.2 Soil characteristics

The soil is derived from Mt. Usu and Mt. Tarumae volcanic ash and is classified as Mollic Andosol (IUSS Working Group WRB, 2006). The soil layers were divided into Ap1, Ap2, 2C, 3A, 4A and 4G, the characteristics of each layer are shown in Table 3.1.

Table 3.1. Soil layers and properties of Shizunai Experimental Livestock Farm in Shin-hidaka

Horizon	Depth (cm)	Bulk density (g cm^{-3})	pH	TC (%)	TN (%)	C:N
Root	-2	-	-	-	-	-
Ap1	0-7	0.94	5.64	3.7	0.27	13
Ap2	7-16	0.91	5.63	4.1	0.29	14
2C	16-29	0.55	5.67	1.3	0.16	8.2
3A	29-44	0.56	5.46	8.1	0.53	15
4A	44-50	0.75	5.63	4.3	0.26	17

TN: total nitrogen; TC: total carbon. “−” denotes not applicable.

In the fall of 2005, this site was renewed, and Timothy (Phleum pretense L.) was sown. Before 2010, less than 5 horses were grazing per hectare from spring to autumn regular every year. Regular grazing activities stopped since 2010, but cattle and horses were sometimes grazing temporarily to relay to other fields or to feed on uncut leaves before snowfall. Fertilization and harvesting have been carried out since 2009 on this site. Average yield from 2009 to 2016 was 79 Mg DM (Dry Matter) ha^{-1} yr^{-1} and mean fertilizer input was 86, 71, 104 kg ha^{-1} in the order of N, P_2O_5, K_2O. Except for 2010, an average of 10 Mg FM (Fresh Matter) ha^{-1} yr^{-1} compost was applied after second harvest. In addition, 20 Mg FM ha^{-1} yr^{-1} urine fertilizer was applied after second harvest in 2012. After 2016 and prior to the soil sampling in this region, no fertilizers were applied to this site.

3.1.2 Experimental Farm in Sapporo

3.1.2.1 Climate conditions

The experimental site had a humid continental climate characterized by cold winters and warm summers, without apparent wet or dry seasons. The annual precipitation at the study site from 2010 to 2022 was approximately 1146 mm, and the mean annual temperature was 9.2°C according to the AMeDAS located in Sapporo (43°03'38.01"N, 141°19'44.16"E). The highest daily temperatures were observed in August, averaging 26.4°C, whereas the lowest daily temperatures were observed in January, averaging –6.4°C. The snow cover period generally lasted from December to March of the following year.

3.1.2.2 Soil information

Prior to the experiment from 2023, the site was used to cultivate crops, such as maize and potatoes, using conventional methods. The land was tilled twice a year (0–20 cm) and chemical fertilizers were applied according to local fertilization standards. The soil type was Fluvisol, and its initial properties are listed in Table 3.2.

Table 3.2. Soil properties of Experimental Farm of the Field Science Center for Northern Biosphere in Sapporo

Horizon	Depth (cm)	Bulk Density (g cm^{-3})	pH	TC (%)	TN (%)	C: N	Clay (%)	Silt (%)	Sand (%)
Ap1	0-20	1.05	5.75	2.61	0.24	11.1	25.7	27.4	46.9
Ap2	20-33	1.29	5.92	2.00	0.18	10.9	24.7	30.9	44.5
Bw	33-50	1.14	6.03	1.39	0.15	8.84	21.2	22.3	56.5

3.2 Analysis of gas and soil samples

3.2.1 CO_2 concentration analysis

This study utilized two methods for CO_2 concentration analysis. The first method involved collecting gas samples using Tedlar bags, followed by CO_2 concentration measurements with an infrared CO_2 analyzer (ZFP9GC11, Fuji Electric, Tokyo, Japan). The second method employed CO_2 probe (GMP 343, Vaisala, Vantaa, Finland) for direct and continuous measurement.

3.2.2 Soil chemistry properties

3.2.2.1 Soil sample preparation

In the incubation experiment, all plant roots were removed from the soil prior to incubation (Chapter 4). In the field experiment, plant residues were removed using a 2 mm soil sieve after each soil sampling. For both experiments, freshly collected soil samples were stored in a refrigerated chamber at 4°C and analyzed within one month.

3.2.2.2 Soil pH and EC

Soil samples were extracted with a soil-to-water ratio of 1:5 using deionized water and shaken for 1 h, and the pH and EC were measured using a pH meter (F-43, HORIBA, Kyoto, Japan) and an EC meter (CM-30V, DKK-TOA, Tokyo, Japan), respectively. Before each measurement, the pH meter and EC meter were calibrated using pH 4 and pH 7 of standard solutions and deionized water, respectively.

3.2.2.3 Soil NO_3^--N, water-soluble organic carbon (WSOC) and water-soluble inorganic carbon (WSIC)

Soil water extract was filtered through a 0.45 μm filter paper. The NO_3^--N concentration was measured using an ion chromatography (DIONEX ICS-1000, Thermo Fisher Scientific, MA, USA), calibrated using 5 ppm NO_3^--N standard and deionized water. The water-soluble organic carbon (WSOC) and water-soluble inorganic carbon (WSIC) concentrations were measured using a TOC analyzer (TOC-L, Shimadzu, Tokyo, Japan), calibrated using deionized water, 10 ppm, 50 ppm total carbon standard and deionized water, 5 ppm, 10 ppm inorganic carbon standard, respectively.

3.2.2.4 Soil NH_4^+-N

Soil samples were extracted with a soil-to-KCl solutions(2 mol L^{-1}) ratio of 1:10 and shaken for 1 h, then filtered through a 0.45 μm filter paper, and then measured using the indophenol blue method (Scheiner, 1976).

3.2.3 SOC components

3.2.3.1 SOC analysis

Since the soils at the two sites investigated in this study are slightly acidic, the total carbon content considered as the SOC content (Mustapha et al., 2023; Rennert and Herrmann, 2022). Total carbon analysis was conducted using an elemental analyzer (Elementar, vario EL cube, Langenselbold, German) . Specifically, collected soil samples were air-dried, sieved by 2 mm soil sieve. Coarse organic matter, e.g. plant tissue and dead animals, will be removed. The air-dried soil was then crushed using a mortar and pestle to a particle size of less than 2 mm. Carbon content in powdered soil samples will be analyzed by the elemental analyzer (Elementar, vario EL cube, Langenselbold, Germany) based on high-temperature combustion, and total carbon was regarded as SOC because of the absence of carbonates in the acidic soil (Mustapha et al., 2023; Rennert and Herrmann, 2022).

3.2.3.2 LOC and ROC

LOC content was analysis according to the method described in Tirol-Padre and Ladha (2004). Specifically, the air-dried soil containing 10-15 mg of carbon from which organic material had been removed, as described in Section 3.2.3.1. was weighed into a 50 mL centrifuge tube and treated with 25 mL of 333 mM $KMnO_4$. Then, shake the centrifuge 6 h and centrifuge at 2000 rpm for 5 min. Dilute the supernatant and extract solution 250 times. Using 0, 0.2, 0.5, 1.0, and 1.5 mM $KMnO_4$ standard solution to create a standard curve. $KMnO_4$ consumed (difference in $KMnO_4$ contents of sample and extract) is converted to LOC. 1 mM $KMnO_4$ is consumed by oxidation of 9 mg of LOC (Eq. 3.1).

$$LOC = 9\frac{mg\ C}{mmol} \times N \times \frac{1}{W} \times k \times 100\% \quad \text{(Eq. 3. 1)}$$

where, N is the molar amount of potassium permanganate consumed during the reaction (mol). W is the weight of the soil sample used in the analysis (mg). k is the ratio of fresh soil weight to dry soil weight.

ROC is calculated as the difference between SOC and LOC (Eq. 3.2).

$$ROC = SOC - LOC \quad \text{(Eq. 3. 2)}$$

3.2.3.3 MBC and WSOC

Fumigation–extraction method (Vance et al., 1987) was used to determine MBC. Specifically, about 10 g fresh soil samples were fumigated with ethanol-free chloroform for 24 h at 25°C in an evacuated extractor. The remaining samples were treated as control. Fumigated and non-fumigated soils were extracted with 50 ml 0.5 mol L^{-1} K_2SO_4 and shaken for 1 h. The extracts then filter through a 0.45 μm filter paper. The difference in carbon concentration (analyzed by TOC analyzer described in Section 3.2.2.3) between the fumigated and non-fumigated extractions was used to calculate MBC (Eq. 3.3)

$$MBC = (C_f - C_{nf})/K_{EC} \quad \text{(Eq. 3. 3)}$$

Where C_f and C_{nf} are the carbon concentrations of fumigated and non-fumigated extractions, respectively. K_{EC} is the conversion factor which equals 0.45 (Wu et al., 1990).

WSOC was measured by the method described in Section 3.2.2.3.

3.3 Statistical analysis

Data analysis and model fitting were performed using R software (version 4.4.0).

4. Application of Different Organic Fertilizers

4.1 Introduction

Organic fertilizers play an important role in reducing SOC losses or increasing SOC stocks, and are increasingly regarded as a strategic approach to soil carbon management and sustainable agriculture (Bhattacharya et al., 2016; Powlson et al., 2011; Verma et al., 2020b). Numerous studies have demonstrated that organic amendments can significantly enhance SOC stocks, improve soil fertility, and act as buffers against the negative effects of intensive cultivation and poor nutrient management. For example, Xu et al. (2025) reported that the application of organic fertilizers enhanced the stabilization of microbial residues through the formation of Fe/Al oxides, thereby promoting SOC accumulation. Even over short periods, such as a single growing season, organic inputs have been shown to increase SOC content, improve nutrient availability, and stimulate microbial activity (Ren et al., 2021). In addition, organic fertilizers can promote plant growth, reduce nutrient leaching, and improve soil physical structure, contributing to more resilient and productive agricultural systems (Duan et al., 2024; Yan and Gong, 2010; Zhao et al., 2017; Zhao et al., 2024). However, the term “organic fertilizer” encompasses a wide variety of materials with highly heterogeneous characteristics. These differences in origin, composition, and degree of decomposition may lead to inconsistent results in terms of carbon retention and environmental performance.

Hokkaido, Japan, is a critical region for agricultural production, characterized by large-scale forage cultivation and livestock farming. In this context, recycling agricultural waste has become an essential measure to enhance soil fertility and reduce environmental pollution. In recent years, to achieve sustainable agricultural development, the Hokkaido government has actively promoted the use of organic fertilizers, particularly compost and resource-recycled livestock waste. In 2021, the Japanese government introduced the "Green Food System Strategy," which aims to expand organic farming to 25% of arable land (approximately 1 million hectares) and reduce the use of chemical pesticides and fertilizers by 2050. Hokkaido has responded to this strategy by implementing relevant policies and measures that encourage farmers to adopt organic farming practices. These efforts not only reduce chemical fertilizer usage but also mitigate greenhouse gas emissions by increasing SOC content. Despite years of organic fertilizer application in agricultural systems, its specific effects can vary under different environmental and soil conditions. For example, Hokkaido’s unique Andosol soils, characterized by high organic matter content and water retention capacity, may respond differently to organic fertilizers compared to other soils. However, research on the effects of organic fertilizer application on soil carbon dynamics and greenhouse gas emissions in Hokkaido's agricultural systems remains relatively limited.

Compost, a solid organic fertilizer produced through the aerobic decomposition of animal manure or plant residues, is one of the most widely used organic amendments in agricultural systems. During composting, the degradation of lignin and cellulose promotes the humification of organic matter, stabilizes nutrients, and converts them into plant-available forms such as humic and fulvic acids (Song et al., 2016; Wei et al., 2007; Zhou et al., 2014). This process enhances the overall stability of the compost and reduces the likelihood of rapid mineralization and greenhouse gas emissions after soil application (Albrecht et al., 2011; Wu et al., 2024). However, the high degree of stabilization in compost may limit the immediate availability of carbon and nutrients for microbial activity, thereby slowing down its decomposition and nitrogen mineralization rates

(Ahmed et al., 2023; Bellino et al., 2015). Therefore, quantifying the short-term decomposition dynamics of compost is essential for evaluating its effectiveness as a strategy to mitigate soil carbon loss and to inform optimized field management practices.

Raw slurry (slurry) is a liquid material that has not undergone anaerobic fermentation, which is rich in ammonium nitrogen, phosphorus, potassium, and other water-soluble nutrients. Due to its rapid nutrient supply and high crop uptake efficiency, slurry is considered an effective substitute for nitrogen fertilizers (Xu et al., 2024). In studies conducted in Hokkaido, slurry application demonstrated significant soil improvement effects, including enhanced nutrient supply capacity and reduced chemical fertilizer use (Kitamura et al., 2021). However, the low C:N ratio of slurry may lead to rapid nitrogen mineralization upon application, significantly increasing N_2O emissions, especially under high soil moisture conditions (Han et al., 2013). On the other hand, the alkalinity of slurry may alleviate the inhibitory effects of soil acidification on microbial activity, thereby influencing soil carbon cycling (Tampio et al., 2016). The rapid decomposition characteristics of slurry could have adverse effects on short-term soil carbon balance, raising the challenge of balancing crop growth needs with greenhouse gas emission risks through appropriate application rates.

Digestate is the residual liquid fraction after anaerobic fermentation, with lower carbon content but higher water content and alkalinity compared to slurry. Previous studies have shown that, compared to raw slurry, digestate typically contains higher concentrations of nitrogen (N), phosphorus (P), and potassium (K), along with lower levels of odor (Calusinska et al., 2018; Immovilli et al., 2008). However, as the fermentation process consumes a significant portion of the organic carbon in the raw slurry, the carbon content in the digestate is generally lower. From the perspective of soil carbon enhancement, slurry may therefore offer greater potential than digestate. However, comparative studies on this topic are limited. In addition, both slurry and digestate can rapidly stimulate soil microbial communities, potentially increasing the risk of SOC mineralization. Studies have reported that the addition of labile carbon to these liquid fertilizers can induce strong priming effects, leading to elevated greenhouse gas emissions (Velthof and Mosquera, 2011). Therefore, clarifying the differences in carbon turnover and retention mechanisms between slurry and digestate is essential for understanding how organic fertilizers with distinct biochemical properties affect SOC dynamics.

Organic fertilizers vary in physical form, chemical characteristics, and carbon content, which may lead to significant differences in their decomposition behavior and the associated impacts on SOC retention and CO_2 emissions. Considering compost manure, raw slurry, and digestate as sources of SOC, this chapter evaluated SOC changes, cumulative CO_2 emissions, and soil carbon retention performance across treatments, and further analyzed the associated soil properties and other gas fluxes to elucidate the mechanisms of carbon turnover and stabilization. We hypothesized that (1) compost manure would exhibit the slowest CO_2 emission rate and the lowest cumulative emissions owing to its solid form; (2) digestate would result in lower CO_2 emissions than raw slurry as a consequence of reduced carbon content; and (3) SOC accumulation would correspond to the amount of carbon input applied in each treatment.

4.2 Materials and methods

4.2.1 Soil collection

In June 2022, three random 0.5 m × 0.5 m sampling areas were established within the grassland region described in Chapter 3 (Fig. 4.1). Soil samples were collected from a depth of up to 20 cm in each area, and all collected soil was thoroughly mixed. The mixed soil was then passed through a 2 mm sieve to remove plant organic matter and air-dried for one month.

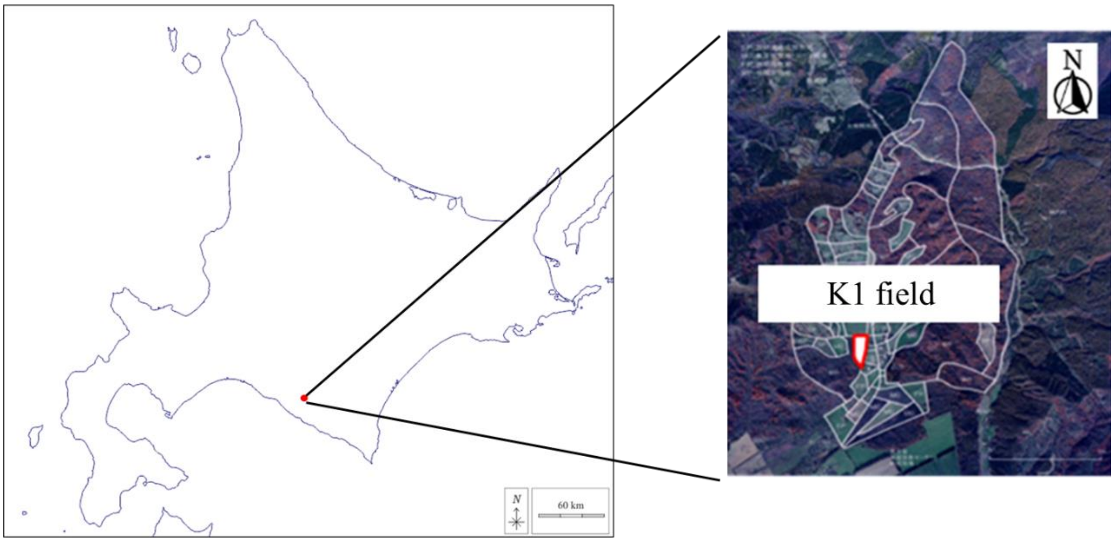

Fig. 4.1. Information about study field.

4.2.2 Fertilizer collection

In June 2022, compost manure was obtained from the compost storage facility at the Shizunai Experimental Livestock Farm and was primarily derived from fermented cattle excreta, horse excreta, and bedding litter via aerobic composting. The collected compost manure was refrigerated at 4°C for subsequent property analysis and incubation experiments. In July 2022, raw slurry was collected from the cattle barn at the Experimental Farm of the Field Science Center for Northern Biosphere, whereas the digestate was obtained from the effluent tank of the adjacent anaerobic digester. The collected slurry and digestate were stored in 1 L plastic bottles and refrigerated at 4°C for subsequent property analysis and incubation experiments (Fig. 4.2).

Fig. 4.2. Collection of compost manure (a), slurry (b) and digestate (c).

4.2.3 Properties of fertilizers

The collected organic fertilizers were dried in an oven at 105°C for 24 hours, and their moisture content was calculated by comparing their weights before and after drying. For pH measurement, 5 g of each fertilizer sample was mixed with 50 mL of deionized water, shaken for 1 hour, and the pH was measured using the pH meter described in Chapter 3. The three organic fertilizers were processed using the sulfuric acid digestion method (Hseu, 2004). Total nitrogen content was analyzed using ion chromatography, as described in Chapter 3. Potassium oxide (K_2O) was quantified using a Polarized Zeeman Atomic Absorption Spectrophotometer (Z-5010, Hitachi High-Tech, Tokyo, Japan), and phosphorus pentoxide (P_2O_5) was quantified using the colorimetric method (Peachey et al., 1973). For total carbon and WSOC analysis, air-dried and fresh fertilizer was used respectively, and their total carbon content was quantified using the same method described for soil total carbon measurement in Chapter 3. The organic matter (OM) content was determined by the loss-on-ignition method (Ball, 1964). Briefly, approximately 1 g of pulverized fertilizer sample was placed in a muffle furnace and subjected to combustion at 550°C for 4 hours. The percentage of OM was calculated from the mass difference between the samples before and after the ignition process. The properties of the fertilizers are shown in Table 4.1.

Table 4.1. Properties of 3 types of fertilizers

	Compost manure	Raw Slurry	Digestate
Dry matter (%)	24.8±1.57 a	4.85±0.38 b	3.72±0.02 b
pH	9.11±0.06 a	8.28±0.10 b	8.51±0.03 b
TN (% FM)	0.72±0.05 a	0.19±0.01 b	0.21±0.03 b
NH_4^+-N (% FM)	0.07±0.01 a	0.10±0.00 a	0.13±0.00 a
P_2O_5 (% FM)	1.78±0.13 a	0.24±0.01 b	0.25±0.02 b
K_2O (% FM)	1.26±0.07 a	0.28±0.00 b	0.29±0.01 b
TC (% FM)	11.7±0.28 a	2.94±0.08 b	1.91±0.08 c
OM (% FM)	22.4±0.13 a	4.62±0.03 b	3.18±0.02 c
WSOC (% FM)	0.49±0.10 a	0.33±0.04 b	0.27±0.03 b
C/N	16.3	15.3	9.11

Different letters represent significant differences between fertilizer ($p < 0.05$). Data represents means ± S.D. ($n = 3$). TN: total nitrogen; TC: total carbon; OM: organic matter; WSOC: water-soluble organic carbon

4.2.4 Incubation settings

This study included five treatments: no fertilizer (NF), inorganic fertilizer (IF), compost manure (M), raw slurry (S) and digestate (D). Each treatment had three replicates and separate incubation bottles were designated for gas and soil analysis, resulting in a total of 5 × 3 × 2 = 30 incubation bottles.

Before incubation, 300 g of air-dried soil was placed in glass bottles (95 mm diameter and 180 mm height). Water was added to adjust the soil moisture to 60% of the maximum water holding capacity (MWHC). The soil was thoroughly mixed and pre-incubated aerobically at 25°C for 7 days under aerobic conditions. During the pre-incubation period, water was replenished every two days to maintain consistent moisture content.

The compost manure was manually broken into small pieces (approximately 10 mm) to improve uniformity before application. The raw slurry and digestate were thoroughly mixed by shaking immediately before application and then applied directly. After fertilizer application, the soil and fertilizer were thoroughly mixed. All bottles were incubated under aerobic conditions at 25°C for 91 days. Throughout the incubation period, the bottles were loosely covered with perforated aluminum foil to maintain aerobic conditions while minimizing evaporation when gas was not being collected. Soil moisture was maintained at 60% of MWHC by adding water every 2 to 3 days.

To facilitate the temporal interpretation of treatment effects, the 91-days incubation period was divided into three periods: early (P_E: days 1–7), middle (P_M: days 8–35), and late (P_L: days 36–91). This classification was consistently applied to both data visualization and statistical analyses.

4.2.5 Fertilization management

To align with the practical conditions described by Kitamura et al. (2021), the fertilizer application was designed based on the annual fertilization rates at the soil collection site. Specifically, the nutrient upper limits for N, P_2O_5, and K_2O were set at 0.24 mg g^{-1}, 0.19 mg g^{-1}, and 0.42 mg g^{-1}, respectively.

For IF treatment, inorganic fertilizers were applied to reach these upper limits using ammonium sulfate for N, fused phosphate for P_2O_5, and potassium sulfate for K_2O. In the organic fertilizer treatments (M, S, and D), each organic material was applied to reach the upper limit of a single target nutrient (N, P_2O_5, or K_2O), with the remaining nutrients supplemented with inorganic fertilizers to ensure nutrient equivalence across treatments. The specific application rates and nutrient contributions of each treatment are shown in Fig. 4.3.

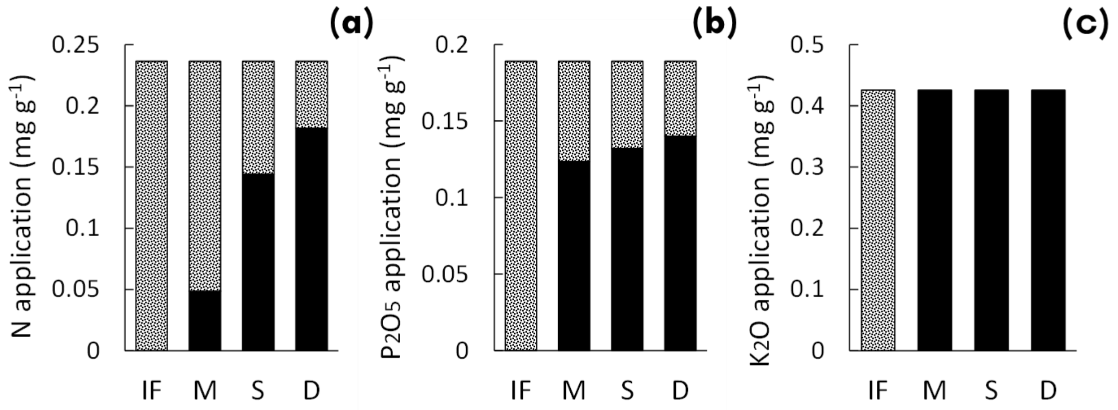

Fig. 4.3. Application rates of N (a), P_2O_5 (b), K_2O (c) and nutrient contribution for each treatment. IF: Inorganic fertilizer; M: Compost manure; S: Raw slurry; D: Digestate.

Since the fertilization design was based on N, P_2O_5, and K_2O levels rather than carbon content, the amount of carbon input varied among the organic fertilizer treatments. Table 4.2 shows the specific carbon input amounts for each organic fertilizer treatment.

Table 4.2. Carbon input in each organic fertilizer treatment

Treatment	Organic Fertilizer input (g)	TC (% FM)	Carbon input (g)
M	14.4	11.7	1.69
S	56.3	2.94	1.66
D	55.2	1.91	1.05

M: Compost manure; S: Raw slurry; D: Digestate. TC: Total carbon

4.2.6 Gas and soil sampling

Gas sampling was conducted on 1, 3, 5, 7, 14, 21, 28, 35, 42, 49, 56, 63, 77, and 91 days after incubation. On each sampling day, the incubation bottles were briefly flushed with purified air to remove residual gases and then sealed with an airtight plastic lid. A 300 mL Tedlar bag pre-filled with purified air was connected via flexible tubing. The bottles were then incubated under the same conditions (25°C) for 24 h. Subsequently, the gas samples were collected from the Tedlar bags and analyzed for CO_2, N_2O, CH_4, and NO concentrations: CO_2 concentration was determined according to the first method described in Chapter 3. Calibration was performed before each measurement using pure N_2 gas (0 ppm) and CO_2 standard gas (1860 ppm). The readings were recorded as voltage values (mV), and CO_2 concentration (ppm) was calculated by multiplying the voltage value by 20. NO concentration was determined using a NO-NO_2-NO_x Analyzer (42iQ, Thermo Scientific, Tokyo, Japan), Calibration was performed using 8 concentrations of standard NO gas (0, 0.004, 0.01, 0.02, 0.04, 0.1, 0.2, and 2 ppm) before measurements. CH_4 and N_2O concentration was determined using a gas chromatograph (GC-2014, Shimazu, Tokyo, Japan). Calibration curves were prepared for CH_4 at 4 standard gas points (1.98, 4.79, 9.94 and 994 ppmv) and for N_2O at 4 standard gas points (0.3, 0.6, 1.5, 6, and 30 ppmv). All collected gas samples were analyzed within 2 hours after sampling. The gas flux (mg kg^{-1} day^{-1} for CO_2 and μg kg^{-1} day^{-1} for N_2O, CH_4, NO) on sampling day was calculated using Eq. 4.1.

$$\boldsymbol{Gas\ flux} = \left(\frac{\boldsymbol{V}}{\boldsymbol{m}}\right) \times \left(\frac{\boldsymbol{dC}}{\boldsymbol{dt}}\right) \times \left(\frac{\boldsymbol{273}}{\boldsymbol{T}}\right) \times \frac{\boldsymbol{M}}{\boldsymbol{22.4}} \quad \text{(Eq. 4.1)}$$

where, *V* is the headspace volume of the incubation bottle (mL), *m* is the dry soil weight (kg), *dC/dt* is the rate of change in gas concentration per unit time (m^3 m^{-3} day^{-1}), *T* is the incubation temperature (298.15 K), and *M* is the molar mass of the target gas (44, 44, 16, and 30 g mol^{-1} for CO_2, N_2O, CH_4 and NO, respectively). The N_2O/NO ratio was calculated as the ratio of the respective gas flux and was used as an indicator of denitrification intensity (Bouwman et al., 2002). The cumulative gas emissions were calculated using the trapezoidal rule based on the gas fluxes measured on each sampling day.

Soil sampling was conducted on days same with gas sampling, and soil properties including pH, EC, NH_4^+-N concentrations and NO_3^--N concentrations by the methods described in Chapter 3. SOC pools were also measured using soil samples collected at the beginning and end of the incubation period, which were quantified using the SOC analysis methods described in Chapter 3.

4.2.7 Data calculations

To evaluate the fate of carbon input and carbon sequestration performance of each organic fertilizer, we calculated two integrated indices, carbon decomposition progress (CDP) and carbon balance efficiency (CBE), which represent the extent of carbon transformation and net carbon retention efficiency, respectively. These indices integrate the amount of carbon input, cumulative CO_2 emissions, and the net increase in SOC relative to the unfertilized control (N treatment). CH_4 was not considered because of its negligible magnitude compared with that of CO_2. The CDP and CBE were calculated as follows (Eq. 4.2 and Eq. 4.3).

$$CDP = \frac{\Delta SOC + \Delta C_{CO2}}{C_{input}} \times 100\% \quad \text{(Eq. 4.2)}$$

$$CBE = \frac{\Delta SOC - \Delta C_{CO2}}{C_{input}} \times 100\% \quad \text{(Eq. 4.3)}$$

where, ΔSOC represents the difference in SOC content at the end of incubation between each organic fertilizer treatment and N treatment (g kg^{-1}). ΔC_{CO2} is the difference in cumulative CO_2 emissions between each organic fertilizer treatment and the N treatment (g C kg^{-1}). C_{input} denotes the amount of carbon applied through organic fertilizers (g kg^{-1}).

To estimate the field-scale increase in SOC and ensure consistency with the Chapter 5, we applied a stock-change approach for the 0–20 cm layer, upscaling mass-based SOC changes to field-scale SOC change (Mg ha^{-1}) using Eq.4.4.

$$\Delta SOC_{field-scale} = BD \times z \times A \times (SOC_{treat} - SOC_{NF}) \quad \text{(Eq. 4.4)}$$

where, BD is the bulk density of field soil (g cm^{-3}), z is the tillage depth (0.2 m), A is the conversion factor from hectares to square meters (10^4 m^2 ha^{-1}), SOC_{treat} is the SOC concentration in each treatment at the end of incubation (g g^{-1}), and SOC_{NF} is the SOC concentration in the NF treatment at the end of incubation (g g^{-1}).

4.2.8 Statistical and multivariate analysis

Differences in cumulative gas emissions, CDP, CBE, and SOC pools among treatments were tested using a one-way ANOVA. When a significant difference was observed ($p <$ 0.05), Tukey's HSD test was performed for multiple comparisons.

A linear mixed-effects model (LMM) was used to evaluate the treatment effects at each incubation stage, similar to the approach used by Yang et al. (2025). In each model, treatment was included as a fixed effect, whereas sampling day and replication were treated as random effects.

Correlation network analysis was conducted to visualize the correlation structure among the variables (Guo et al., 2023a). Specifically, we first calculated the direct correlations of CO_2 flux with soil properties and other gas fluxes and then identified secondary correlations between variables that were directly associated with CO_2 flux. Spearman's rank correlation coefficients were computed for all variable pairs within each treatment, and only significant correlations ($p < 0.05$) were included in the network visualization.

Redundancy analysis (RDA) was performed to examine the associations between CDP- or CBE-related indicators and other associated variables, focusing on system-level responses after organic fertilizer application. Changes in CDP, CBE, SOC, and cumulative CO_2 emissions were set as the response variables, whereas the explanatory variables included changes in soil properties, SOC components, and cumulative emissions of other gases. All variables were standardized prior to analysis and scaling type 2 was employed to emphasize the distribution of treatment-level samples.

4.3 Results

4.3.1 Evaluations of CO_2 flux and cumulative emissions under different treatments

Temporal changes in CO_2 flux across the different treatments are shown in Fig. 4.4. All organic fertilizer treatments exhibited a similar trend over the 91-day incubation period. CO_2 flux peaked during P_E, gradually declined during P_M, and stabilized during P_L. Notably, a relatively stable plateau during P_M was observed in M. Among all the treatments, the highest CO_2 flux recorded for S on day 1 (321 mg kg^{-1} day^{-1}) was significantly higher than the peak values observed for M and D (101 and 83.2 mg kg^{-1} day^{-1}, respectively, $p < 0.05$,). According to the LMM results, the CO_2 flux in S during P_E was significantly higher than that in M and D (Table 4.3). However, the significant difference in CO_2 flux between S and M disappeared during P_M and P_L, although both remained significantly higher than in D. Relatively stable CO_2 fluxes throughout the incubation period were observed in NF and IF, with no significant difference between them, and both were significantly lower than in all organic fertilizer treatments. Fig. 4.5 shows the cumulative CO_2 emissions at the end of the incubation period for each treatment group. All organic fertilizer treatments exhibited significantly higher cumulative CO_2 emissions than the NF and IF treatments, with no significant difference observed. Among the organic treatments, the cumulative emissions in S were the highest, significantly exceeding those in M, which were also significantly higher than those in D.

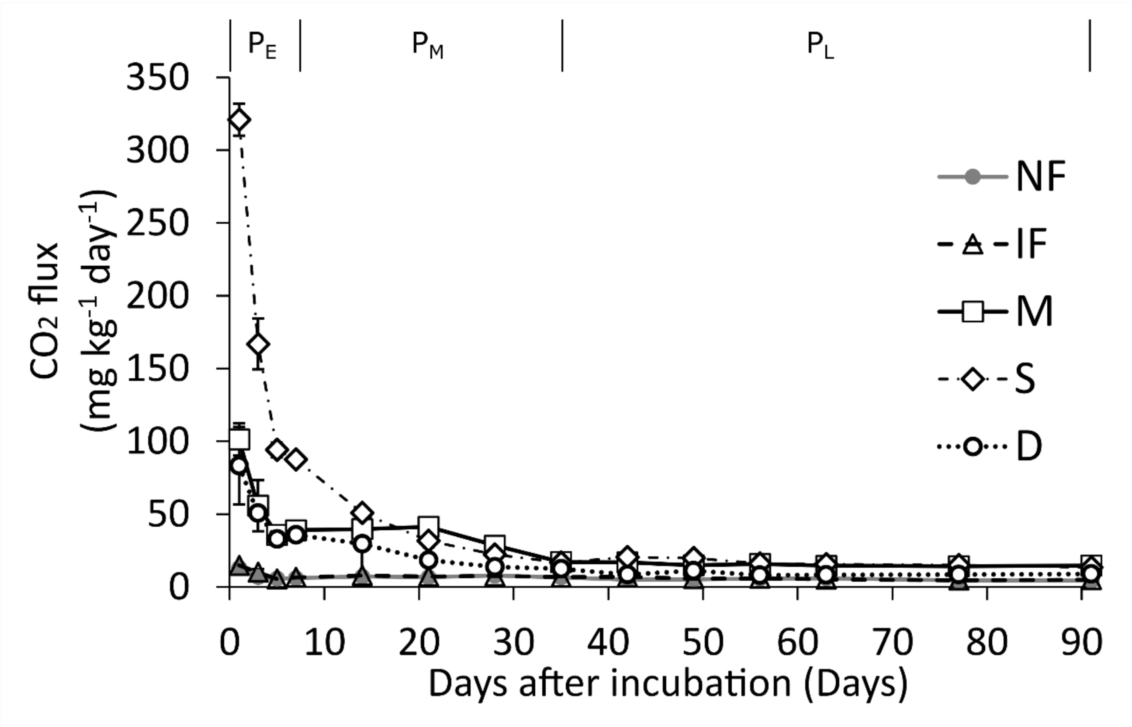

Fig. 4.4. Changes in CO_2 flux among all treatments during the incubation. Data represents means ± standard deviation (n = 3). P_E, P_M, P_L represent early period (Days 1-7), middle period (Days 8-35) and late period (Days 36-91). NF: No fertilizer; IF: Inorganic fertilizer; M: Compost manure; S: Raw slurry; D: Digestate.

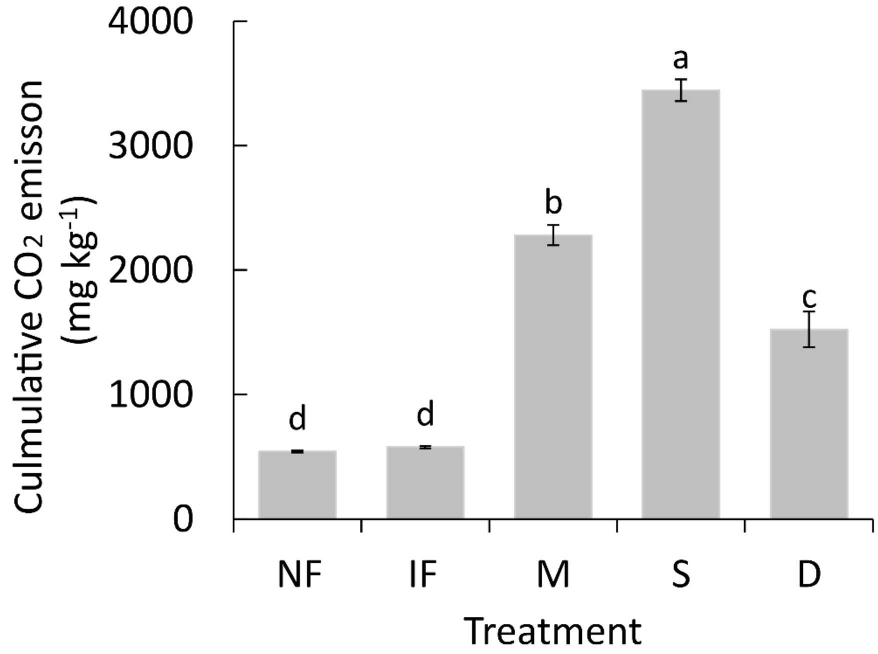

Fig. 4.5. Cumulative CO_2 emissions among all treatments after the incubation. The error bars show the standard deviation (n = 3). Different letters indicate significant differences among treatments at $p < 0.05$. NF: No fertilizer; IF: Inorganic fertilizer; M: Compost manure; S: Raw slurry; D: Digestate.

Table 4.3. Linear Mixed Model (LMM) results of gas flux and soil properties under different treatments during each period

	Period	Treatment				
		NF	IF	M	S	D
CO_2 flux ($mg\ kg^{-1}\ day^{-1}$)	P_E	7.84 c	9.22 c	58.0 b	167 a	50.6 bc
	P_M	7.01 c	7.29 c	31.6 a	30.3 a	18.5 b
	P_L	5.02 c	5.54 c	15.2 a	16.7 a	8.80 b
CH_4 flux ($\mu g\ kg^{-1}\ day^{-1}$)	P_E	5.38 b	5.43 b	5.52 b	63.8 a	16.1 b
	P_M	5.95 a	6.10 a	6.11 a	6.14 a	6.18 a
	P_L	5.99 a	5.84 a	5.81 a	5.73 a	5.69 a
NO flux ($ng\ kg^{-1}\ day^{-1}$)	P_E	0.71 c	1.77 bc	3.38 bc	8.71 b	25.8 a
	P_M	0.42 c	2.41 c	4.17 bc	9.00 a	7.71 ab
	P_L	0.43 d	4.77 b	5.88 a	4.36 b	3.27 c
N_2O flux ($\mu g\ kg^{-1}\ day^{-1}$)	P_E	6.62 c	9.50 c	198 b	329 a	290 a
	P_M	4.97 c	7.40 c	85.2 b	131 ab	174 a
	P_L	3.14 c	5.70 bc	71.2 a	11.1 bc	20.2 b
N_2O/NO	P_E	9.55 b	5.71 b	71.2 a	48.5 a	14.6 b
	P_M	11.8 bc	3.31 c	21.6 b	18.1 b	33.1 a
	P_L	7.34 b	1.24 c	13.3 a	2.66 bc	7.61 b
pH	P_E	5.07 b	5.06 b	5.09 b	5.97 a	6.14 a
	P_M	5.00 ab	4.76 b	4.86 abc	4.69 c	5.09 a
	P_L	4.99 a	4.34 d	4.43 c	4.56 b	4.61 b
EC ($mS\ m^{-1}$)	P_E	9.59 c	50.8 a	33.8 ab	23.4 bc	23.2 bc
	P_M	10.6 c	34.1 b	44.7 a	38.6 b	34.2 b
	P_L	11.5 d	33.0 c	49.9 a	41.6 b	45.1 b
NO_3^--N conc. ($mg\ kg^{-1}$)	P_E	11.2 ab	11.2 ab	15.1 a	6.8 b	8.7 b
	P_M	13.0 b	21.2 b	36.0 a	37.3 a	32.5 a
	P_L	15.2 b	39.9 b	61.9 a	59.1 a	64.1 a
NH_4^+-N conc. ($mg\ kg^{-1}$)	P_E	1.85 c	51.6 a	28.2 b	31.6 b	27.7 b
	P_M	0.88 d	31.3 a	18.7 b	4.39 cd	8.71 c
	P_L	0.403 b	2.64 a	2.90 a	0.813 b	1.32 b

Values represent the estimated marginal means (emmeans) during each incubation period. Different letters indicate significant differences among treatments at $p < 0.05$. P_E: early period (1–7 days after incubation); P_M: middle period (8–35 days); P_L: latter period (36–91 days). NF: No fertilizer; IF: Inorganic fertilizer; M: Compost manure; S: Raw slurry; D: Digestate.

4.3.2 Evaluations of SOC pools, CDP and CBE under different treatments

The SOC, LOC, and ROC concentrations at the end of the incubation period are shown in Fig.4.6. All organic fertilizer treatments significantly increased SOC concentrations compared to NF and IF, with the highest value observed in S (33.9 g kg^{-1}), followed by D and M (33.2 and 32.5 g kg^{-1}, respectively). Among organic fertilizer treatments, the SOC concentration in S was significantly higher than that in M, whereas no significant differences were observed between D and the other organic treatments. In terms of SOC fractions, ROC accounted for a dominant proportion, ranging from 69.8% to 72.4%. Compared with NF and IF, both LOC and ROC concentrations were significantly higher in S, and the ROC concentration was also significantly elevated in D. In contrast, no significant differences in LOC or ROC concentrations were observed in M. In addition, no significant differences in the LOC or ROC concentrations were observed among the three organic fertilizer treatments.

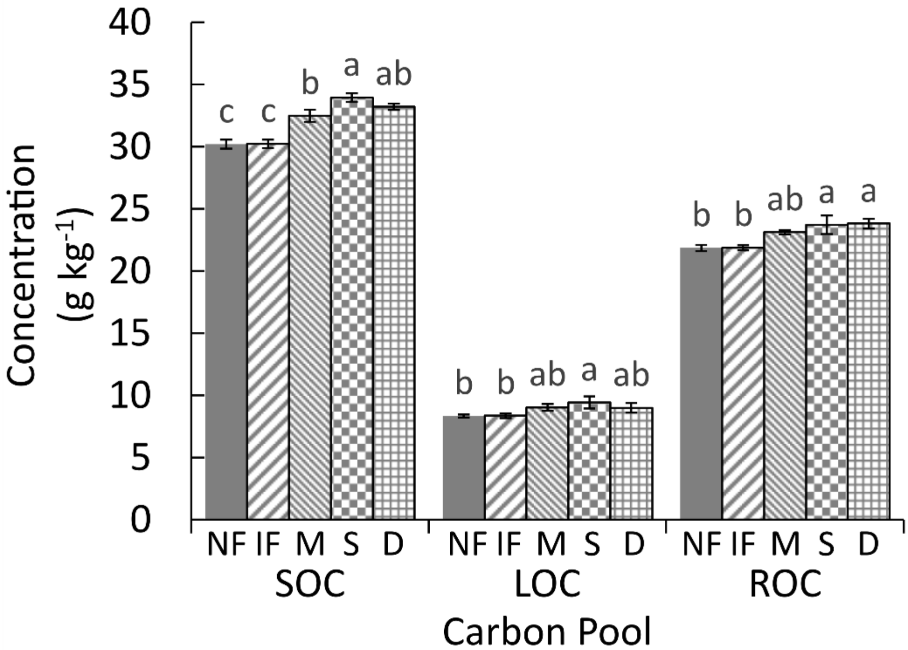

Fig. 4.6. Soil organic carbon (SOC), labile organic carbon (LOC) and recalcitrant organic carbon (ROC) concentrations among all treatments after the incubation. The error bars show the standard deviation (n = 3). Different letters indicate significant

differences among treatments at $p < 0.05$. NF: No fertilizer; IF: Inorganic fertilizer; M: Compost manure; S: Raw slurry; D: Digestate.

The MBC and WSOC concentrations at the end of the incubation period are shown in Fig.4.7. Although both parameters tended to be higher in organic fertilizer treatments than in the NF and IF treatments, the differences were not significant ($p > 0.05$).

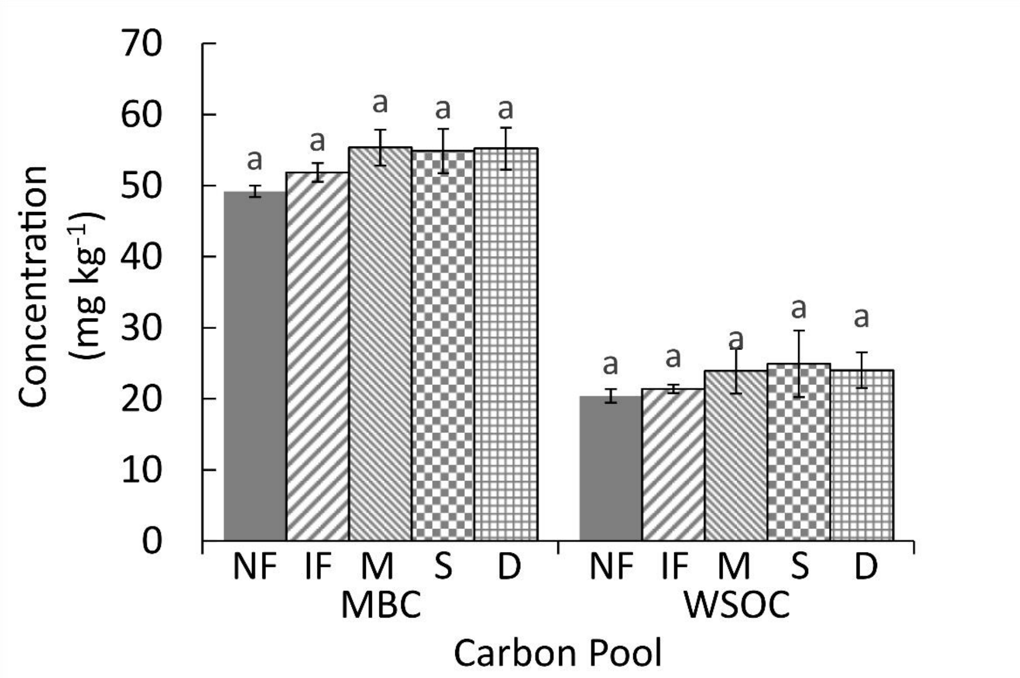

Fig. 4.7. Microbial organic carbon (MBC) and water-soluble organic carbon (WSOC) concentrations among all treatments after the incubation. The error bars show the standard deviation (n = 3). Different letters indicate significant differences among treatments at $p < 0.05$. NF: No fertilizer; IF: Inorganic fertilizer; M: Compost manure; S: Raw slurry; D: Digestate.

Table 4.4 shows the CDP and CBE values at the end of the incubation period. CDP was significantly higher in S and D than in M, with no significant differences between S and D. CBE was significantly higher in D than in S and M, while no significant differences were found between S and M.

Table 4.4. Carbon Decomposition Progress (CDP) and Carbon Balance Efficiency (CBE) under different organic treatments

	M	S	D
CDP (%)	51.61 ± 8.73 b	81.12 ± 6.02 a	97.98 ± 7.23 a
CBE (%)	29.53 ± 9.30 b	47.16 ± 6.53 b	74.24 ± 7.81 a

Values represent the mean ± standard deviation (n = 3). Different lowercase letters indicate significant differences between the treatments ($p < 0.05$). M: Compost manure; S: Raw slurry; D: Digestate.

4.3.3 Changes in other gas fluxes and soil properties

Significant CH_4 flux peaks were observed only in S on Days 1 and 3, reaching 205 and 99.6 μg kg^{-1} day^{-1}, respectively ($p < 0.05$; Fig. 4.8a). Correspondingly, the CH_4 flux in S was significantly higher than that in the other treatments only during P_E (Table 4.3).

The NO fluxes in S and D followed a rise–fall pattern during the incubation period; however, their peak timings differed, occurring during P_M in S and during P_E in D. During P_E, the NO flux in D was significantly higher than that in all the other treatments, whereas during P_M, the NO flux in S was significantly higher than that in all the other treatments except D. In contrast, the NO flux in M exhibited a continuously increasing trend, with the highest value observed during the P_L (Fig. 4.8b, Table 4.3). A similar rise–fall trend in N_2O flux was observed in S and D. However, the N_2O flux in M showed a distinct pattern, which decreased during P_E and then stabilized thereafter (Fig. 4.8c). Notably, the N_2O flux in M was significantly lower than that in the other organic treatments during P_E. However, it was the highest among all treatments during P_L (Table 4.3). A pronounced peak in N_2O/NO (>100) was observed on day one in M, and this ratio remained consistently above 10 throughout the incubation period. In contrast, a decreasing trend was observed for N_2O/NO in S and D after P_M, and at the end of the incubation, their values were not significantly different from those in the IF (Fig. 4.8d).

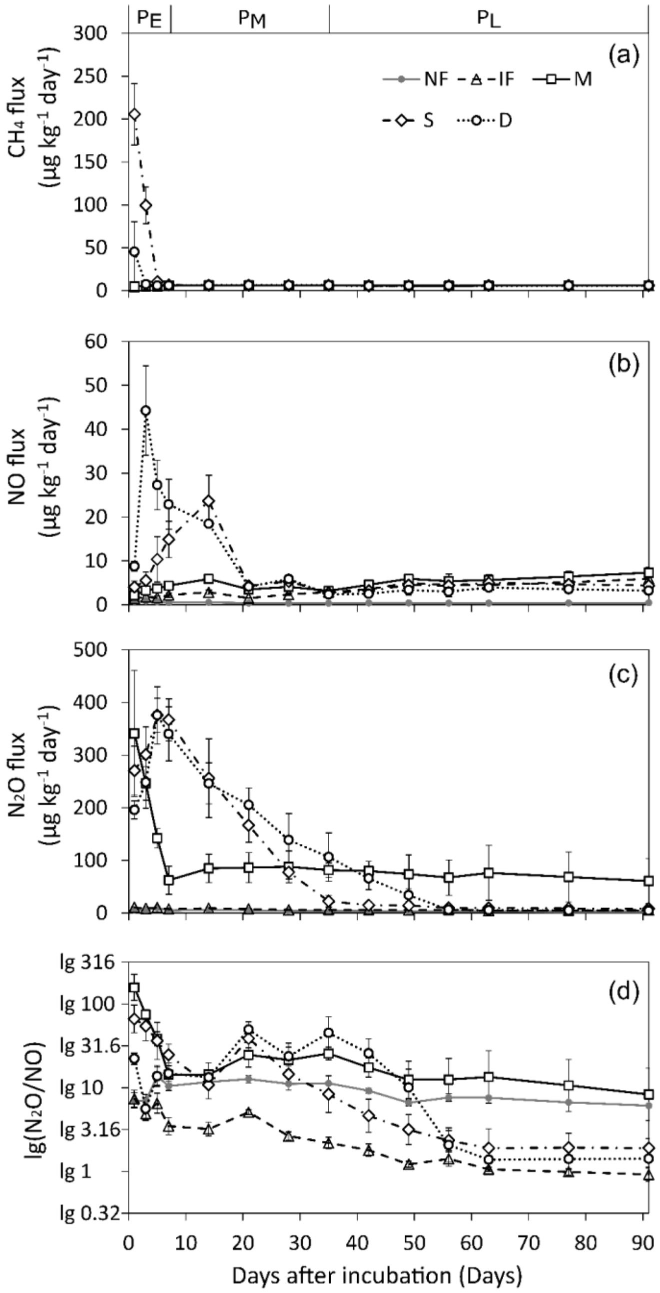

Fig. 4.8. Changes in CH_4 (a), NO (b), N_2O (c) flux and lg(N_2O/NO) (d) among all treatments during the incubation. Data represents means ± standard deviation (*n* = 3). P_E, P_M, P_L represent early period (Days 1-7), middle period (Days 8-35) and late period (Days 36-91). NF: No fertilizer; IF: Inorganic fertilizer; M: Compost manure; S: Raw slurry; D: Digestate.

The cumulative CH_4 emissions in the S treatment were significantly higher than those in the other treatments. In contrast, no significant differences were observed in cumulative N_2O or NO emissions among the organic fertilizer treatments (Table 4.5).

Table 4.5. Cumulative emissions of CH_4, N_2O and NO under different treatments after the incubation

	NF	IF	M	S	D
CH_4 (mg kg^{-1})	0.54 ± 0.02 b	0.53 ± 0.00 b	0.53 ± 0.03 b	1.13 ± 0.09 a	0.61 ± 0.07 b
NO (mg kg^{-1})	0.04 ± 0.00 b	0.32 ± 0.02 b	0.45 ± 0.05 a	0.62 ± 0.05 a	0.70 ± 0.11 a
N_2O (mg kg^{-1})	0.37 ± 0.10 b	0.59 ± 0.34 b	7.86 ± 2.51 a	8.48 ± 0.20 a	9.79 ± 1.75 a

Values represent means ±standard deviation (n=3). Different lowercase letters indicate the significant difference between treatments (p<0.05).

In all organic fertilizer treatments, the soil pH initially increased, followed by a decline during the incubation period. However, the extent of pH elevation was lower in M than in S and D, and the pH in M was significantly lower than that in S and D during P_L (Fig. 4.9a, Table 4.3). Both EC and NO_3^--N concentrations exhibited a general increasing trend across the organic fertilizer treatments, whereas both parameters in M entered a plateau phase during the P_L (Fig. 4.9b, 4.9c). In contrast, NH_4^+-N concentrations followed a rise–fall pattern in all organic treatments, while the decline in M was notably slower than that in S and D. As a result, the NH_4^+-N concentrations remained significantly higher in M treatment during both P_M and P_L (Fig. 4.9d, Table 4.3).

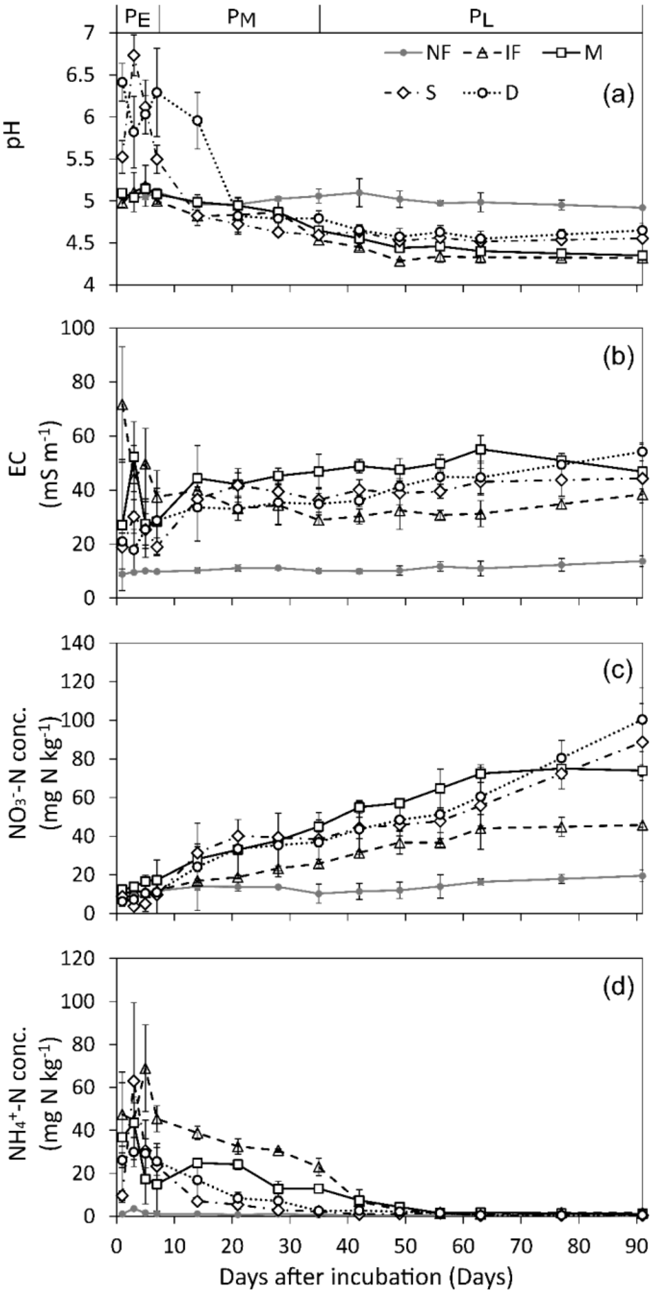

Fig. 4.9. Changes in pH (a), EC (b), nitrate nitrogen (NO_3^--N) concentration (c), ammonium nitrogen (NH_4^+-N) concentration (d) among all treatments during the incubation. Data represents means ± standard deviation (*n* = 3). P_E, P_M, P_L represent early period (Days 1-7), middle period (Days 8-35) and late period (Days 36-91). NF: No fertilizer; IF: Inorganic fertilizer; M: Compost manure; S: Raw slurry; D: Digestate.

4.3.4 Correlation structure and multivariate drivers of carbon flux and retention

A correlation network was constructed with CO_2 flux designated as the focal node to explore its association with soil properties and other gas fluxes (Fig. 4.10). Compare to the correlations in NF and IF, the CO_2 flux exhibited consistent and relatively strong correlations with pH and NH_4^+-N and NO_3^--N concentrations in organic fertilizer treatments, forming a stable core module. Among three organic fertilizer treatments, the overall network connectivity in M appeared weaker, with reduced edge strength and fewer secondary associations. Variations were also observed in the gas-related nodes: the CH_4 flux was disconnected in M, whereas the NO flux and NO/N_2O were unlinked in S and D, respectively. Notably, the correlation between CO_2 and NO fluxes was negative in M ($r = -0.76, p < 0.05$) but positive in D ($r = 0.77, p < 0.05$). While the second-order linkages of the three core soil variables remained largely consistent across treatments, the NO and N_2O correlations differed in sign between M ($r = -0.75$, $p < 0.05$) and D ($r = 0.77$, $p < 0.05$), indicating treatment-specific patterns in nitrogenous gas co-variation.

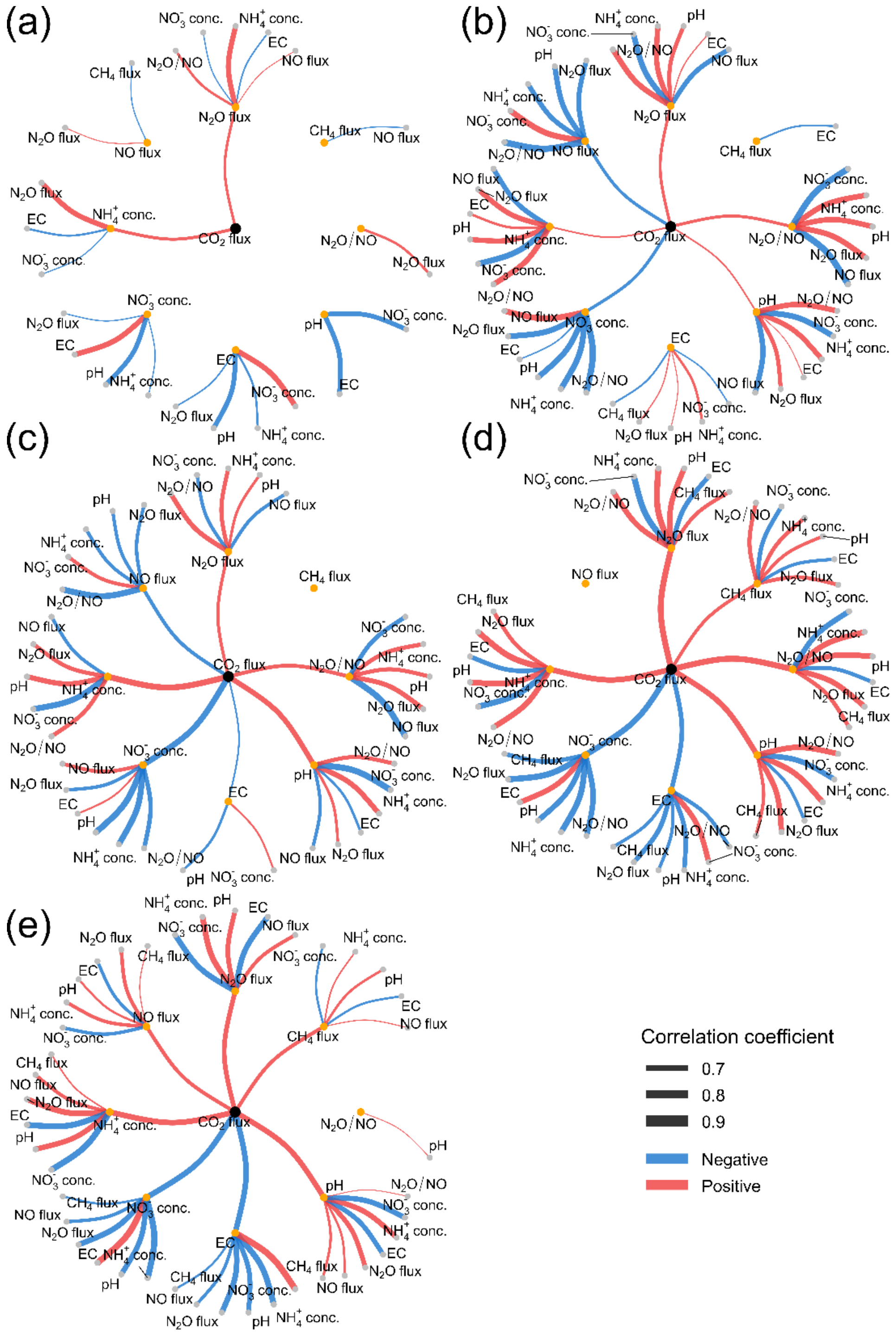

Fig. 4.10. Correlation coefficient networks of gas and soil properties factors to the CO_2 flux under NF: No fertilizer (a); IF: Inorganic fertilizer (b); M: Compost manure (c), S: Raw slurry (d) and D: Digestate treatment (e). Edges represent significant correlations ($p < 0.05$).

The RDA results after removing highly collinear variables (cumulative NO emissions, EC change, WSOC change, and MBC change) are shown in Fig. 4.11. RDA1 and RDA2 explained 86.2% and 11.6% of the total variance, respectively. Sample point D was mainly distributed in the first quadrant and was clearly separated from those of M and S, which clustered in the fourth quadrant. The CDP and CBE vectors were oriented in similar directions. SOC showed a significant positive correlation with CDP ($r = 0.68$, $p < 0.05$), whereas cumulative CO_2 emissions were not significantly correlated with either CDP or CBE. Among the explanatory variables, changes in NO_3^--N concentration and cumulative N_2O emissions were the strongest drivers of the CBE and CDP, as well as their component variables within the RDA space.

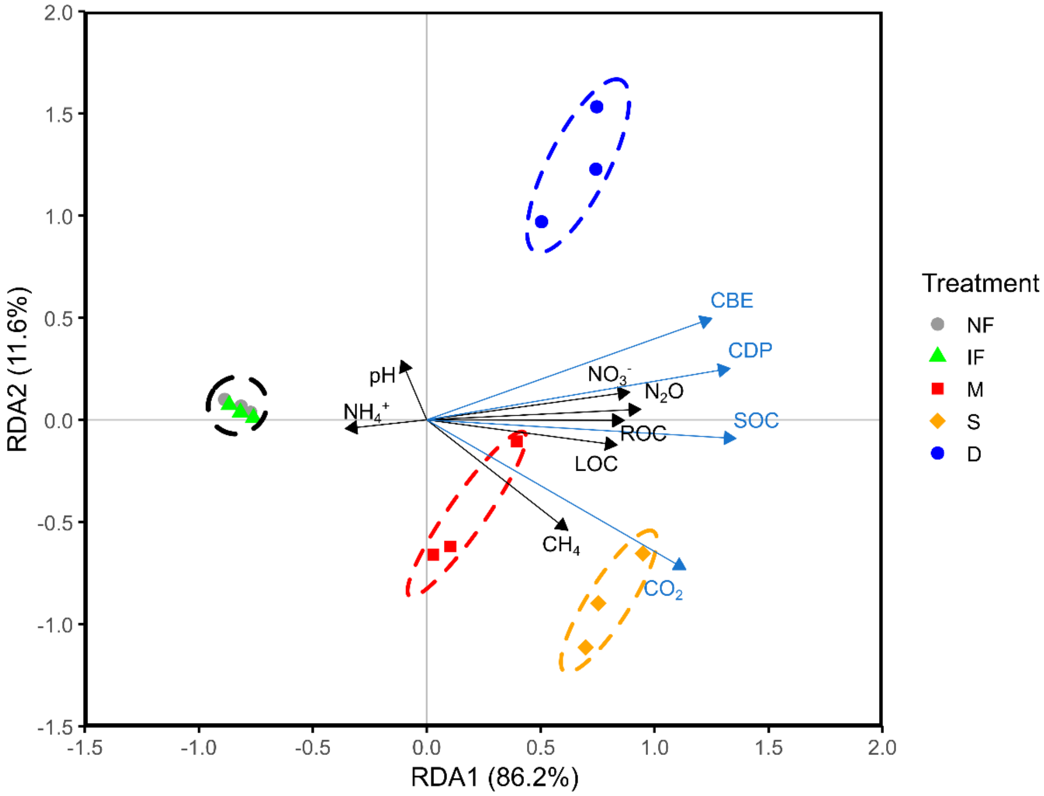

Fig. 4.11. Redundancy analysis (RDA) of the CDP, CBE, SOC change, cumulative CO_2 emissions and gas, soil properties factors. CDP: Carbon Decomposition Progress; CBE: Carbon Balance Efficiency; SOC, LOC, ROC: changes in soil organic carbon, labile organic carbon and recalcitrant organic carbon before and after incubation; CO_2, CH_4, N_2O: cumulative gas emissions after the incubation; pH, NO_3^-, NH_4^+: changes in pH, nitrate nitrogen (NO_3^--N) conc. and ammonium nitrogen (NH_4^+-N) conc. before and after incubation). NF: No fertilizer; IF: Inorganic fertilizer; M: Compost manure; S: Raw slurry; D: Digestate.

4.3.5 Field-scale SOC change

The field-scale SOC changes were calculated using the SOC concentrations obtained from each treatment after the incubation experiment in combination with the field soil bulk density (Fig. 4.12). The estimated field-scale SOC changes for organic fertilizer treatments ranged between 3.09 and 4.80 Mg ha^{-1}.

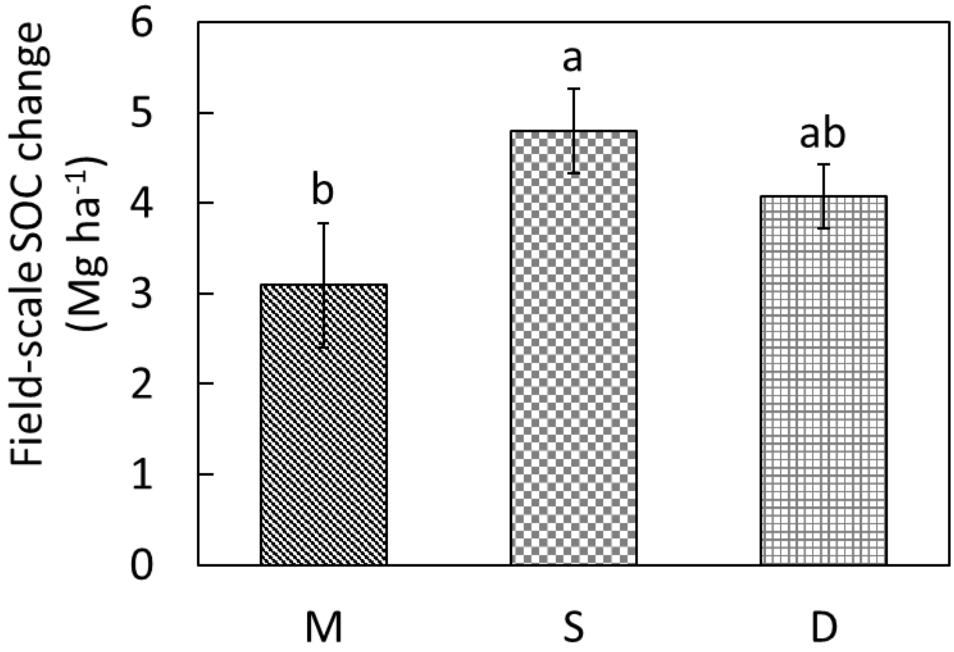

Fig. 4.12. Field-scale SOC changes in different organic fertilizer treatments. The error bars show the standard deviation (n = 3). Different letters indicate significant differences among treatments at $p < 0.05$. M: Compost manure; S: Raw slurry; D: Digestate.

4.4 Discussion

Although the application of organic fertilizers is widely recognized for its positive impact on SOC (Maillard and Angers, 2014; Zhong et al., 2010), and this study consistently confirmed such effects (Fig. 4), distinct differences in carbon dynamics were observed among the fertilizer types. These differences were evident not only in cumulative CO_2 emissions and SOC, but also in changes in soil properties and the fluxes of other related gases. Of the three initial hypotheses, only the second was supported by the results, which predicted that the digestate would produce less CO_2 than the raw slurry, owing to its reduced carbon content (Fig.2). In contrast, the first hypothesis regarding the lower emissions of CO_2 in M was not confirmed, and SOC accumulation did not increase in direct proportion to carbon input, in contrast to the third hypothesis. To better interpret these divergent patterns, the following sections discuss the treatment-specific responses, possible mechanisms, and implications for fertilizer management.

4.4.1 Compost manure treatment: Limited carbon transformation and soil feedback responses

Among all organic fertilizer treatments, despite having the highest carbon input (5.63 mg g^{-1}), the cumulative CO_2 emissions at the end of the incubation in M were significantly lower than those in S (Fig. 4.5). This observation is consistent with previous studies. Impraim et al. (2022) reported that CO_2 emissions from compost-treated soils were significantly lower than those from raw-manure treated soils in a 40-days incubation period. Liyanage et al. (2021) found that compost-amended soils emitted less CO_2 than soils amended with green manure or tea waste, regardless of the initial carbon concentration. Such low emissions are often attributed to the high proportion of stabilized carbon in the compost, which is less accessible for microbial decomposition (Bhogal et al., 2016; Holatko et al., 2022). However, this mechanism does not fully explain the results observed in M. At the end of the incubation period, the ROC content in M was not significantly higher than that in N (Fig. 4.6). And, among the three organic fertilizer treatments, it exhibited the lowest trend. In addition, the SOC content in M was the lowest among the organic treatments and was significantly lower than that in S, whereas the carbon application rate was almost similar in these treatments. These findings suggest that the supposedly stable carbon in compost did not accumulate in the soil as expected, raising the possibility that a portion of the applied carbon was neither mineralized nor retained. This interpretation is further supported by the CDP results. In M, only 51.6% of the applied carbon was converted into either SOC or CO_2 by the end of the incubation, significantly lower than CDP in S and D (Table 4.4). This proportion is consistent with the results reported by San-Emeterio et al. (2023), who observed that approximately 60% of compost-derived carbon was released over a 6-month incubation. The results of low mineralization and low accumulation in M suggest that carbon transformation in compost may be constrained by additional limiting factors.

Microbial respiration and nitrification are typically regulated by the availability of labile carbon and ammonium, with rapid substrate turnover driving the simultaneous emissions of CO_2 and NO (He et al., 2020; Liu and Greaver, 2010). However, in this study, the NO emissions showed no distinct peaks for either M or IF, whereas peaks were recorded in S and D (Fig. 4.8b). This pattern, together with the significant negative correlation between CO_2 and NO fluxes in M (Fig. 8a), indicates that organic amendments in manure did not induce a coupled enhancement of microbial respiration and nitrogen transformation compared to raw slurry and digestate. Nitrogen limitation is unlikely to explain this decoupling, as evidenced by the relatively higher inorganic nitrogen input in M (Fig. 4.3) and its significantly elevated NO_3^--N and comparable NH_4^+-N concentrations during P_E compared to S and D (Table 4.3). Instead, the absence of coupled CO_2 and NO responses is more likely attributable to limited microbial accessibility to compost-derived carbon. Although previous studies have reported that the addition of mineral nitrogen can enhance the microbial utilization of organic substrates (Milkereit et al., 2025; Wu et al., 2025), such effects appeared limited in M despite its substantial inorganic nitrogen input

(Fig. 4.3). This observation suggests that the absence of coupling was not solely due to substrate recalcitrance but was more likely driven by spatially heterogeneous microenvironments, such as compost aggregates in M. In contrast, the raw slurry and digestate were more homogeneous and contained readily available organic substrates, which may have facilitated concurrent microbial processes. This hypothesis was further supported by the patterns of N_2O emissions and the N_2O/NO, which are often used as indicators of the relative contribution of nitrification to denitrification (Bouwman et al., 2002; Li et al., 2015; Liu et al., 2017). N_2O flux in M remained consistently above 50 μg kg^{-1} day^{-1} throughout the incubation, and the N_2O/NO exceeded 100 on day 1 (Fig. 4.8), indicating a denitrification-dominated environment. Notably, N_2O/NO in M showed a steady decline throughout the incubation period, and the total CH_4 emissions did not differ from those in NF (Fig. 4.8d, Table 4.5). This suggests that the overall environment did not reach a sufficiently anaerobic state to induce significant CH_4 emissions, and that the anaerobic microsites may have gradually dissipated or that oxygen diffusion conditions improved over time.

The potential presence of anaerobic microenvironments in M was also reflected in the changes in soil properties. During P_E, the pH in M increased only slightly and did not differ significantly from that in NF (Table 4.3). This response contrasts with previous studies on compost application in field or pot experiments, where composts from various sources significantly raised soil pH by 0.5 to 1.5 units (Ding et al., 2021; Liu et al., 2023). Such discrepancies may be attributed to the slow disintegration of compost peas under the incubation conditions, which could have limited the release of alkaline components. At the end of incubation, soil pH in M was significantly lower than that in the other treatments, potentially indicating the gradual accumulation of acidic metabolites produced by anaerobic processes such as denitrification, which eventually exceeded the pH buffering capacity of the soil. The correlation network analysis further highlighted the distinct response characteristics of the soil system in M. Compared with S and D, the correlation network in M exhibited weaker first-order linkages between CO_2 flux and soil properties, as well as fewer second-order connections among the soil variables themselves (Fig. 4.10). This suggests a lack of coordinated response to external perturbations in the soil system. Such a weakened feedback mechanism may result from the compartmentalization of biogeochemical processes under locally reducing conditions, which spatially decouple carbon decomposition, nitrogen transformation, and EC regulation.

Although the CDP and CBE in M were relatively low in this study, whether this implies a greater potential for long-term SOC accumulation remains uncertain and requires further investigation. Previous studies have suggested that when compost is incorporated into the soil, its soluble organic compounds can rapidly bind to mineral surfaces, forming protective coatings that limit subsequent microbial access and decomposition (Dijkstra and Keitel, 2024). Under such conditions, although early microbial activity may be stimulated by a priming effect, the lack of a continuous carbon supply could drive microbes to decompose native soil organic matter, thereby offsetting the positive effects of compost on SOC accumulation. Long-term compost application often results in elevated fungal activity. This enhances the fungal breakdown of cellulose into low-molecular-weight oligosaccharides, which, in turn, promotes the activity of gram-negative bacteria. These bacteria typically exhibit low carbon-use efficiency, resulting in greater carbon loss and reduced carbon retention in the soil (Miao et al., 2021). Moreover, the lowest pH at the end of the incubation period and consistently elevated N_2O emissions were observed in treatment M. These findings suggest that in practical applications, the risks of soil acidification and increased greenhouse gas emissions associated with compost use should be carefully considered.

4.4.2 Digestate versus raw slurry: Higher carbon-balance efficiency with comparable soil dynamics

Compared with the significantly lower CDP in M, CDP values in both S and D were above 80 % by the end of incubation, and the difference between them was not significant (Table 4.4). This finding indicates that almost all the applied carbon in raw slurry and digestate was converted into either CO_2 or SOC. Nevertheless, despite the much higher carbon input in S, the final SOC content and its fractions did not differ significantly from those in D (Fig. 4.6 and 4.7). Moreover, CBE was significantly higher in D than in S, whereas CBE in S did not differ from that in M (Table 4.4). This discrepancy was mainly attributed to CO_2 emissions, as the cumulative CO_2 flux in S was significantly higher than that in D throughout the incubation period (Fig. 4.4, Table 4.3). This pattern can be linked to the distinct anaerobic digestion process and substrate composition of the two materials. During anaerobic digestion, readily degradable carbon is consumed first, leaving the digestate enriched in semi-degradable components, such as soluble proteins or cellulose, which are less available for microbial mineralization (Lamolinara et al., 2022; van Midden et al., 2024; Zhong et al., 2011). This is also reflected by the slightly higher OM:TC ratio of the digestate (1.66) compared to that of the raw slurry (1.57), indicating a higher proportion of non-carbon components per unit carbon in digestate-derived organic matter (Table 4.2). Notably, despite the lower C:N ratio of digestate than raw slurry (Table 4.2), the condition that, in theory, should enhance microbial activity and accelerate carbon mineralization (Chen et al., 2014; Lv et al., 2018) was not observed. Previous studies have reported similar results; digestate application can induce negative priming effects and promote SOC stabilization (S. H. Villarino et al., 2025). Furthermore, digestate C:N has been positively correlated with CO_2 emissions because a higher C:N stimulates fungal activity, thereby increasing CO_2 release (Barduca et al., 2021). These observations suggest that the SOC enhancement efficiency was higher in D owing to its more stable carbon composition and reduced carbon loss despite the smaller carbon input. In contrast, the large carbon input in S was not effectively retained as SOC, reflecting a lower carbon-use efficiency.

Although contrasting SOC enhancement efficiencies were observed between in S and D, the soil physicochemical responses were largely similar. No significant differences were observed in the temporal dynamics of soil properties between the two treatments. In the correlation network, the CO_2 flux maintained strong first- and second-order relationships with the key soil variables. This indicates a well-coupled relationship between carbon processes and the soil environment, which is distinct from the loosely structured network in M (Fig. 4.9 and 4.10). However, the differences in gas emissions were still evident. During P_E, a distinct CH_4 emission peak was observed, and the cumulative CH_4 emissions were significantly higher than those in D. In contrast, no significant CH_4 peak was observed in D and its cumulative CH_4 emissions were comparable to those in NF. Methanotrophs inhibit agricultural soils (Singla and Inubushi, 2014; Walling and Vaneeckhaute, 2020), and CH_4 fluxes typically peak on the day of organic fertilizer application (Czubaszek and Wysocka-Czubaszek, 2018). The occurrence of CH_4 peaks in both treatments, regardless of magnitude, suggests that the

CH_4 concentrations exceeded the threshold for microbial oxidation at that time. The absence of an insignificant peak in D might be attributed to the higher availability of nitrogen in the digestate, which could stimulate the activity of methanotrophs and suppress CH_4 emissions (Egene et al., 2022). In addition, the NO peak in D occurred during P_E, earlier than that in S. This implies that nitrification in D responded more rapidly to increased nitrogen availability (Egene et al., 2022; Foereid et al., 2021). These gas flux differences reinforce the view that the digestate led to smaller transient carbon losses, thus achieving a higher carbon balance efficiency than the slurry despite their overall similar soil responses. Nevertheless, small fluctuations in the N_2O/NO during P_M in D suggest a potential risk of intensified denitrification following digestate application (Badagliacca et al., 2024; Zilio et al., 2023).

A meta-analysis integrating 17 different studies on digestate application reported that approximately 68% of the carbon in digestate remains relatively stable in soil with a mean residence time of 1.2 years (Andrade Díaz et al., 2024). This value was slightly lower than the CBE observed in D in the present study (74.24%). However, during the P_L, the CO_2 flux in S and D remained significantly higher than that in NF or IF (Table 4.3), suggesting that the CBE may continue to decline after the incubation period. However, results from long-term incubation experiments have consistently indicated that digestate achieves a higher carbon retention efficiency than raw slurry (Thomsen et al., 2013). Field conditions, however, are governed by interacting factors, such as temperature, soil moisture, and precipitation, which make organic matter decomposition and SOC stabilization markedly more complex than under controlled incubation. Several field trials have reported markedly lower carbon retention efficiencies for both digestate and raw slurry (Liang et al., 2021; Villarino et al., 2025). Therefore, despite the favorable short-term results observed in the present study, additional long-term field studies are essential before the carbon sequestration potential of digestates can be confirmed for practical agricultural applications.

4.4.3 Decomposition pathways and nutrient couplings: Re-examining carbon retention indicators

The amounts of retained SOC and CO_2 emissions (mineralization) are commonly regarded as direct indicators of fertilizer performance (Khalsa et al., 2020; Li et al., 2018; Yang et al., 2021). However, when the biochemical composition or decomposition environment of materials differs substantially, endpoint measurements alone may be insufficient to elucidate the underlying transformation trajectories. In the present study, limited carbon release and modest SOC accumulation occurred in M. This outcome was attributed not only to the relatively stable carbon composition of compost manure but also to the slow-disintegrating physical structure: large compost particles tend to have limited contact with the surrounding soil, thereby restricting microbial mineralization (Dijkstra and Keitel, 2024). Therefore, increased focus should be directed toward decomposition trajectories and nutrient release kinetics determined by the origin and structural characteristics of the material when comparing different types of organic amendments.

Although soil carbon and nitrogen cycles are generally tightly coupled under natural conditions (Hendricks et al., 2022; Nazir et al., 2024), the addition of organic fertilizers can potentially alter or disrupt this relationship. In the present study, CO_2 emissions and SOC content were primarily explained by the levels of ROC and LOC changes and CH_4 emissions, whereas nitrogen-related variables showed low explanatory power (Fig. 4.11). This suggests that short-term changes in carbon dynamics depend more on the intrinsic characteristics of the carbon pool. In contrast, soil nitrogen dynamics exhibited relatively stronger loadings for CBE and CDP, which are two key indices for evaluating the carbon performance of organic materials. This indicates that nitrogen-related processes should be considered when assessing the SOC enhancement potential of different amendments.

4.5 Conclusion

This study evaluated the effects of compost manure, raw slurry, and digestate on soil carbon dynamics from the perspectives of decomposition kinetics and soil feedback. All three organic fertilizers promoted SOC accumulation; however, the CBE varied depending on the material properties. Compost manure application induced localized anaerobic microsites, which led to the partial decoupling of carbon and nitrogen processes at the bulk soil scale, thereby limiting both CDP and SOC accumulation and ultimately resulting in the lowest CBE. In contrast, raw slurry and digestate exhibited comparable CDP at the end of incubation, whereas the digestate achieved a higher CBE with a lower carbon input, suggesting that anaerobic digestion can enhance carbon use efficiency and mitigate immediate carbon mineralization losses. Moreover, the dynamics of soil nitrate, ammonium, and N_2O emissions explained variations in CDP and CBE more effectively than the SOC fractions, highlighting the key regulatory role of nitrogen dynamics in shaping the carbon balance. Overall, the combined evaluation of decomposition rates and soil feedback provided a more robust assessment of the carbon sequestration potential of different organic fertilizers than considering the final SOC or CO_2 emissions alone. Given the variability in field temperature, moisture, and management practices, further assessments under diverse environmental conditions are necessary.

5. Enhanced Rock Weathering

5.1 Introduction

As mentioned in chapter 1, there are two approaches to reducing soil CO_2 emissions, broadly. The first involves reducing emissions at the source, such as suppressing microbial or root respiration. For instance, regulating soil moisture through irrigation was reported to inhibit microbial activity and thereby reduce CO_2 emissions (Zhong et al., 2021). The second approach involves reabsorbing the CO_2 that has already been produced and sequestering it back into the soil, effectively reducing net CO_2 emissions such as afforestation/reforestation and soil organic carbon sequestration (Fuss et al., 2018). Among these, enhanced rock weathering (ERW), as a method of CO_2 reabsorption and sequestration, has gained widespread attention in recent years as a viable CDR strategy.

ERW artificially crushes silicate rocks to increase their surface area, thereby enhancing their natural weathering processes to remove atmospheric CO_2 (Beerling et al., 2020; Strefler et al., 2018). Briefly, dissolution of silicate minerals releases cations, converting dissolved CO_2 into bicarbonate (HCO_3^-) and under some conditions forming secondary minerals or dissolved silica. HCO_3^- either precipitates as calcium carbonate or leaches through the soil into the global water system, eventually discharging into the oceans (Berg and Banwart, 2000; Hartmann et al., 2013). Once in the ocean, HCO_3^- acts as a carbon sink, increasing the ocean alkalinity and counteracting ocean acidification (Gore et al., 2019; Rau and Caldeira, 1999). Therefore, understanding the carbon cycle in farmlands is essential to evaluate the effects of ERW on soil–plant ecosystems. However, many studies on the potential of ERW to reduce CO_2 emissions have been based on calculations of changes in metal ions or soil carbon (Beerling et al., 2020; Lefebvre et al., 2019; Lewis et al., 2021). Owing to the complexity and variability of field environments and complexity of CO_2 measurements (Leuning et al., 2008; Zhou et al., 2021), direct proof of CO_2 emission reduction by ERW in agricultural fields remains limited, highlighting the need for field experiments.

ERW not only sequesters atmospheric CO_2 via weathering but also releases metal ions, such as Ca, Mg, and K, providing mineral nutrients to crops (Hartmann et al., 2013; Jariwala et al., 2022). Release of HCO_3^- and Si via mineral weathering reduces soil Al toxicity and improves the soil pH (Elisa et al., 2016; Patrícia Vieira da Cunha et al., 2008). However, changes in soil properties resulting from these processes can enhance microbial activity, thereby increasing the soil CO_2 emissions. Borges et al. (2019) reported that increased soil silicate concentrations related to higher phosphorus availability lead to elevated CO_2 emissions. Dietzen et al. (2018) indicated that silicate mineral application increases soil pH to a level sufficient to overcome aluminum toxicity, without any significant difference in the cumulative net CO_2 flux between olivine-amended and control soils. Therefore, exploring the impact of ERW on soil properties, such as soil pH and moisture, is essential to evaluate its CO_2 removal potential as changes in these soil properties alter the activity of soil microorganisms and plant root systems. Moreover, differences in the properties of rhizosphere and non-rhizosphere soils cannot be ignored in weathering processes as root exudates affect the soil structural stability, water retention capacity, and microbial community composition (Fu et al., 2022; Kobierski et al., 2018). Partial pressure of CO_2 in rhizosphere soil is higher than that in non-rhizosphere soil (Drigo et al., 2013; Hinsinger et al., 2009), implying that the weathering process in rhizosphere soil is more active than that in non-rhizosphere soil. To date, differences in the weathering processes in rhizosphere and non-rhizosphere soil conditions have not been thoroughly investigated.

Estimation of the net biome production (NBP) is important to assess the ecosystem carbon budget (Shimizu et al., 2009). Carbon flows into ecosystems primarily from plant photosynthates, which are converted into organic matter. This organic matter is transported from the leaves to the roots, with a portion exuded into the rhizosphere. Conversely, carbon flow from ecosystems consists of CO_2 emissions from organic matter decomposition, artificial harvesting, and leaching. Carbon flow changes within the rhizosphere and non-rhizosphere soils induced by ERW must be accounted for in ecosystems treated with rock powder. Evaluating the carbon budget of farmland ecosystems using ERW via direct measurement of carbon flow may yield results different from those of previous reports using soil carbon changes as the only evaluation method (Guo et al., 2023b; Kantola et al., 2023).

This study aimed to quantify the influence of basalt rock powder addition on soil carbon emission from rhizosphere and non-rhizosphere soils and determine the main driving factors for these effects. Furthermore, we clarified and compared the carbon budgets of fields with and without rocks. It was hypothesized that the application of basalt rock powder decreases soil carbon loss by absorbing atmospheric CO_2 via mineral weathering and producing bicarbonate ions in the rhizosphere and non-rhizosphere soils, thereby improving the field carbon budget.

5.2 Materials and methods

5.2.1 Site description

The study was conducted at the Experimental Farm of the Field Science Center for Northern Biosphere, Hokkaido University (Sapporo, Hokkaido, Japan; 43°04'17.4" N 141°20'24.6" E) in 2023. The experimental site had a humid continental climate characterized by cold winters and warm summers, without apparent wet or dry seasons. The annual precipitation at the study site was approximately 1146 mm, and the mean annual temperature was 9.2℃. The highest daily temperatures were observed in August, averaging 26.4℃, whereas the lowest daily temperatures were observed in January, averaging –6.4℃. The snow cover period generally lasted from December to March of the following year.

5.2.2 Experimental settings

In this study, two treatment plots were designed, one without (NB) and one with (B) basalt application, each with three replicates. Soybean (*Glycine max* (L.) Merr.) cultivar Yukihomare was used in this study. The size of each plot was 15.4 m^2 (4.4 m × 3.5 m) with a buffer zone between the plots. A non-crop area of 4.4 m × 1 m was established in the southern part of each plot to measure CO_2 emissions without root respiration, representative images of each treatment plot (comprising six plots) are provided in Fig. 5.1.

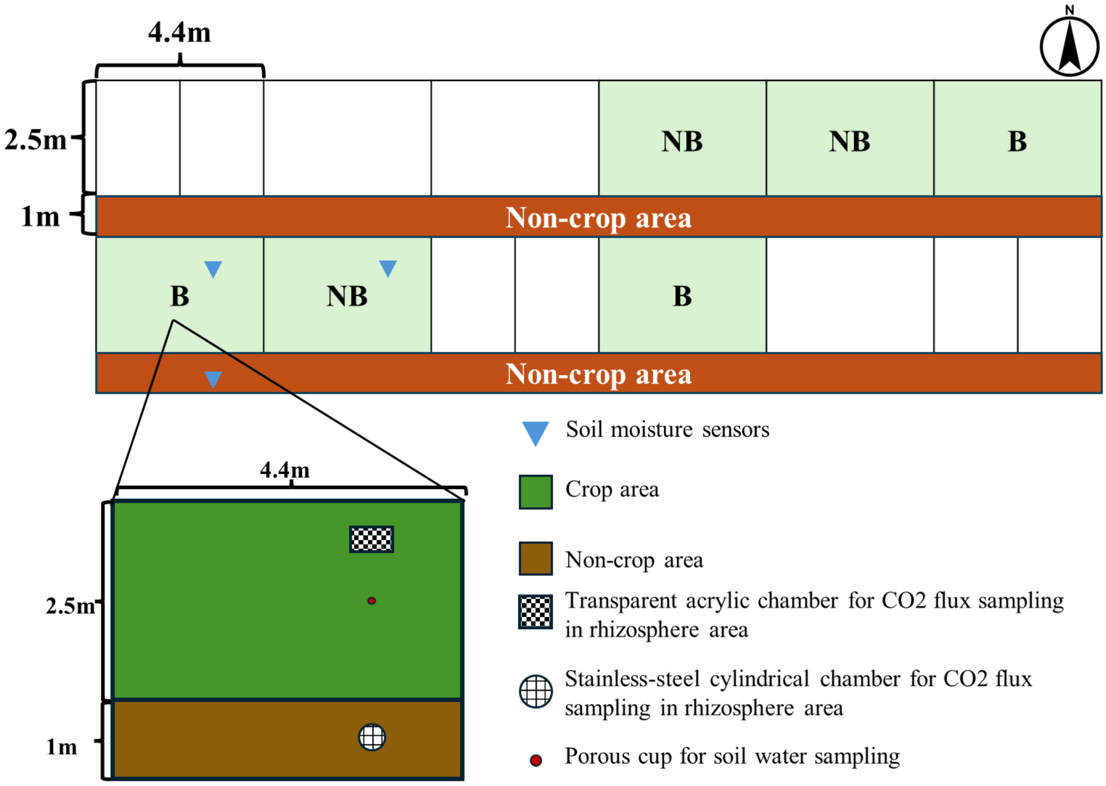

Fig. 5.1. Images of experimental settings. B: Basalt application; NB: No basalt application.

Soybeans were planted in the crop-growing area at a density of approximately 7.27 plants per square meter. On May 19th, based on the bulk density of the 20-cm soil layer, 9.52% of the soil weight (150 t ha^{-1}) of basalt powder was evenly applied to the B treatment plot and then thoroughly mixed with the 0–20 cm soil layer through tillage. The reasons for applying basalt at 9.52 wt% are that previous studies have reported that applying basalt at 20 wt% can reduce crop yield, whereas no adverse effects on crop yield have been reported for the application of basalt at 10 wt% (Haque et al., 2020). To ensure consistency and maximize experimental outcomes, the maximum allowable application rate of basalt was chosen for the field experiment. The rock mass ratio with particle size less than the value reached 80% of the basalt powder (P80) was 57.66 μm and the detailed concentrations of mineral composition are provided in Table 5.1.

Table 5.1. Mineral composition of basalt rock.

Mineral	Concentration	S.D.	Unit	Mineral	Concentration	S.D.	Unit
P_2O_5	0.197	0.001	%	Nb	3.54	0.4	μg g^{-1}
Na_2O	3.82	0.05	%	Mo	0.205	0	μg g^{-1}
MgO	5.06	0.016	%	Ru	1.53	0.48	μg g^{-1}
Al_2O_3	13.13	0.01	%	Rh	0	0	μg g^{-1}
SiO_2	56.32	0.02	%	Pd	1.59	0.45	μg g^{-1}
SO_3	5.04E-05	0	%	Ag	1.44	0.49	μg g^{-1}
Cl	6.58E-03	7.30E-05	%	Cd	0.205	0	μg g^{-1}
K_2O	0.269	0.0009	%	In	0.305	0	μg g^{-1}
CaO	7.74	0.004	%	Sn	1.63	0.85	μg g^{-1}
Ti	4874	6	μg g^{-1}	Sb	0.405	0	μg g^{-1}
V	254	2	μg g^{-1}	Te	0.505	0	μg g^{-1}
Cr	44.3	0.59	μg g^{-1}	I	0.605	0	μg g^{-1}
MnO	1412	2	μg g^{-1}	Cs	0.805	0	μg g^{-1}
Fe_2O_3	9.29	0.004	%	Ba	117	6.7	μg g^{-1}
Co	1.01	0	μg g^{-1}	La	1.51	0	μg g^{-1}
Ni	11.1	0.33	μg g^{-1}	Ce	1.51	0	μg g^{-1}
Cu	26.1	0.46	μg g^{-1}	Hf	5.04	1.5	μg g^{-1}
Zn	61.9	0.55	μg g^{-1}	Ta	0.805	0	μg g^{-1}
Ga	13.7	0.26	μg g^{-1}	W	0.505	0.15	μg g^{-1}
As	0.205	0	μg g^{-1}	Au	2.03	1.4	μg g^{-1}
Se	0.105	0	μg g^{-1}	Hg	3.77	1.4	μg g^{-1}
Rb	11.2	0.28	μg g^{-1}	Tl	0.205	0	μg g^{-1}
Sr	184	0.4	μg g^{-1}	Pb	7.38	0.4	μg g^{-1}
Y	21.2	0.2	μg g^{-1}	Bi	0.305	0	μg g^{-1}
Br	0.205	0	μg g^{-1}	Th	0.305	0	μg g^{-1}
Zr	56.45	0.37	μg/g	U	0.305	0.12	μg/g

On May 24th, fertilizers were applied in the forms of $(NH_4)H_2PO_4$ and K_2SO_4 at rates of 178.17 and 148.09 kg ha^{-1}, respectively, followed by another round of tillage to incorporate them into the 0–20 cm soil layer. Sowing was performed on June 1st. After sowing, to prevent birds from damaging the seeds, a fiber bird net covered the entire crop-growing area until June 17th. The thinning was performed on June 22th. Harvesting was conducted on September 21th, which was also the end of the measurement period.

To compare the differences between the measured parameters in the two treatment areas during specific growth stages of soybeans, the entire measurement period was divided into five intervals according to the growth stages of soybeans: S0, S1, S2, S3, and S4, representing before sowing (May 22nd to May 31st), the vegetative stage (June 1st to July 13th), the flowering stage (July 14th to July 31th), the pod-filling stage (August 1st August 21st), and the maturity stage (August 22nd to September 21st).

5.2.3 Measurement of CO_2 flux

The CO_2 flux was measured in both the non-crop area described as F_{CO2} and the crop area representing net ecosystem exchange (NEE) using the static closed chamber method (Shimizu et al., 2009). An example of the CO_2 flow in a crop or non-crop area is shown in Fig. 5.2.

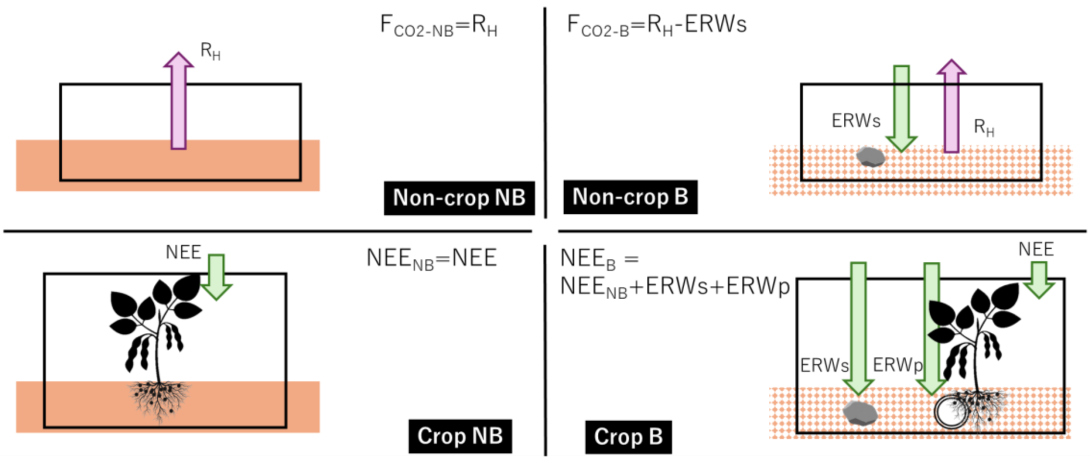

Fig. 5.2. Examples of CO_2 flow in B and NB in the crop and non-crop areas. R_H: heterotrophic respiration, NEE: net ecosystem exchange, $F_{CO2\text{-}NB}$: CO_2 flux in non-rhizosphere soil in NB, $F_{CO2\text{-}B}$: CO_2 flux in non-rhizosphere soil in B, NEE_{NB}: CO_2 flux in rhizosphere soil in NB, NEE_B: CO_2 flux in rhizosphere soil in B, ERWs: ERW-induced CO_2 removal in non-rhizosphere soil, ERWp: ERW-induced CO_2 removal in rhizosphere soil.

In non-crop areas, CO_2 flux was measured every two days for one week after the application of basalt powder and fertilizers, and then every 7–15 days thereafter. To minimize the influence of diurnal temperature variation, measurements were taken between 8:00 AM and 11:00 AM on the measurement days. During the measurement, a stainless-steel cylindrical chamber with a diameter of 20 cm and height of 25 cm was placed on a chamber base that had been inserted 3 cm into the soil and leveled after tillage. (Fig. 5.3).

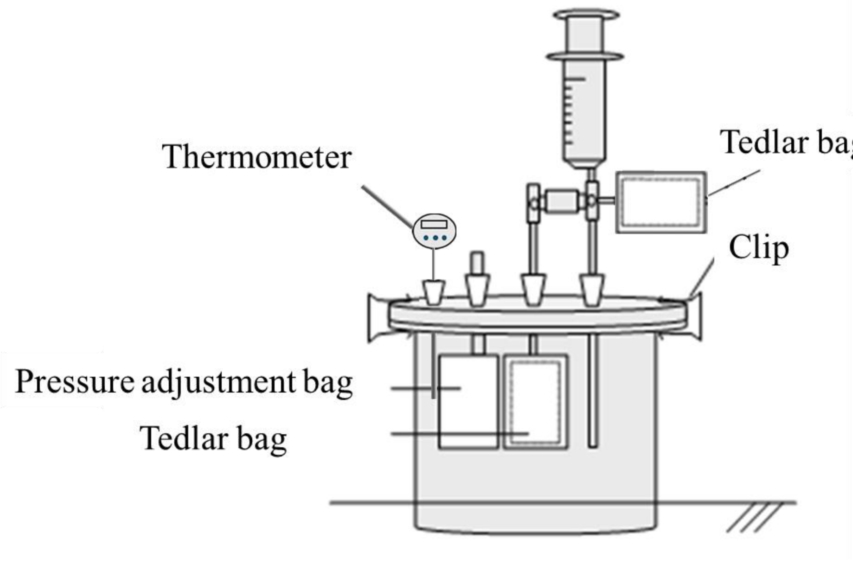

Fig. 5.3. Schematic diagram of the chamber setup in the non-crop area.

The gap between the chamber and the chamber base was sealed with water (Fig. 5.4).

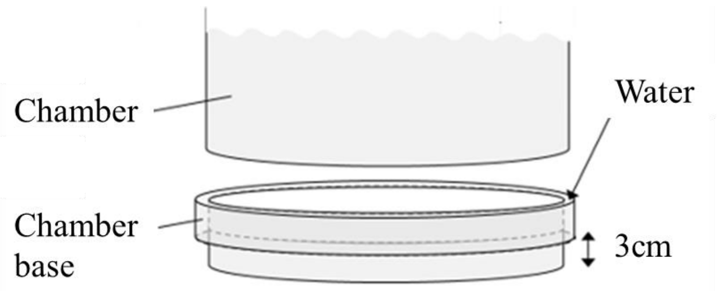

Fig. 5.4. Schematic diagram of the connection between the chamber and the chamber base.

Gas samples of approximately 300 mL were extracted from the chambers at 7, 17, and 27 min after setup and collected in Tedlar bags. The CO_2 concentration in the gas samples was analyzed using an infrared CO_2 gas analyzer described in Chapter 3. CO_2 flux was calculated using a three-point regression. In the crop-growing area, NEE was measured using the static closed chamber method, including soybean plants in the chamber. CO_2

flux measurements began on June 22nd, with a frequency of once every 7–15 days. The measurement times were the same as those for the non-crop areas. During the measurement, a transparent acrylic chamber (60 cm in length, 40 cm in width, and 55 cm in height) was placed on a chamber base set up after the removal of the bird net (Fig. 5.5). The gap between the chamber and chamber base was sealed with water.

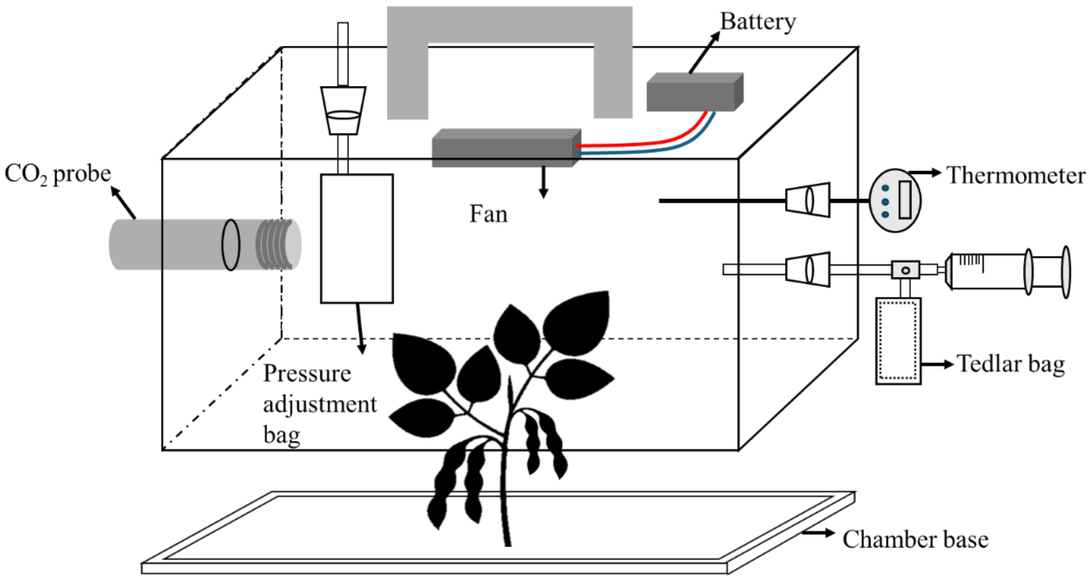

Fig. 5.5. Schematic diagram of the chamber setup in the crop area.

A CO_2 probe (GMP 343, Vaisala, Vantaa, Finland) was used to measure the CO_2 concentration inside the chamber every 15 seconds, and linear regression of the concentrations within the first 7 minutes after setup was used to calculate the CO_2 flux.

The CO_2 flux (kg CO_2 ha^{-1} day^{-1}) for the sampling day was calculated using Eq. 4.1.

$$f_{CO2} = \rho \times (\frac{V}{A}) \times (\frac{dC}{dt}) \times (\frac{273}{T}) \times \frac{M}{22.4} \quad \text{(Eq. 4. 5)}$$

where, ρ represents the CO_2 density (1.977 mg mL^{-1}), V is the gas volume of the chamber (mL), A is the base area of the chamber (cm^2), (dC/dt) is the rate of change in gas concentration per unit time (cm^3 cm^{-3} day^{-1}), T is the temperature measured by thermometer (°C), and M is the molar mass of CO_2 (44).

5.2.4 Soil physical and chemical properties

To assess the effects of basalt application on soil properties and to analyze the factors influencing CO_2 removal through weathering, we measured key soil properties at regular intervals to monitor changes over the investigation period. After fertilization and tillage, thermometers (TR-52, T&D, Nagano, Japan) were installed in the crop-growing area of each plot to continuously measure the soil temperature at a depth of 5 cm and to record data every hour. The soil volumetric water content (VWC) at a depth of 5 cm in the crop-growing area of the first replicates of NB and B (Fig. 5.1) was measured using soil moisture sensors (CDC-TEROS-12, Meter Japan, Saitama, Japan), and the data were recorded every hour. On each gas sampling day, the surface soil was collected at a depth of 5 cm (three samples for each plot), and the VWC was measured by creating a fitting curve between the VWC of the second and third replicates and the first replicate. This fitting curve, along with the sensor data from the first replicate, was used to estimate the hourly VWC changes for the second and third replicates.

During each gas sampling, surface soil at a depth of 5 cm (sampled at three points) from the crop-growing area was collected to analyze soil chemical properties, including pH, EC, NO_3^--N and NH_4^+-N concentrations, WSOC, and WSIC. The method of the analyzation is described in Chapter 3. The measurement methods for WSIC and WSOC are identical, since their values can be simultaneously determined using the TOC analyzer.

5.2.5 F_{CO2} and NEE models

Based on the data of CO_2 flux and corresponding soil property values at specific time points, to identify the hourly F_{CO2} and NEE, this study fitted models for them. For the F_{CO2} model, the soil temperature and soil moisture models mentioned by Suseela et al. (2012) (Eq. 5.1) was used.

$$F_{CO2} = a * exp\ (k * T) * [(\theta - \theta_{min})(\theta_{max} - \theta)]^b \qquad \text{(Eq. 5.1)}$$

where, a is the F_{CO2} when the soil temperature is 0°C, k and b are the sensitivity of F_{CO2} to soil temperature and soil moisture content, respectively. θ_{max} and θ_{min} are the maximum and minimum VWC during the investigation period, T is the soil temperature at a depth of 5 cm, and θ is VWC at a depth of 5 cm.

As NEE equals the CO_2 absorbed by plant photosynthesis (GPP: Gross Primary Production) minus the CO_2 emitted by ecosystem respiration (R_E: Ecosystem Respiration) (Shimizu et al., 2009), the models were fitted separately for GPP and R_E. The GPP was modeled using the photosynthetic light-response curves proposed by Ögren and Evans (1993) (Eq. 5.2), whereas R_E was modeled using the temperature calculation formula used by Flanagan and Johnson (2005) (Eq. 5.3). Thus, the calculation formula for the NEE was obtained (Eq. 5.4).

$$GPP = \frac{\phi I + m - \sqrt{(\phi I + m)^2 - 4\Theta\phi I m}}{2\Theta} \qquad \text{(Eq. 5. 2)}$$

$$R_E = a * exp\ (k * T) \qquad \text{(Eq. 5. 3)}$$

$$NEE = \frac{\phi I + m - \sqrt{(\phi I + m)^2 - 4\Theta\phi I m}}{2\Theta} - ae^{k*T} \qquad \text{(Eq. 5. 4)}$$

where, ϕ is the maximum quantum yield, m is the light-saturated photosynthetic rate (an asymptote), Θ is the convexity (set to 0.9 in this study), I is the hourly photosynthetic photon flux density (PFD) measured by a meteorological observation tower which was set up beside the field, a is the R_E when the soil temperature is 0°C, k is the sensitivity of R_E to soil temperature and T is the soil temperature at a depth of 5 cm.

Subsequently, $ERWs$ and $ERWp$, which represent CO_2 removal in the non-rhizosphere and rhizosphere soil were calculated using Eq. 5 and 6 (Fig. 5.2), respectively.

$$ERW_s = F_{CO2-NB} - F_{CO2-B} \qquad \text{(Eq. 5. 5)}$$

$$ERW_p = NEE_B - NEE_{NB} - ERW_s \qquad \text{(Eq. 5. 6)}$$

where, $F_{CO2\text{-}NB}$ and $F_{CO2\text{-}B}$ are the CO_2 flux in non-rhizosphere areas in NB and B treatments, respectively, and NEE_{NB} and NEE_B are the NEE in NB and B, respectively. Positive values indicate CO_2 removal and negative values indicate CO_2 emissions.

Cumulative amounts of F_{CO2}, NEE, $ERWs,$ and $ERWp$ were calculated by linear interpolation of the gas flux and fitted as follows:

$$Cumulative\ CO_2\ emission\ or\ abosorbtion = \sum(\frac{f_i+f_{i+1}}{2} * t) \qquad \text{(Eq. 5. 7)}$$

where, f_i is the fitted value of the i th CO_2 flux, and t is the time interval between two fitted values (1 h).

5.2.6 Net primary production (NPP) and carbon leaching (L)

On September 21th, four mature soybean plants were collected from each treatment area. The plants were separated into seeds, pods, stems, and roots. These parts were then dried at 70°C for 72 h, weighed, and subsequently ground into powder. The carbon content of each part was measured using an elemental analyzer (vario EL cube, Elementar Analysensysteme GmbH, Langenselbold, Germany). The NPP was calculated based on the dry weight and carbon concentration of each part.

The leaching of carbon is determined by the carbon concentration in the soil water and the hydrological conditions (precipitation and evapotranspiration). Soil water at a depth of 30 cm was collected monthly after a rainy event on June July 11th, August 27th, and September 15th using a porous cup at a pressure of 70 kPa generated by a negative pressure pump (DIK-3954, DAIKI, Saitama, Japan). The organic and inorganic carbon contents of the leachate were measured using a TOC analyzer. Evapotranspiration was calculated using the Penman equation as mentioned in Miura and Okuno, (1993) (Eq. 5.8).

$$ET_{pen} = \frac{\Delta}{\Delta+\gamma} * \frac{S}{l} + \frac{0.26\gamma\left(1+\frac{u_2}{100}\right)}{\Delta+\gamma} * (e_{sa} - e_a) \quad \text{(Eq. 5. 8)}$$

where, Δ represents the slope of the vapor pressure curve (mbar °C^{-1}), γ is the psychrometric constant (0.66 mbar °C^{-1}), S is the net solar radiation (MJ m^{-2}), l is the latent heat of vaporization of water (MJ kg^{-1}), u_2 is the wind speed at a height of 2 m (m s^{-1}), e_{sa} is the saturation vapor pressure (mbar), and e_a is the actual vapor pressure of the air (mbar). Environmental data, including wind speed, relative humidity, and air temperature, were observed using a meteorological tower set up next to the experimental field, while sunshine duration data were obtained from the Automated Meteorological Data Acquisition System (AMeDAS) located in Sapporo (43°03'38.01"N, 141°19'44.16"E).

Carbon leaching (L), including organic carbon leaching (OL) and inorganic carbon leaching (IL), was calculated as the product of the amount of percolating water and carbon concentration in the soil water. OL and IL were calculated using Eq. 5.9 and Eq. 5.10:

$$OL = \sum_{month} c_{OL} * max\,\{0, P - ET_{pen}\} \quad \text{(Eq. 5. 9)}$$

$$IL = \sum_{month} c_{IL} * max\,\{0, P - ET_{pen}\} \quad \text{(Eq. 5. 10)}$$

where, c_{OL} and c_{IL} are the concentration of organic carbon and inorganic carbon in the soil water, and P is the total monthly precipitation. ET_{pen} is the monthly evapotranspiration.

5.2.7 Calculation of NBP

To evaluate the carbon budget of the entire soybean field, the NBP was calculated using the following equation mentioned in Shimizu et al., (2009):

$$NBP = NPP - R_H + ERW_s + ERW_p - E - L \quad \text{(Eq. 5. 11)}$$

where, *NPP*, *ERWs*, *ERWp* and *L* are the net primary production, the CO_2 removal in non-rhizosphere and rhizosphere soil, and the carbon leaching, respectively. R_H is the heterotrophic respiration, which was the cumulative amount of CO_2 flux in non-rhizosphere area of NB treatment (i.e. cumulative F_{CO2} in NB treatment). *E* is the artificial harvest, which was the aboveground NPP in this study. Positive NBP values represent the carbon sequence, whereas negative values represent carbon loss.

Ultimately, the carbon loss mitigation caused by ERW was calculated by comparing the NBP between the B and NB treatment areas.

5.2.8 Statistical analysis

Statistical analysis applied in this chapter was described in chapter 3. Model performance was evaluated using the explained variance (R^2) (Eq. 5.12):

$$R^2 = 1 - \frac{\sum_{i=1}^{n}(x_i - x_{i-pre})^2}{\sum_{i=1}^{n}(x_i - \bar{x})^2} \quad \text{(Eq. 5. 12)}$$

A two-sample *t*-test was used to assess the differences in gas emissions between the two treatment intervals. A Linear Mixed Model (LMM) was used to evaluate the differences in soil properties between two treatments during each period. Linear regression analysis was used to determine the associations between the soil properties and ERWs or ERWp on each sampling day.

5.3 Results

5.3.1 Soil properties

During the investigation period, the temperature ranged from 10 to 30°C. Multiple heavy rainfall events with daily precipitation > 25 mm were observed in S1, S2, and S4, whereas relatively long rainfall events with precipitation < 10 mm were observed in S3 (Fig. 5.6a). Soil temperature and VWC generally exhibited trends similar to those of air temperature and precipitation. During the investigation period, no significant difference in the soil temperatures was observed in B and NB. Notably, VWC in B was significantly lower than that in NB ($p < 0.05$), irrespective of the period, with the decrease ranging from 0.53% to 4.97% (Fig. 5.6b; Table 5.2).

The mean soil pH in NB ranged from 5.76 to 5.97, which was significantly lower than that in B regardless of the time period ($p < 0.05$; Fig. 5.7a; Table 5.2). However, EC in B was higher than that in NB during S0 and S1, with no significant differences observed throughout the investigation period (Fig. 5.7b; Table 5.2). Soil NO_3^--N and NH_4^+-N concentrations were high in S0 and S1 and gradually decreased with no significant differences between the two treatments (Fig. 5.7c and d; Table 5.2). WSOC concentrations were not significantly different between the two treatments. However, WSIC concentration in B was significantly higher than that in NB in S3 and S4 with an increase of 2.38 and 1.31 mg kg^{-1}, respectively ($p < 0.05$; Fig. 5.8a and b; Table 5.2).

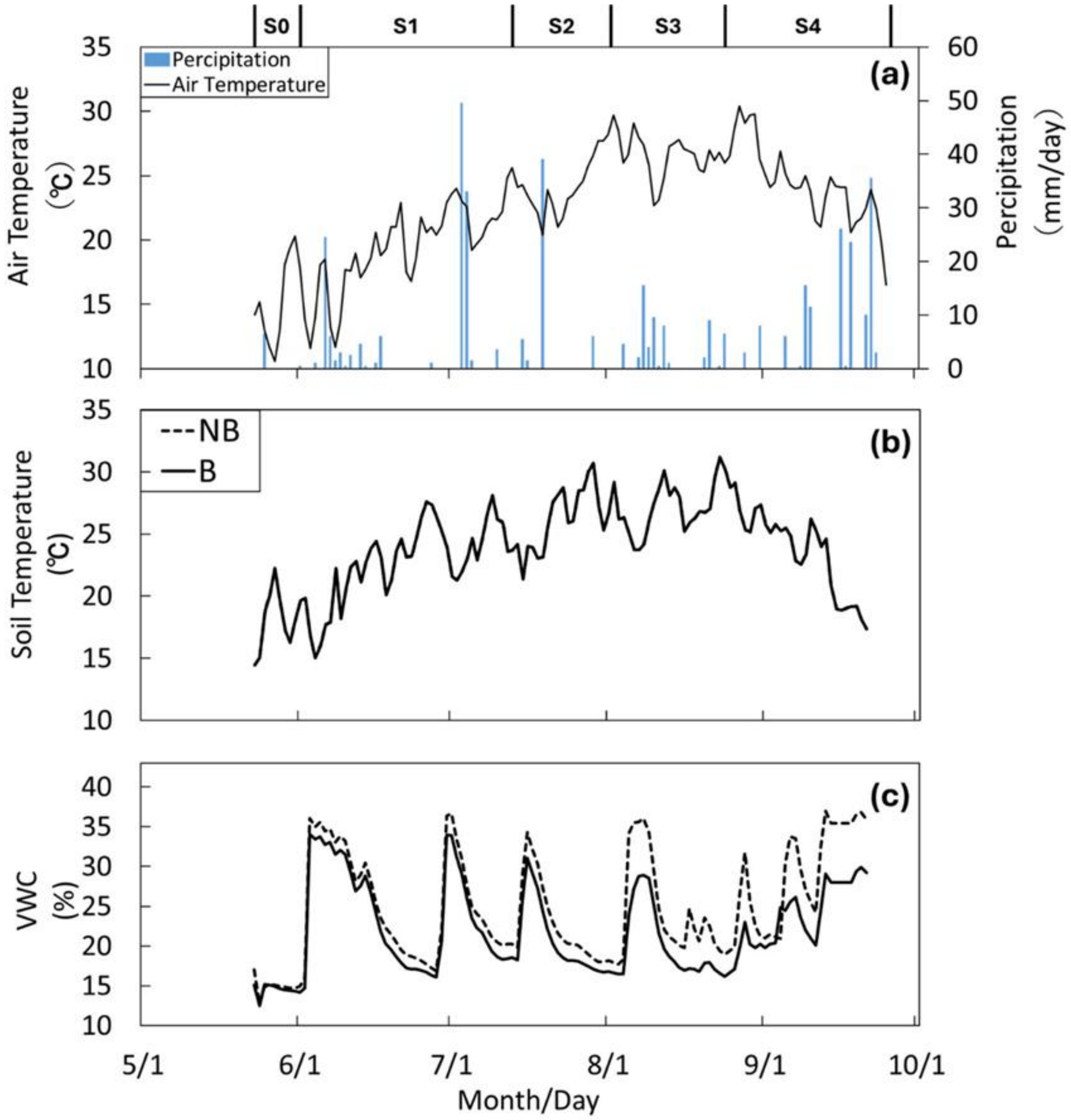

Fig. 5.6. Daily variations in air temperature and precipitation (a), soil temperature (b) and volumetric water content (VWC) (c). Data represents means. S0, S1, S2, S3, S4 represent before sowing (May 22nd to May 31st), the vegetative stage (June 1st to July 13th), the flowering stage (July 14th to July 31st), the pod-filling stage (August 1st to August 21st), and the maturity stage (August 22nd to September 21st), respectively.

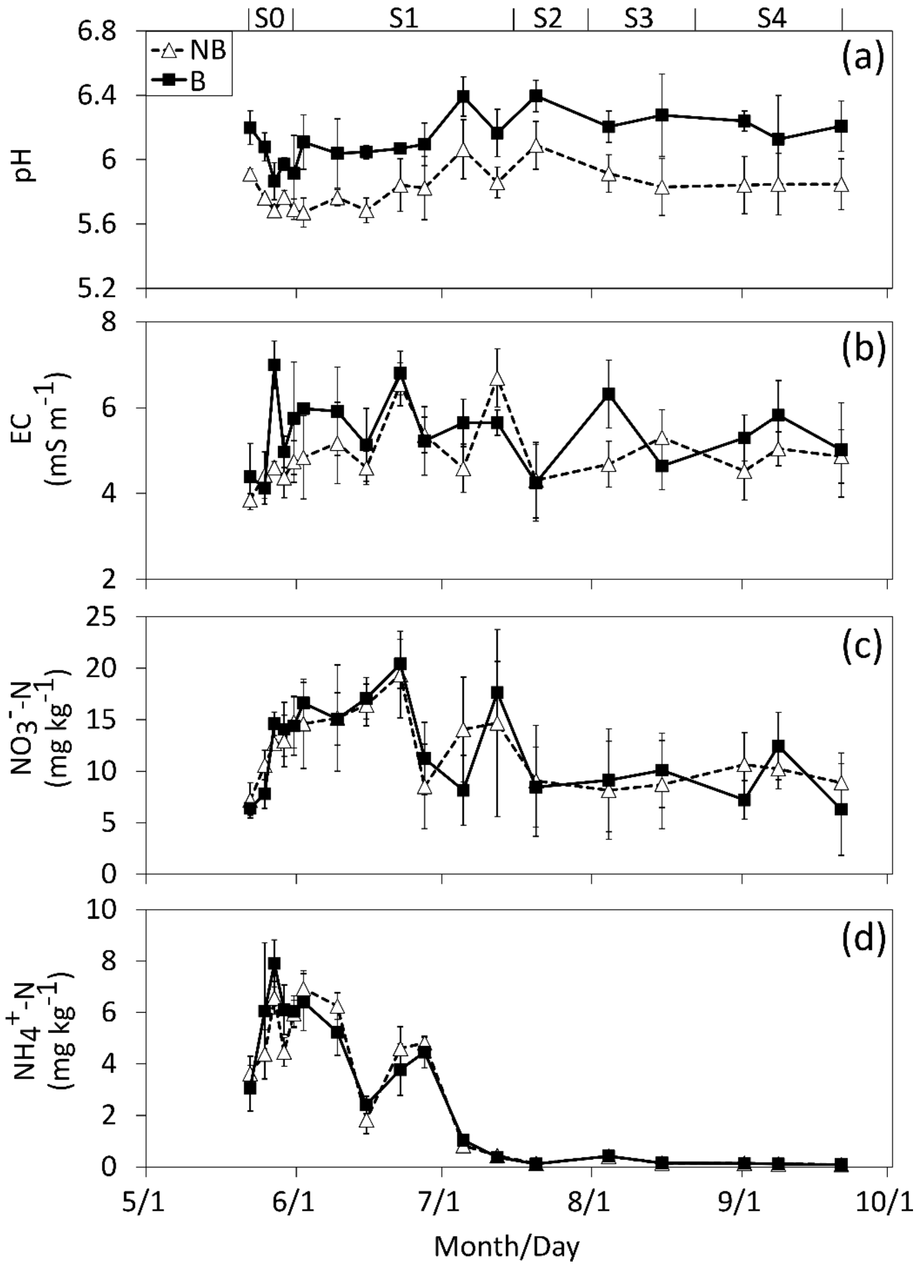

Fig. 5.7. Seasonal variations in pH (a), EC (b), nitrate nitrogen (NO_3^--N) (c) and ammonium nitrogen (NH_4^+-N) (d) concentrations. Data represents means ± S.D. (n = 3). S0, S1, S2, S3, S4 represent before sowing (May 22nd to May 31st), the vegetative stage (June 1st to July 13th), the flowering stage (July 14th to July 31st), the pod-filling stage (August 1st to August 21st), and the maturity stage (August 22nd to September 21st), respectively.

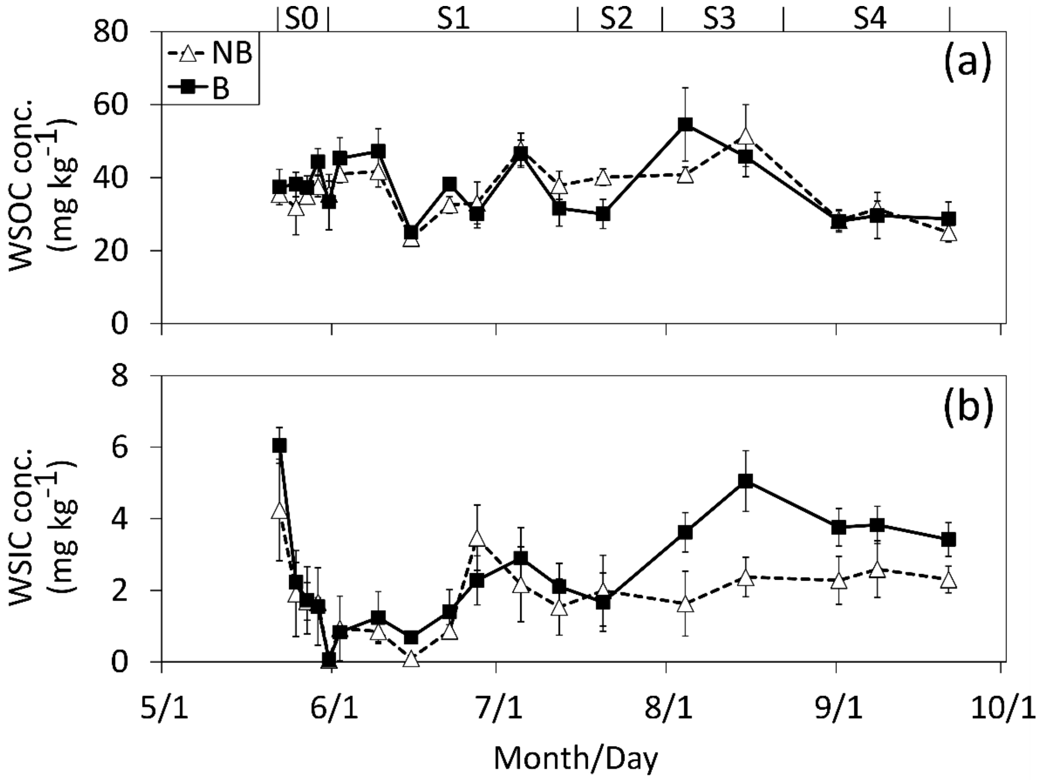

Fig. 5.8. Seasonal variations in water-soluble organic carbon (WSOC) (a) and water-soluble inorganic carbon (WSIC) (b) concentrations. Data represents means ± S.D. (n = 3). S0, S1, S2, S3, S4 represent before sowing (May 22nd to May 31st), the vegetative stage (June 1st to July 13th), the flowering stage (July 14th to July 31st), the pod-filling stage (August 1st to August 21st), and the maturity stage (August 22nd to September 21st), respectively.

Table 5.2. Linear Mixed Model (LMM) results of soil properties between treatments during each period.

		S0	S1	S2	S3	S4
Soil Temperature (℃)	NB	17.7	22.7	26.3	26.7	24.3
	B vs NB	-0.01 ns	-0.00 ns	-0.01 ns	0.00 ns	-0.01 ns
VWC (%)	NB	15.4	25.5	23.1	24.7	28.1
	B vs NB	-0.53 **	-1.62 **	-2.24 **	-4.36 **	-4.97 **
pH	NB	5.76	5.81	5.97	5.87	5.85
	B vs NB	0.27 **	0.32 **	0.31 *	0.37 **	0.35 **
EC ($mS\ m^{-1}$)	NB	4.35	5.19	5.50	5.00	4.81
	B vs NB	1.22 *	0.60 †	-0.55 ns	0.49 ns	0.57 ns
NO_3^--N conc. ($mg\ kg^{-1}$)	NB	10.9	14.7	11.87	8.42	9.92
	B vs NB	-0.55 ns	0.06 ns	1.17 ns	1.18 ns	-1.27 ns
NH_4^+-N conc. ($mg\ kg^{-1}$)	NB	4.63	4.21	0.28	0.27	0.09
	B vs NB	0.80 *	-0.32 ns	-0.04 ns	0.01 ns	-0.00 ns
WSOC conc. ($mg\ kg^{-1}$)	NB	34.7	36.5	38.7	45.6	28.0
	B vs NB	3.30 ns	2.27 ns	-7.85 ns	4.74 ns	0.85 ns
WSIC conc. ($mg\ kg^{-1}$)	NB	2.26	1.40	1.74	1.97	2.37
	B vs NB	0.24 ns	0.17 ns	0.14 ns	2.38 **	1.31 **

The row labeled "NB" represents the mean soil properties under the NB treatment during the specified period. The row labeled "B vs NB" represents the difference in soil properties between the B and NB treatments (positive values indicate higher values in the B treatment compared to NB, while negative values indicate the reverse). The accompanying suffix specifies the statistical significance of the observed difference (**: $p < 0.01$; *: $p < 0.05$; †: $p < 0.1$; ns: $p > 0.1$) (VWC: volumetric water content; WSOC: water-soluble organic carbon; WSIC: water-soluble inorganic carbon). S0, S1, S2, S3, S4 represent before sowing (May 22nd to May 31st), the vegetative stage (June 1st to July 13th), the flowering stage (July 14th to July 31st), the pod-filling stage (August 1st to August 21st), and the maturity stage (August 22nd to September 21st), respectively.

5.3.2 Calculation of ERWs and ERWp

To calculate the fluxes and cumulative amounts of F_{CO2} and assess NEE during the investigation period, we fitted F_{CO2} with soil temperature and VWC and NEE with hourly PFD and soil temperature, respectively. The modeling results are summarized in Tables 5.3 and 5.4. Significant fitting equations of F_{CO2} and NEE were generated under all treatments and replicates, with soil temperature and VWC accounting for 38–62% of F_{CO2}, and PFD and soil temperature accounting for 69–81% of NEE.

Table 5.3. Coefficient values and coefficient determination in the fitting equations of CO_2 flux in non-rhizosphere (F_{CO2}) against soil temperature and volumetric water content (VWC).

treatment	replication	a	k	b	R^2
NB	1	1.10	0.045	0.681	0.43*
	2	0.953	0.067	0.602	0.53*
	3	0.557	0.036	0.834	0.62**
B	1	0.215	0.020	1.13	0.55**
	2	0.235	0.041	1.04	0.38*
	3	1.13	0.057	0.696	0.46*

**: $p < 0.01$; *: $p < 0.05$

Table 5. 4 Coefficient values and coefficient determination in the fitting equations of Ecosystem Exchange (NEE) against photosynthetic photon flux density (PFD) and soil temperature.

treatment	replication	φ	m	a	k	R^2
NB	1	0.097	452	211	0.012	0.79*
	2	0.104	469	223	0.012	0.81*
	3	0.094	449	210	0.010	0.81**
B	1	0.115	429	214	0.006	0.69*
	2	0.123	450	244	0.003	0.71*
	3	0.128	452	259	0.001	0.70*

**: $p < 0.01$; *: $p < 0.05$

Using the fitting equations for F_{CO2} and NEE, we assessed the daily emission/absorption trends of F_{CO2} and NEE over time during the investigation period (Fig. 5.9). During the investigation period, no significant difference was observed in the cumulative F_{CO2} of NB and B. However, cumulative F_{CO2} was slightly lower in B. Daily mean ERWs in S0, S2, and S3 were approximately 3-times higher than those in S1. Notably, ERWs in S4 was negative, indicating high CO_2 emissions from the non-rhizosphere soils in B (Table 5.5). Cumulative NEE in B was significantly higher than that in NB throughout the study period. Specifically, daily mean ERWp in S4 was 90.3% higher than that of the entire period. This period was the major contributor to the overall average ERWp during the entire period (Fig. 5.9b; Table 5.6).

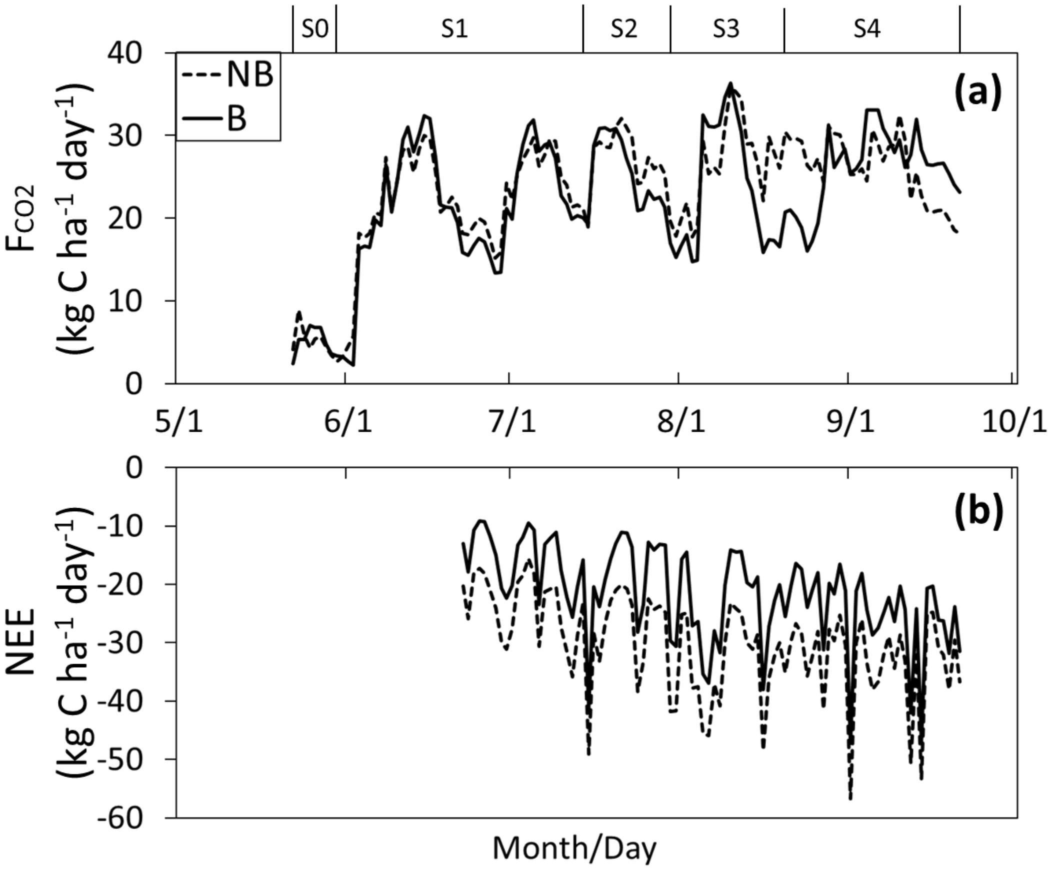

Fig. 5.9. Variations in daily emission of CO_2 flux in non-rhizosphere (F_{CO2}) (a) and net ecosystem exchange (NEE) (b). Data represents means. S0, S1, S2, S3, S4 represent before sowing (May 22nd to May 31st), the vegetative stage (June 1st to July 13th), the flowering stage (July 14th to July 31st), the pod-filling stage (August 1st to August 21st), and the maturity stage (August 22nd to September 21st), respectively.

Table 5. 5 Cumulative amounts of CO_2 flux in non-rhizosphere area (F_{CO2}) and ERWs for each period. S0, S1, S2, S3, S4 represent before sowing (May 22th to May 31th), the vegetative stage (June 1st to July 13th), the flowering stage (July 14th to July 31th), the pod-filling stage (August 1st to August 21th), and the maturity stage (August 22th to September 21th), respectively.

Period	F_{CO2} (Mg C ha^{-1})		ERWs	Daily Mean ERWs
	NB	B	(Mg C ha^{-1})	(kg C ha^{-1} day^{-1})
S0	0.05±0.01 a	0.05±0.01 a	0.00±0.01	0.06±1.60
S1	0.97±0.07 a	0.94±0.10 a	0.02±0.12	0.57±2.80
S2	0.47±0.05 a	0.44±0.06 a	0.03±0.08	1.83±4.32
S3	0.57±0.06 a	0.50±0.07 a	0.07±0.09	3.33±4.40
S4	0.80±0.07 a	0.82±0.08 a	-0.02±0.10	-0.56±3.34
Total	2.86±0.26 a	2.75±0.30 a	0.11±0.43	0.89±3.23

The values represent the mean ± standard deviation (n = 3). Different lowercase letters indicate significant differences between treatments ($p < 0.05$).

Table 5.6. Cumulative amounts of net ecosystem exchange (NEE) and ERWp for each period. S0, Si, S2, S3, S4 represent before sowing (May 22th to May 31th), the vegetative stage (June 1st to July 13th), the flowering stage (July 14th to July 31th), the pod-filling stage (August 1st to August 21st), and the maturity stage (August 22th to September 21th), respectively.

Period	NEE (Mg C ha^{-1})		ERWp	Daily Mean ERWp
	NB	B	(Mg C ha^{-1})	(kg C ha^{-1} day^{-1})
S1	-0.52±0.03 a	-0.34±0.01 b	0.16±0.13	7.11±5.72
S2	-0.52±0.03 a	-0.35±0.01 b	0.14±0.08	3.16±1.96
S3	-0.69±0.04 a	-0.49±0.01 b	0.14±0.10	7.61±5.61
S4	-1.04±0.05 a	-0.79±0.02 b	0.27±0.12	12.8±5.69
Total	-2.77±0.16 a	-1.97±0.06 b	0.69±0.43	6.71±4.15

The values represent the mean ± standard deviations (n = 3). Different lowercase letters indicate significant differences between treatments ($p < 0.05$).

5.3.3 Correlations between ERWs, ERWp and soil properties

Soil property data collected on each gas sampling day and daily ERWs and ERWp values on the same day were subjected to a linear regression analysis. ERWs exhibited a significant negative correlation with daily mean VWC ($R^2 = 0.69$; $p < 0.05$) and increased with increasing WSOC concentration ($R^2 = 0.19$; $p < 0.1$). ERWp was negatively correlated with NH_4^+-N concentration ($R^2 = 0.56$; $p < 0.05$). In contrast to ERWs, ERWp was positively correlated with daily mean VWC ($R^2 = 0.38$; $p < 0.1$; Fig. 5.9). Correlation heatmaps for soil properties associated with ERWs and ERWp are shown in Fig. 5.1.

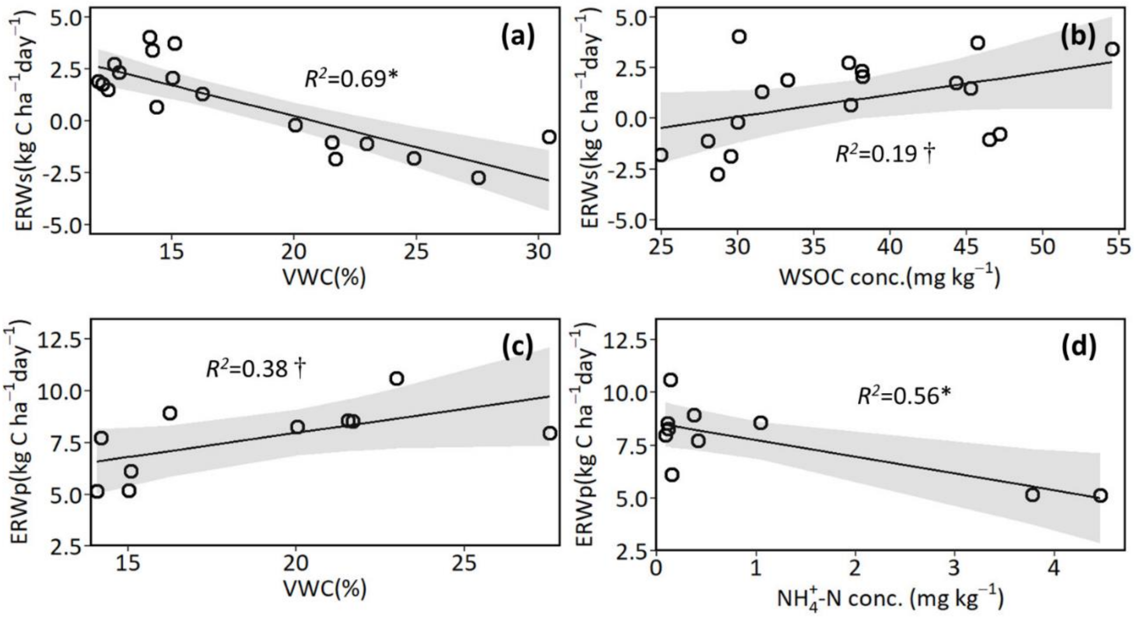

Fig. 5.10. Correlations between daily cumulative ERWs and daily mean volumetric water content (VWC) (a) and water-soluble organic carbon (WSOC) conc. (b), and between daily ERWp and VWC (c) and NH_4^+-N concentration (d). The points in the scatter plot represent the soil properties from each soil sampling days and the corresponding daily cumulative ERWs or ERWp on that day. Grey filled area represents 95% confidence interval. *: $p < 0.05$, †: $0.05 < p < 0.1$.

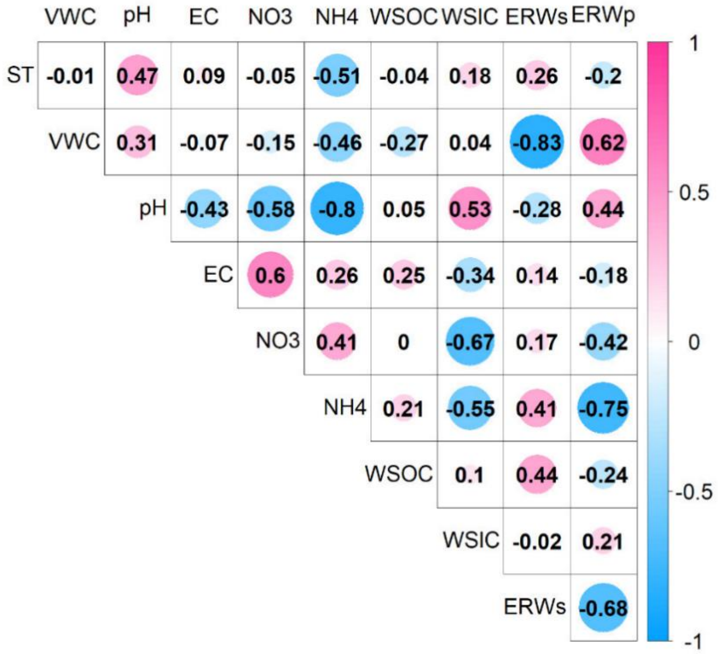

Fig. 5.11. Correlation analysis of soil properties and daily cumulative ERWs, ERWp. ST is soil temperature, VWC is volumetric water content, NO3 is NO_3^--N conecntration, NH4 is NH_4^+-N concentration, WSOC is water-soluble organic carbon concentration, WSIC is water-soluble inorganic carbon concentration, ERWs is daily cumulative ERW-induced CO_2 removal in non-rhizosphere soil, ERWp is daily cumulative ERW-induced CO_2 removal in rhizosphere soil. The value is Pearson correlation coefficient.

5.3.4 Carbon budget

Although NPP and E were relatively higher in B than in NB (Table 5.7), no significant difference was observed between in NB and B. However, OL in NB was higher than that in B, whereas IL in NB was lower than that in B. Moreover, the amount of leached carbon was approximately an order of magnitude smaller than the NPP and R_H, as indicated above.

Table 5.7. Cumulative amounts of net primary production (NPP), carbon export (E), organic carbon leaching (OL) and inorganic carbon leaching (IL).

Treatment	NPP (Mg C ha^{-1})	E (Mg C ha^{-1})	OL (kg C ha^{-1})	IL (kg C ha^{-1})
NB	2.57±0.14 a	2.40±0.14 a	8.79±0.68 a	1.76±0.19 a
B	2.63±0.17 a	2.46±0.17 a	7.54±0.56 a	2.00±0.15 a

The values represent the mean ± standard deviations (n = 3). Different lowercase letters indicate significant differences between treatments ($p < 0.05$).

All NBP components, except R_H, ERWs, and ERWp, are shown in Fig. 5.12. Regardless of the treatment, NBP was negative, indicating carbon loss and altered carbon budget. However, carbon loss in B was –1.90±0.73 Mg C ha^{-1}, which was 29.4% less than that in NB (–2.69±0.41 Mg C ha^{-1}); however, no significant difference ($p > 0.05$) was observed in the NBP of the two treatments.

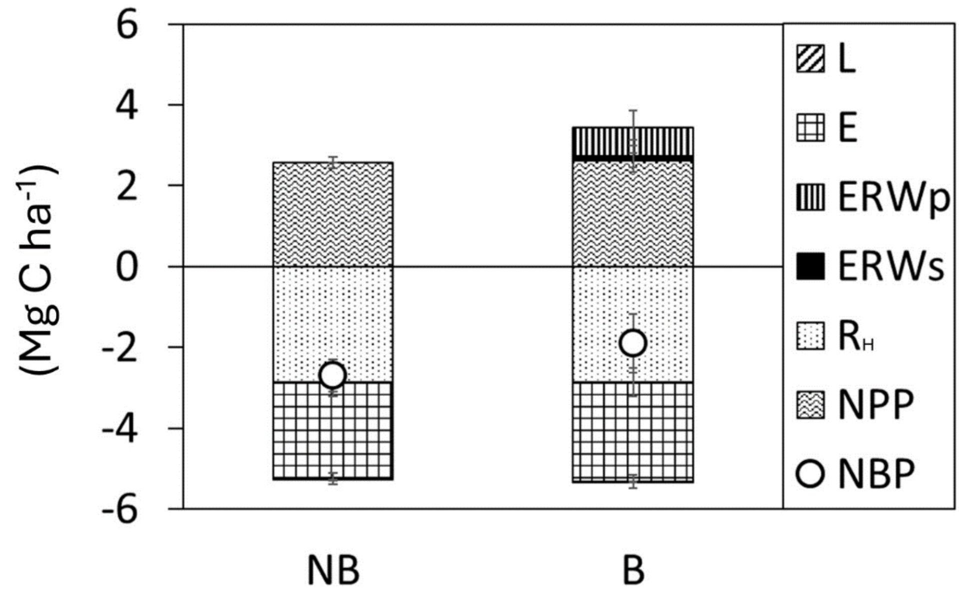

Fig. 5.12. Net biome production (NBP) and its components in NB and B. (L, E, R_H, NPP represent carbon leaching, carbon export, the cumulative amount of CO_2 flux in non-rhizosphere area of NB treatment and net primary production, respectively. ERWs

and ERWp are CO_2 removal in the non-rhizosphere and rhizosphere soil. The error bars show the standard deviations. (n = 3).

5.4 Discussion

5.4.1 Response of soil properties

Soil temperature and volumetric water content are key factors influencing soil respiration and the rate of rock weathering. In this study, the application of basalt powder did not significantly affect soil temperature, but it did significantly reduce soil VWC (Table 5.2). Previous research on the impact of ERW on soil water content has been inconsistent. Some studies suggest that the application or coverage of rock powder can increase soil water content by improving moisture movement within soil pores, reducing evaporative losses, or enhancing soil water retention capacity (de Oliveira Garcia et al., 2020; Medeiros et al., 2024; Ribeiro et al., 2020). Conversely, other studies indicate that the application of rock powder can decrease soil total porosity, thereby reducing soil VWC (Vienne et al., 2022; Wang et al., 2020). A plausible explanation is that basalt fines partially infilled larger pores, altering the pore-size distribution, which may have contributed to the observed decrease in soil water content. Immediate tilling after rock powder application and a relatively low soil bulk density may also reinforce this effect. However, while the soil pores occupied by basalt may lead to a slight decrease in VWC, the water retention capacity of the soil could potentially be enhanced (Ribeiro et al., 2020).

For the chemical properties of the soil, the pH in B was significantly higher than that in NB throughout the study period (Table 5.2). This is consistent with previous studies reporting that ERW can increase soil pH (Guo et al., 2023b; Ramos et al., 2015). Improvement in soil pH under acidic soil conditions positively affects soil nutrient retention and alleviates soil Al toxicity, thereby promoting crop growth (Buss et al., 2024; Dang et al., 2022; Xia et al., 2020). The bicarbonate generated from the weathering of primary minerals, such as plagioclase (a major component of basalt), is the main cause of the pH increase. Additionally, the release of metal cations (e.g., Mg, Ca) during this process is also a reason for the tendency of increased soil EC observed with basalt application in this study. These results suggest that ERW has the potential to replace currently widely used pH ameliorants such as lime.

It was observed that the basalt application had no significant impact on soil NO_3^--N or NH_4^+-N concentrations(Table 5.2). The variation in soil nitrogen primarily results from the application of fertilizers or plant growth, since the weathering of basalt does not produce nitrogen products, the short-term application of basalt does not directly affect soil nitrogen dynamics (Lan et al., 2021; Luo et al., 2024; X. Wu et al., 2024). The variation in WSOC in the topsoil (0-20 cm) mainly comes from humic acids (Jin et al., 2023; Tao and Lin, 2000). In this study, since there was no application of organic fertilizers, the changes in WSOC concentration should be primarily due to the leaf fall or root death of soybeans, rather than the application of basalt. On the other hand, WSIC mainly exists in the form of carbonates (Lu et al., 2020; Wang and Alva, 1999), and numerous previous studies have reported the promotion of soil inorganic carbon sinks by rock powder application (Dang et al., 2022; Guo et al., 2023b; Kelland et al., 2020). Additionally, this study shows that during periods S3 and S4, the WSIC in B was significantly higher than that in NB (Table 5.2). Moreover, it has been reported that the weathering of basalt spans a long time period, and even with enhanced weathering treatments, a substantial portion of the basalt may remain unweathered after decades (de

Oliveira Garcia et al., 2020; Li et al., 2016). The results of WSIC suggest that a long-term time scale is required to evaluate the impact of ERW on soil inorganic carbon pools.

5.4.2 CO_2 removal in non-rhizosphere soil

In this study, ERWs was applied to evaluate CO_2 removal in non-rhizosphere soils, which is influenced by two factors: CO_2 uptake through weathering and changes in soil microbial respiration. No significant differences in F_{CO2} were observed between B and NB through to the study period, and the ERWs throughout the investigation period were not consistently positive. ERWs did not necessarily promote carbon sequestration (Table 5.5). This result indicates that changes in soil properties induced by basalt application may enhance soil microbial respiration, thereby leading to relatively lower ERWs values in the outcomes. Throughout the investigation period, soil pH in B was higher than that in NB (Fig. 5.7 a). Numerous studies have shown that an increase in pH in acidic soils can enhance microbial respiration by increasing the solubility of soil organic matter, alleviating the inhibitory effect of acidity on microbial growth, and reducing metabolic stress on microbes (Anderson et al., 2018; Jones et al., 2019; Malik et al., 2018). Consequently, the relatively higher pH of B led to a decrease in ERWs. However, the soil microbial respiration response to the impact of basalt application on soil properties is not solely a "promotion”. The lower VWC in B may inhibit soil microbial respiration. Reported studies have shown that when VWC is below 38%, increasing moisture can enhance R_H by improving substrate diffusion and increasing enzyme activity (Chen et al., 2018; Knowles et al., 2015). In this study, VWC remained below the threshold throughout the entire period, regardless of the treatment. Additionally, the negative correlation between ERWs and VWC (Fig. 5.6 a) and the negative ERWs observed during S4, where

VWC was relatively high (Table 5.2), indirectly indicated that increased soil moisture may enhance soil microbial respiration, thereby reducing ERWs values. Hence, because the effectiveness of ERW in non-rhizosphere soil is constrained by the microbial respiration response, carbon removal through ERW in non-crop areas may require more stringent soil conditions.

Previous studies have discussed the conditions under which rock weathering enhances carbon sequestration. Research utilizing reaction transport models (RTM) or the Soil Cycles of Elements simulator for Predicting Terrestrial regulation of greenhouse gases (SCEPTER) has indicated that carbon sequestration capacity can be enhanced under conditions of higher temperature, increased water content, and acidic soils, owing to increased dissolution or reaction rates (Baek et al., 2023; Kelland et al., 2020). However, model simulations of sequestration capacity often overlook the impact of soil biota, including soil microorganisms and plant roots, on CO_2 removal during weathering processes. Particularly under conditions of higher temperatures and soil moisture, rock weathering is not only enhanced, but microbial respiration is also relatively increased (Zhang et al., 2010), which can offset the CO_2 sequestered by the weathering process, resulting in lower levels of ERWs. Accordingly, further research on the response of soil microorganisms to rock application is essential for effectively implementing ERW technology for CO_2 sequestration in the field.

5.4.3 CO_2 removal in rhizosphere soil

Differing from the response of soil microbial respiration to soil properties included in ERWs, the ERWp reflecting CO_2 removal in rhizosphere soils is more regulated by the impact of crop roots on soil respiration. Compared with F_{CO2}, NEE in B was significantly higher than that in NB, regardless of the period, and ERWp was also significantly positive (Table 5.6). Throughout soybean growth, organic compounds, including organic acids and saponins, are exudated (Liang et al., 2013; Tsuno et al., 2018), and the death of fine roots increases the organic components in the soil. These organic compounds can accelerate mineral dissolution through complexation with cations, thereby promoting the weathering process (Barreto et al., 2021; Lawrence et al., 2014). The higher WSIC in the later stages of the investigation in S3 and S4 may indirectly support this facilitative effect. In contrast, metal ions (e.g., Al and Fe) produced by weathering can enhance the chemical stability of organic carbon, thus promoting soil organic carbon sequestration (Buss et al., 2024; Chen et al., 2022). These interactions may explain the relatively high ERWp values. Additionally, studies have shown that during the pod-filling stage (S3), the exudation of nitrogen-containing compounds by soybean roots increases significantly (Ofosu-Budu et al., 1990). As the soybean enters the maturation stage (S4), the death of roots also increases, and dead roots return to the SOC (Kosslak et al., 1997). This also explains the higher daily mean ERWp in S3 and S4 (Table 5.6). Root exudation is also influenced by soil properties. Studies have indicated that root exudate production increases with increasing soil moisture content (Dijkstra and Cheng, 2007). This was reflected in the marginally significant ($p < 0.1$) positive correlation between ERWp and VWC observed in this study (Fig. 5.10c), further indicating the role of plant roots in the weathering process. The negative correlation between ERWp and NH_4^+-N concentration (Fig. 5.10d), for two reasons. First, ammonium dihydrogen phosphate was used as a nitrogen fertilizer. After fertilization, a large amount of NH_4^+-N entered the soil when the soybeans were sown and had not yet developed root systems. As soybeans grow, they directly absorb NH_4^+-N (Joseph et al., 1976; Klotz and Horst, 1988), resulting in a higher degree of root development when the NH_4^+-N conc. was lower, and consequently, ERWp was higher. Second, nitrifying bacteria in the soil utilize NH_4^+-N to produce nitrate-N, releasing hydrogen ions during the process. These free hydrogen ions can enhance the weathering process by promoting the dissolution of primary minerals (Banfield et al., 1999; Zhao et al., 2023), resulting in an increased ERWp.

The co-stimulatory effects of organic exudates from well-developed plant root systems and weathering processes may lead to higher levels of ERWp, possibly offering more suitable agricultural management conditions for ERW. For instance, basalt powder can be applied in crop fields with more developed root systems and higher levels of exudates, or with higher levels of root-derived CO_2 in partial pressure. Additionally, better irrigation conditions and organic fertilizer application may increase the CO_2 sequestration capacity in the field by promoting crop root growth (Chen et al., 2019; Luan et al., 2020). However, the composition and production rate of root exudates vary among different crops and under different soil conditions (Carvalhais et al., 2011; Miller et al., 2019), and the relationship between increased soil respiration due to irrigation, organic fertilizer application, and enhanced weathering remains unclear. Further field experiments are required to verify the rationality of these management practices.

5.4.4 Carbon budget

Several studies have been conducted on the carbon budget related to ERW, most of which calculated the carbon budget based on changes in soil inorganic carbon (Guo et al., 2023b; Kelland et al., 2020). However, under acidic soil conditions similar to this study, the main component of soil inorganic carbon (HCO_3^-) exhibits high decomposition rates and low contents, making it difficult to directly measure SIC for calculating the carbon budget (Mi et al., 2008; Sheng et al., 2016). In this study, we employed a method to evaluate the carbon budget based on CO_2 emissions and crop harvests, which has been previously applied in pasture and rotation field studies (Loubet et al., 2011; Shimizu et al., 2015). This method may offer a new approach for assessing the carbon budget of basalt powder in acidic soils.

In the overall calculation of NBP, the natural carbon losses from the ecosystem are primarily attributed to R_H. The reduction in carbon losses caused by basalt application, achieved through the removal of CO_2 produced by soil respiration, was determined using ERWs and ERWp (Fig. 5.12). In this study, CO_2 removal due to ERW was 0.81 ± 0.17 Mg C ha^{-1}, which corresponds to the removal of 28% of the CO_2 emitted by microbial respiration (2.86 ± 0.35 Mg C ha^{-1}). This value still holds potential for further improvement. The P80 of the basalt powder used in this study (57.66 μm) is larger than the optimal particle size range (10-30 μm) mentioned in Beerling et al. (2018). It has been reported that reducing the P80 of rock powder by five times can increase carbon sequestration by 33%, although this would also result in higher CO_2 emissions from rock powder production (Guo et al., 2023b). Additionally, despite crushing basalt into a powder to enhance weathering, the process is still time-consuming. Kelland et al. (2020) proposed that the carbon capture process might take one to five years to demonstrate the CO_2 capture capability after a single application of basalt powder. Lefebvre et al. (2019) indicated that ERW have considerable potential for long-term CO_2 removal. Therefore, the total CO_2 removal observed in the first year of basalt powder application in this study may only represent a part of the weathering process.

In addition to CO_2 emissions and CO_2 removal via ERW (ERWs and ERWp, respectively), plant harvests and carbon leaching were also measured in this study to determine specific NBP (Fig. 5.12). No significant differences were observed in NPP and C exports of the two treatments (Table 5.7), contradicting previous reports that basalt increases the crop yield by enhancing the essential nutrients (Blanc-Betes et al., 2021; Luchese et al., 2021). Crop yield is influenced by multiple factors including climate and soil conditions. In the present study, in B, a lower VWC was observed during the investigation period, whereas water stress limited soybean growth (Foroud et al., 1993; Wijewardana et al., 2018). Additionally, some studies have indicated that the yield-increasing effect of ERW is not significant under semi-arid and semi-humid climatic conditions (Guo et al., 2023a). This indicates that the yield-increasing effect of ERW may require consideration of the influence of field meteorological conditions and initial soil properties. Organic carbon leaching in NB and B were 8.79 ± 0.68 and 7.54 ± 0.56 kg C ha^{-1}, respectively (Table 5.7). As organic carbon leaching is influenced by soil properties and climatic conditions, even within acidic soil systems similar to those in this study, the reported range can vary substantially. Nevertheless, organic carbon leaching values in this study fell within the previously report ranging from 5.5 to 74 kg C ha^{-1} yr^{-1} (Kindler et al., 2011; Long et al., 2015). Notably, there were no significant differences in leaching between the treatments for either organic or inorganic carbon, indicating that the application of rock powder does not increase carbon loss via leaching in short-term. Furthermore, the carbon flux of leaching is nearly an order of magnitude smaller than that of the other pathways, thereby exerting minimal influence on the overall carbon budget.

Here, no significant differences were observed in the plant yield and carbon leaching. Therefore, variations in NBP within the study area mainly stemmed from differences in CO_2 emissions (ERWs and ERWp; Table 5.7; Fig. 5.12). Carbon loss in B was reduced by 29.4% lower than that in NB, even though the difference was not statistically significant (Fig. 5). This value aligns with previous studies on maize/soybean systems, where ERW reduced carbon loss by 23% to 42% (Kantola et al., 2023). However, studies disagree on which flux drives the ERW-induced improvement in the farm carbon balance loss mitigation. In our study, the removal in CO_2 emissions primarily mitigated carbon loss, while research of Kantola et al., (2023) indicated that ERW mainly reduced carbon loss by promoting crop biomass. Additionally, studies have reported that an increase in soil inorganic carbon is a significant pathway through which ERW improves carbon budget (Azeem et al., 2022; Haque et al., 2020). Rock powder can enhance the carbon balance by increasing soil microaggregates, and redistribution soil organic carbon has also been reported (Reifschneider et al., 2021). Considering the differences in CO_2 absorption between the rhizosphere and non-rhizosphere areas observed in this study, a more detailed mechanistic investigation of weathering processes around crop roots is necessary to determine the impact of ERW on the carbon budget in farmland systems. However, as this study did not specifically measure soil carbon pools, the differential responses of soil organic and inorganic carbon pools to ERW could be a focus of future research.

5.5 Conclusion

In conclusion, ERW technique reduced CO_2 emissions in both the rhizosphere and non-rhizosphere soils, with more pronounced effects in the rhizosphere soil. Some soil property responses to ERW, such as increased soil pH, promoted soil microbial respiration, indicating that the application of basalt powder to ERW in non-crop soils requires more stringent soil conditions. However, in the rhizosphere soil, crop root systems and root-induced rock weathering mutually enhance each other, suggesting that the ERW technique has wide application potential in agricultural crop fields, particularly in crop fields with vigorous root activity and exudate output. Additionally, ERW mitigated soil carbon loss, providing a new solution for farmland carbon balance. However, further research is necessary to elucidate the mechanisms by which ERW improves the carbon budget.

6. General discussion

6.1 Mechanisms of efficiency differences in two carbon loss mitigation strategies

This study systematically compared organic fertilizer applications and ERW as carbon loss mitigation strategies. The findings showed significant differences in short-term efficiency between the two approaches. Organic fertilizers exhibited markedly higher carbon mitigation efficiency compared to ERW within the 91-days incubation period. Specifically, carbon loss mitigation rate relative to the control was 3.09, 4.80, and 4.08 Mg C ha^{-1} for compost, slurry, and digestate, respectively (Fig 4.12). While enhanced rock weathering achieved only 0.79 Mg C ha^{-1} over approximately 6 months of field trials. The fundamental cause of this efficiency disparity lies in the inherently different mechanisms through which these methods intervene in carbon cycling processes.

Organic fertilizers achieve carbon mitigation by directly introducing exogenous organic carbon into soil, representing an input-side intervention approach that rapidly enhances soil organic carbon pools (Lazcano et al., 2013). From a carbon cycling perspective, organic fertilizers essentially constitute carbon that has been pre-fixed from atmospheric CO_2 through plant photosynthesis and animal metabolic processes, then directly applied to soil systems (Diacono and Montemurro, 2010; Liu et al., 2006; Yang and Zhang, 2023). This pre-fixed carbon source bypasses the complex transformation processes from atmospheric CO_2 to SOC stock, thereby enabling rapid carbon sequestration effects. The rapid increase in soil organic carbon content observed in the 91-days incubation experiment demonstrates the advantage of this direct input approach.

The efficiency differences among organic fertilizer types further reveal the critical influence of carbon quality on mitigation effectiveness. Digestate exhibited the highest

CBE, primarily attributed to the structural modifications of organic matter during anaerobic fermentation. During anaerobic digestion, readily decomposable carbohydrates and proteins are preferentially degraded to produce methane, while recalcitrant components such as lignin are retained (van Midden et al., 2024; Zhong et al., 2011). This process endows the organic carbon in digestate with enhanced stability, resulting in reduced rapid mineralization losses after application. In contrast, raw slurry contains substantial amounts of labile components (Andrade Díaz et al., 2024), leading to higher CO_2 emissions and relatively lower CBE after application. Although compost provided the largest carbon input, its carbon release and transformation processes were relatively slow due to physical structural constraints, preventing it from fully realizing its carbon mitigation potential during the short-term incubation experiment.

In contrast, ERW directly captures CO_2 from the atmosphere through mineral weathering reactions, representing an indirect carbon sequestration approach. The core mechanism involves weathering reactions between silicate minerals, atmospheric CO_2, and water, forming dissolved bicarbonate ions that ultimately achieve long-term carbon storage in the form of carbonates (Beerling et al., 2018; Guo et al., 2023b). The carbon loss mitigation effect of this approach in field experiments was significantly lower than that of organic fertilizers, reflecting fundamental differences in reaction kinetics and energy requirements between geochemical and biochemical processes.

Rock weathering reactions require overcoming relatively high activation energy barriers, and under ambient temperature and pressure conditions, the dissolution rates of silicate minerals are inherently slow (Baek et al., 2023; Li et al., 2016). Furthermore, the weathering process depends on diffusion and mass transfer of reactants and products at mineral surfaces, which further constrains overall reaction rates (Dietzen et al., 2018b).

Notably, enhanced rock weathering exhibited higher efficiency in rhizosphere soils, primarily associated with biological enhancement by plant root systems. Root exudates, such as citric acid and malic acid, can combine metal ions on mineral surfaces, accelerating mineral dissolution (Holden et al., 2024). Simultaneously, the elevated CO_2 concentrations generated by root respiration provide additional reactants for weathering reactions. This bio-geochemical coupling effect partially explains the efficiency differences between rhizosphere and non-rhizosphere soil.

From the perspective of carbon transformation kinetics, these two methods follow distinct reaction patterns and controlling mechanisms. Carbon transformation in organic fertilizers involves complex networks of enzyme-catalyzed biochemical reactions, including extracellular enzyme depolymerization of macromolecular organic matter, microbial uptake and metabolism of small molecular compounds (Conant et al., 2011). These biochemical reactions are characterized by relatively low activation energies and rapid reaction rates, enabling rapid progression under suitable temperature and moisture conditions. The temporal variations in CO_2 emission curves among different organic fertilizers in the incubation experiment also reflect the intrinsic decomposition characteristics and stability differences of their organic components.

Carbon sequestration through ERW is a purely chemically-controlled process, primarily involving mineral surface protonation, metal ion release, and establishment of carbonic acid-bicarbonate equilibrium in solution (Berg and Banwart, 2000; Patrícia Vieira da Cunha et al., 2008). These reactions exhibit relatively small rate constants and are highly dependent on chemical environmental parameters such as temperature, pH, and ionic strength (Borges et al., 2019). Unlike biological reactions, the rates of rock weathering reactions remain relatively stable over time, without exhibiting the pattern of initial rapid response followed by gradual decline observed in organic fertilizers. However, it is noteworthy that although carbon sequestration through enhanced rock weathering is essentially a geochemical reaction, it still depends on biological process regulation in soil environments. Mineral weathering reactions require suitable pH conditions, adequate moisture, and continuous reactant supply, which are largely influenced by soil microbial activities and plant root physiological processes (Lawrence et al., 2014; Liang et al., 2013).

This cross-process regulation exists in both methods, creating a symmetry: the biochemical processes of organic fertilizers are constrained by physical structures (such as the slow release from compost), while the geochemical processes of rock weathering are enhanced by biological activities. This regulatory complexity indicates that in soil, a multiphase composite system, no single process can function independently, and optimal effects can only be achieved through synergistic interactions among multiple factors.

In general, organic fertilizers application and ERW represent two fundamentally different carbon loss mitigation strategies: the former achieves rapid carbon accumulation by utilizing carbon resources already fixed in the biosphere, while the latter directly removes CO_2 from the atmosphere through geochemical processes. These mechanistic differences not only explain the significant disparity in their short-term efficiency but also suggest potential distinctions in long-term carbon sequestration stability and environmental adaptability.

6.2 Applicability boundaries and methodological limitations

The effectiveness of carbon loss mitigation strategies depends on the interactions among three key factors, material properties, environmental conditions, and temporal dynamics. Therefore, the selection of soil carbon loss mitigation strategies is often constrained by specific application environments and practical conditions. When facing degraded farmlands severely deficient in organic matter and requiring rapid soil quality improvement, the direct carbon input advantage of organic fertilizers is fully realized (Saia et al., 2015; Weyers and Spokas, 2011). In this study, digestate, slurry, and compost, all significantly enhanced SOC content in the short term, providing possibilities for rapid restoration of soil ecological functions. However, achieving these immediate effects depends on stable organic feedstock supply, and in regions with underdeveloped livestock industries or limited agricultural waste resources, large-scale promotion of organic fertilizers often faces the practical challenge of feedstock shortage (Golicz et al., 2019; Tong et al., 2017). More critically, the carbon loss mitigation effects of organic fertilizers require continuous application for maintenance, and once application ceases, the resulting soil improvement effects gradually diminish (Dijkstra and Keitel, 2024). This dependency may become a limiting factor in rural areas with unstable economic conditions or insufficient labor force. Meanwhile, this study also found that organic fertilizer application produces substantial amounts of greenhouse gases other than CO_2, which is consistent with extensive previous research (Chirinda et al., 2010b; He et al., 2023; Kitamura et al., 2021; Verma et al., 2020b), making environmental impact assessment of organic fertilizers prior to application critically important.

In contrast, ERW demonstrates unique dual benefits in acidic soil environments with low pH and mineral nutrient deficiency. Basalt powder application not only achieves direct atmospheric CO_2 capture but also releases alkaline ions and mineral nutrients that effectively improve soil chemical environments, creating more suitable conditions for crop growth (Elisa et al., 2016; Hicks et al., 2022; Patrícia Vieira da Cunha et al., 2008).

This multifaceted effect has significant application value in regions where acidic soils are widely distributed. However, ERW faces dual challenges of slow reaction rates and environmental sensitivity. This study found that under high precipitation conditions, enhanced soil microbial respiration may offset or even exceed the carbon sequestration effects of rock weathering, leading to reduced net carbon loss mitigation effectiveness. This sensitivity to moisture conditions limits the stable application of this method in regions with highly variable precipitation. Additionally, studies have indicated that under acidic soil conditions, CO_2-driven weathering of silicate rock powder accounts for less than 1% of total weathering, highlighting that current CDR estimation methods for ERW still contain uncertain components (Holden et al., 2024).

The two strategies exhibit distinct adaptability differences across various agricultural production systems. In intensive annual cropping systems, organic fertilizers can be organically integrated with existing fertilization regimes, achieving coordinated unification of soil carbon loss mitigation and nutrient supply through partial replacement of chemical fertilizers (Liang et al., 2021; Ramteke et al., 2024). Particularly, liquid organic fertilizers such as digestate, with their nutrient composition and application methods similar to conventional liquid fertilizers, are readily accepted and adopted by farmers. However, organic fertilizers have relatively high management requirements during storage, transport, and application processes, and improper handling may pose risks of pathogen contamination or nutrient losses, which could become application barriers in regions with relatively backward technical levels.

ERW demonstrates greater application potential in perennial crop systems, particularly in orchards and forestlands with well-developed root systems and vigorous rhizosphere activities. Plant root-secreted organic acids and continuous root respiration provide favorable conditions for weathering reactions, enabling this method to achieve better carbon sequestration effects (Aziez et al., 2022; Dijkstra and Cheng, 2007). However, this dependency simultaneously means that weathering efficiency decreases significantly in areas with sparse root systems or during fallow periods. More importantly, the mining, processing, and transportation of silicate minerals involve substantial energy consumption and carbon emissions. In regions with scarce mineral resources or long transportation distances (Guo et al., 2023a), these indirect emissions may significantly diminish the net carbon loss mitigation effects.

From an economic feasibility perspective, both strategies face cost-benefit trade-offs. Organic fertilizers have relatively low production costs, particularly compost and digestate produced from local agricultural wastes, but their transport radius is limited, making cross-regional distribution economically unfavorable. On the other hand, although ERW provides long-term effects, it requires substantial initial investment, especially as the specific particle size requirements for rock powder increase processing costs. In the absence of policy support or carbon trading market incentives, farmers may lack sufficient economic motivation to adopt these technologies.

It is noteworthy that the temporal scale characteristics of the two strategies determine their applicability differences under various policy objectives. For soil improvement projects requiring short-term demonstrated effectiveness, the rapid response characteristics of organic fertilizers make them the preferred choice. For long-term climate change mitigation strategies, the persistent carbon sequestration effects of ERW better align with policy objectives, despite its slow onset. This temporal scale difference is also reflected in evaluation systems: this study focused more on short-term changes, potentially underestimating the long-term value of enhanced rock weathering while overestimating the sustained effects of organic fertilizers.

Overall, organic fertilizers and ERW are not universally applicable solutions but require selection and optimization according to specific soil conditions, climate environments, agricultural system features, and socioeconomic contexts. This study demonstrates that nitrogen dynamics can better reflect the carbon decomposition patterns of different organic fertilizers, while rhizosphere environment significantly influences the CO_2 removal effectiveness of ERW. Therefore, comprehensive evaluation of nitrogen dynamics and accurate assessment of root system characteristics at different growth stages are essential considerations in practical applications. In practice, location-specific implementation of different strategy combinations may be essential for achieving optimal carbon loss mitigation outcomes.

6.3 Potential and challenges for synergistic application

As demonstrated in Section 6.2, organic fertilizers and ERW exhibit distinct differences in applicable conditions and methodological characteristics, but these differences simultaneously reveal the potential for synergistic application of both strategies. The complementary characteristics of these two approaches provide a theoretical foundation for developing more efficient and stable soil carbon loss mitigation strategies.

The most prominent synergistic effect manifests in the regulation of soil chemical environment. This study found that although organic fertilizer applications can mitigate soil acidification caused by chemical fertilizers, there remains a certain risk of acidification compared to control, which may become a limiting factor under long-term intensive application. In contrast, ERW can significantly increase soil pH through mineral weathering reactions, with released alkaline ions providing sustained buffering capacity for soil. Therefore, combining appropriate amounts of rock powder with organic fertilizer applications could theoretically effectively eliminate the soil acidification risks potentially associated with organic fertilizers, providing assurance for long-term stability of soil chemical environment. This synergistic pH regulation not only benefits soil health but also creates better environmental conditions for the optimal performance of both methods. Another important synergistic mechanism lies in the promotion of rock weathering processes by organic matter. In this study, ERW exhibited significantly higher CO_2 removing rate in rhizosphere soils compared to non-rhizosphere soils, primarily attributed to the promoting effects of root exudates on mineral dissolution. Organic fertilizer applications significantly increase soil water-soluble organic carbon content, and these soluble organic compounds possess similar chemical activity to root exudates, capable of accelerating silicate mineral dissolution through complexation. Theoretically, organic fertilizer applications can provide additional promoters for rock weathering reactions, thereby enhancing the reaction rates and carbon sequestration efficiency of enhanced rock weathering. This coupling of biogeochemical processes may achieve co-benefit effect, leveraging both the rapid carbon input advantages of organic fertilizers and enhancing the long-term CO_2 remove capacity of rock weathering.

From a temporal scale perspective, synergistic application of both methods may also achieve organic unification of short-term effects and long-term objectives. The rapid response characteristics of organic fertilizers can create more suitable reaction environments for ERW. As time progresses and the direct effects of organic fertilizers gradually diminish, the long-term carbon sequestration effects of rock weathering begin to manifest, achieving smooth transition and sustaining maintenance of carbon loss mitigation effects. This effect may provide agricultural systems with more stable and sustainable carbon management solutions.

However, the synergistic application of both strategies also faces numerous challenges. The most direct issue is the cumulative cost effect. The combined costs of organic fertilizer production, transport, and application with rock powder mining, processing, and transportation may exceed farmers' financial capacity, particularly in the absence of policy subsidies or market incentives. The increased management complexity is also a non-negligible issue. Synergistic application requires precise control of application timing, rates, and methods for both materials, imposing higher demands on management capabilities. Moreover, the potential negative effects arising from interactions between the two methods remain unclear. For instance, different types of organic compounds produced from organic fertilizer decomposition may exert varying effects on rock weathering: while certain organic acids may promote mineral dissolution, whether other metabolic byproducts might have inhibitory effects remains uncertain. On the other hand, whether mineral ions released from rock weathering could affect the decomposition patterns of organic fertilizers. These complex interactions all require dedicated research to answer. Additionally, nutrient balance and ratio optimization when both strategies are applied simultaneously represents a complex technical challenge, as inappropriate combinations may lead to nutrient excess or deficiency, affecting crop growth and soil health. From the perspective of research methodology, the understanding of synergistic effects between the two strategies in this study remains quite limited. This study evaluated the effects of both strategies separately under different experimental conditions (laboratory incubation vs. field experiments) but lacks direct evidence from simultaneous application of both materials under identical conditions. In addition, the short temporal scale of incubation experiments and single growing season of field trials constrained the assessment of long-term synergistic effects.

Future research should focus on mechanism validation and effect evaluation of synergistic application of both strategies. First, dedicated controlled experiments need to be designed to compare the differences between individual and synergistic applications under identical conditions, quantifying the magnitude of synergistic effects. Second, long-term experiments should be conducted to evaluate the cumulative effects and stability of synergistic application across multiple growing seasons. At the mechanistic level, investigation of the interaction mechanisms between organic matter and mineral weathering is needed to elucidate the chemical processes of synergistic carbon sequestration.

6.4 Conclusion

This study compared organic fertilizer applications and ERW as soil carbon loss mitigation strategies under a common evaluation framework, demonstrating that both methods effectively contribute to mitigating soil carbon loss. The effectiveness of soil carbon loss mitigation is fundamentally determined by the interaction of material properties, environmental conditions, and temporal dynamics. Organic fertilizers achieve immediate soil carbon storage increases through direct carbon input, with digestate particularly suitable for short-term soil carbon loss mitigation in aerobic fields due to its ability to avoid rapid decomposition. In contrast, ERW demonstrates soil carbon loss mitigation effects during growing periods in planted fields through interactions with root system activities, offering potential for long-term carbon stabilization in soils. The integrated assessment reveals that digestate is optimal for short-term soil carbon sequestration, while ERW is most suitable for continuous soil carbon loss mitigation in planted fields. For practical technology selection, comprehensive evaluation of nitrogen dynamics and accurate assessment of rhizosphere biomass at different growth stages are critically important considerations. Future research should focus on evaluating the synergistic effects of combining these two approaches to achieve more comprehensive and sustainable carbon loss mitigation strategies.

7. Summary

7.1 Introduction

With global average temperatures predicted to rise by 1.5-2.0°C during the 21st century, reducing greenhouse gas emissions (particularly CO_2) has become an urgent priority (Calvin et al., 2023). Soil represents a significant carbon pool, accounting for 25% of CO_2 exchange between terrestrial ecosystems and the atmosphere (Schlesinger and Andrews, 2000), making soil carbon loss mitigation an important carbon dioxide removal (CDR) strategy. Soil carbon loss mitigation strategies can be primarily classified into two categories. The first involves enhancing soil carbon storage through organic carbon application, although this may potentially increase CO_2 emissions from soil, and research on the efficiency of different organic materials remains limited. The second encompasses CO_2 re-sequestration and stabilization from soil through techniques such as enhanced rock weathering (ERW), while current research on quantifying specific carbon loss mitigation amounts is insufficient. This study aims to quantify and compare carbon loss mitigation amounts achieved through two soil management approaches (organic fertilizer application and ERW) and provide scientific evidence for practical implementation technologies. Specifically, the research conducted: (I) comparison of the effects of different materials on soil carbon pools and carbon budgets and their relative efficiency, and (II) calculation of ERW mitigation amounts and examination of applicable environments.

7.2 Materials and methods

7.2.1 Application of different organic fertilizers

The incubation experiment was conducted using cultivated soil (Andosol) collected from a managed grassland located at the Shizunai Experimental Livestock Farm, Field Science Center for Northern Biosphere of Hokkaido University, Shinhidaka, Hokkaido, Japan. Five treatments were established with three replicates each: no fertilizer (NF), inorganic fertilizer (IF), compost (M), slurry (S), and digestate (D). The soils (300 g air-dried basis) were incubated under aerobic conditions at 25°C for 91 days. Based on field application rates, 14.4, 56.3, and 55.2 g of M, S, and D were added to the soil, corresponding to carbon inputs of 5.63, 5.53, and 3.50 mg g^{-1}, respectively. The incubation period was divided into three phases: early (days 1–7), middle (days 8–35), and late (days 36–91). Gas fluxes of CO_2, N_2O, NO, and CH_4 were measured throughout the experiment. Soil organic carbon (SOC), labile organic carbon (LOC), microbial biomass carbon (MBC), and water-soluble organic carbon (WSOC) were determined using dry combustion, $KMnO_4$ oxidation, chloroform fumigation, and water extraction, respectively. Recalcitrant organic carbon (ROC) was calculated as the difference between SOC and LOC. Carbon dynamics were assessed using two indices. The carbon decomposition progress (CDP) was calculated as $(\Delta SOC + \Delta CO2)/C_{input}$, representing the proportion of decomposed carbon relative to the carbon input. The carbon balance efficiency (CBE) was calculated as $(\Delta SOC - \Delta CO2)/C_{input}$, representing the proportion of net carbon retained. Both ΔSOC and ΔCO2 were defined as fertilizer-induced values, i.e., the difference between fertilized treatments and NF.

7.2.2 Enhance rock weathering

From May to September 2023, a field experiment was conducted at the Experimental Farm of the Field Science Center for Northern Biosphere of Hokkaido University, Sapporo, Hokkaido, Japan. Two treatments were established with three replicates each: a basalt applied treatment (B) with a soil application rate at 150 Mg ha^{-1} in the 15 cm soil layer with incorporation into the soil to a depth of 15cm, and a non-applied treatment (NB). Both treatments included non-crop areas and crop areas, where soybeans were cultivated only in the crop areas. During the cultivation period, CO_2 fluxes from non-crop areas (F_{CO2}) and net ecosystem exchange (NEE, including soybean photosynthesis) from crop areas were measured, along with soil properties including pH, EC, water-soluble organic carbon (WSOC) concentrations, water-soluble inorganic carbon (WSIC) concentrations, NO_3^--N concentrations. Soil temperature and volumetric water content (VWC) at 5 cm depth and photosynthetic photon flux density were monitored. F_{CO2} and NEE were modeled as functions of soil temperature, VWC, and photon flux density. Net primary production (NPP) and harvested export (E) were obtained from the harvested biomass. Leaching (L) was calculated from the product of carbon concentrations in soil solution and drainage water volume. ERWs was defined as the difference in CO_2 emissions between the B and NB non-crop areas. ERWp was calculated as the difference in NEE between B and NB crop areas, after subtracting ERWs. Net biome production (NBP) was then determined as the difference between carbon inputs (NPP, ERWs, ERWp) and outputs (F_{CO2}, L, E). For analysis, the growing season was divided into five stages: before sowing (S0), vegetative stage (S1), flowering stage (S2), pod-filling stage (S3), and maturity stage (S4).

7.3 Results and Discussion

7.3.1 Application of different organic fertilizers

At the end of incubation, SOC was significantly higher in all organic fertilizer treatments compared with NF, whereas cumulative CO_2 emissions did not increase linearly with carbon input and followed the order S > D > M significantly. Despite receiving the highest carbon input, the M treatment exhibited the lowest SOC accumulation. CDP indicated that only 51.6% of the applied carbon was converted into CO_2 or SOC in the M treatment, which was significantly lower than in S (81.12%) and D (97.98%). Correlation network analysis further showed that the associations between CO_2 flux and soil properties were weaker in M than in S and D, particularly the positive correlation with pH and the negative correlation with EC, suggesting the formation of anaerobic microsites by compost particles.

CBE was significantly higher in D (74.24%) than in S (47.16%), indicating that prior anaerobic digestion of easily degradable carbon suppressed rapid carbon mineralization after soil application and thereby contributed to sustained carbon retention. RDA analysis revealed that changes in NO_3^--N concentration and cumulative N_2O emissions positively contributed to CDP and CBE, with stronger predictive power than changes in SOC fractions. Although digestate supplied the lowest amount of carbon, it achieved the lowest CO2 emissions and the highest CBE due to its high conversion efficiency, suggesting that digestate is the most effective option for mitigating soil carbon loss.

7.3.2 Enhanced rock weathering

During the investigation period, the pH in B treatment was significantly higher, while VWC was significantly lower compared to the NB treatment, indicating that basalt application improved soil pH but induced a tendency toward drier conditions. Both ERWs and ERWp showed positive values, suggesting a CO_2 removal effect from ERW. However, the cumulative ERWs value (0.11 ± 0.43 Mg C ha^{-1}) fluctuated across growth stages and became negative under the high-precipitation conditions of S4. The negative correlations between daily cumulative ERWs and pH and VWC suggest that CO_2 remove via weathering was offset by enhanced microbial respiration induced by increased pH and rainfall.

In contrast, the cumulative ERWp value (0.69 ± 0.43 Mg C ha^{-1}) was significantly positive with higher mean values in S3 (abundant root exudates) and S4 (substantial leaf litter input) than in other stages. This result may be attributed to a mutually reinforcing interaction, in which crop growth was stimulated by metal cations released through weathering, while root exudates further promoted rock dissolution through complexation with metal ions.

Although there was no significant difference in NBP between the B and NB treatments during the investigation period, the B treatment tended to show a higher NBP due to reduced CO_2 emissions, indicating the potential carbon loss mitigation effect of ERW, with a mitigation amount of 0.79 Mg C ha^{-1}. Notably, 86.4% of the CO_2 remove was attributed to the planted plot, highlighting the high potential of ERW application in agricultural fields with well-developed root systems.

7.4 Conclusion

This study compared organic fertilizer applications and ERW as soil carbon loss mitigation strategies under a common evaluation framework, demonstrating that both methods effectively contribute to mitigating soil carbon loss. The effectiveness of soil carbon loss mitigation is fundamentally determined by the interaction of material properties, environmental conditions, and temporal dynamics. Organic fertilizers achieve immediate soil carbon storage increases through direct carbon input, with digestate particularly suitable for short-term soil carbon loss mitigation in aerobic fields due to its ability to avoid rapid decomposition. In contrast, ERW demonstrates soil carbon loss mitigation effects during growing periods in planted fields through interactions with root system activities, offering potential for long-term carbon stabilization in soils. The integrated assessment reveals that digestate is optimal for short-term soil carbon sequestration, while ERW is most suitable for continuous soil carbon loss mitigation in planted fields. For practical technology selection, comprehensive evaluation of nitrogen dynamics and accurate assessment of rhizosphere biomass at different growth stages are critically important considerations.

8. Reference

Abbas, F., Hammad, H.M., Ishaq, W., Farooque, A.A., Bakhat, H.F., Zia, Z., Fahad, S., Farhad, W., Cerdà, A., 2020. A review of soil carbon dynamics resulting from agricultural practices. Journal of Environmental Management 268, 110319. https://doi.org/10.1016/j.jenvman.2020.110319

Ahmed, T., Noman, M., Qi, Y., Shahid, M., Hussain, S., Masood, H.A., Xu, L., Ali, H.M., Negm, S., El-Kott, A.F., Yao, Y., Qi, X., Li, B., 2023. Fertilization of Microbial Composts: A Technology for Improving Stress Resilience in Plants. Plants 12, 3550. https://doi.org/10.3390/plants12203550

Albrecht, R., Le Petit, J., Terrom, G., Périssol, C., 2011. Comparison between UV spectroscopy and nirs to assess humification process during sewage sludge and green wastes co-composting. Bioresource Technology 102, 4495–4500. https://doi.org/10.1016/j.biortech.2010.12.053

Amann, T., Hartmann, J., Hellmann, R., Pedrosa, E.T., Malik, A., 2022. Enhanced weathering potentials—the role of in situ CO_2 and grain size distribution. Front. Clim. 4. https://doi.org/10.3389/fclim.2022.929268

Anderson, C.R., Peterson, M.E., Frampton, R.A., Bulman, S.R., Keenan, S., Curtin, D., 2018. Rapid increases in soil pH solubilise organic matter, dramatically increase denitrification potential and strongly stimulate microorganisms from the Firmicutes phylum. PeerJ 6, e6090. https://doi.org/10.7717/peerj.6090

Andrade Díaz, C., Albers, A., Zamora-Ledezma, E., Hamelin, L., 2024. The interplay between bioeconomy and the maintenance of long-term soil organic carbon stock in agricultural soils: A systematic review. Renewable and Sustainable Energy Reviews 189, 113890. https://doi.org/10.1016/j.rser.2023.113890

Andres, R.J., Fielding, D.J., Marland, G., Boden, T.A., Kumar, N., Kearney, A.T., 1999. Carbon dioxide emissions from fossil-fuel use, 1751-1950. Tellus B 51, 759–765. https://doi.org/10.1034/j.1600-0889.1999.t01-3-00002.x

Azeem, M., Raza, S., Li, G., Smith, P., Zhu, Y.-G., 2022. Soil inorganic carbon sequestration through alkalinity regeneration using biologically induced weathering of rock powder and biochar. Soil Ecol. Lett. 4, 293–306. https://doi.org/10.1007/s42832-022-0136-4

Aziez, A.F., Prasetyo, A., Paiman, P., 2022. Root Growth Response of Soybean Under Water Deficit. Journal of Biodiversity and Biotechnology 2, 63–69. https://doi.org/10.20961/jbb.v2i2.66465

Bach, L.T., Gill, S.J., Rickaby, R.E.M., Gore, S., Renforth, P., 2019. CO_2 Removal With Enhanced Weathering and Ocean Alkalinity Enhancement: Potential Risks and Co-benefits for Marine Pelagic Ecosystems. Front. Clim. 1. https://doi.org/10.3389/fclim.2019.00007

Badagliacca, G., Lo Presti, E., Gelsomino, A., Monti, M., 2024. Repeated Solid Digestate Amendment Increases Denitrifying Enzyme Activity in an Acid Clayey Soil. Soil Systems 8, 14. https://doi.org/10.3390/soilsystems8010014

Baek, S.H., Kanzaki, Y., Lora, J.M., Planavsky, N., Reinhard, C.T., Zhang, S., 2023. Impact of Climate on the Global Capacity for Enhanced Rock Weathering on Croplands. Earth's Future 11, e2023EF003698. https://doi.org/10.1029/2023EF003698

Ball, D.F., 1964. Loss-on-Ignition as an Estimate of Organic Matter and Organic Carbon in Non-Calcareous Soils. Journal of Soil Science 15, 84–92. https://doi.org/10.1111/j.1365-2389.1964.tb00247.x

Banfield, J.F., Barker, W.W., Welch, S.A., Taunton, A., 1999. Biological impact on mineral dissolution: Application of the lichen model to understanding mineral weathering in the rhizosphere. Proceedings of the National Academy of Sciences 96, 3404–3411. https://doi.org/10.1073/pnas.96.7.3404

Barduca, L., Wentzel, S., Schmidt, R., Malagoli, M., Joergensen, R.G., 2021. Mineralisation of distinct biogas digestate qualities directly after application to soil. Biol Fertil Soils 57, 235–243. https://doi.org/10.1007/s00374-020-01521-5

Barreto, M.S.C., Elzinga, E.J., Ramlogan, M., Rouff, A.A., Alleoni, L.R.F., 2021. Calcium enhances adsorption and thermal stability of organic compounds on soil minerals. Chemical Geology 559, 119804. https://doi.org/10.1016/j.chemgeo.2020.119804

Beerling, D.J., Kantzas, E.P., Lomas, M.R., Wade, P., Eufrasio, R.M., Renforth, P., Sarkar, B., Andrews, M.G., James, R.H., Pearce, C.R., Mercure, J.-F., Pollitt, H., Holden, P.B., Edwards, N.R., Khanna, M., Koh, L., Quegan, S., Pidgeon, N.F., Janssens, I.A., Hansen, J., Banwart, S.A., 2020. Potential for large-scale CO_2 removal via enhanced rock weathering with croplands. Nature 583, 242–248. https://doi.org/10.1038/s41586-020-2448-9

Beerling, D.J., Leake, J.R., Long, S.P., Scholes, J.D., Ton, J., Nelson, P.N., Bird, M., Kantzas, E., Taylor, L.L., Sarkar, B., Kelland, M., DeLucia, E., Kantola, I., Müller, C., Rau, G., Hansen, J., 2018. Farming with crops and rocks to address global climate, food and soil security. Nature Plants 4, 138–147. https://doi.org/10.1038/s41477-018-0108-y

Béghin-Tanneau, R., Guérin, F., Guiresse, M., Kleiber, D., Scheiner, J.D., 2019. Carbon sequestration in soil amended with anaerobic digested matter. Soil and Tillage Research 192, 87–94. https://doi.org/10.1016/j.still.2019.04.024

Bellino, A., Baldantoni, D., Nicola, F.D., Iovieno, P., Zaccardelli, M., Alfani, A., 2015. Compost amendments in agricultural ecosystems: confirmatory path analysis to clarify the effects on soil chemical and biological properties. The Journal of Agricultural Science 153, 282–295. https://doi.org/10.1017/S0021859614000033

Berg, A., Banwart, S.A., 2000. Carbon dioxide mediated dissolution of Ca-feldspar: implications for silicate weathering. Chemical Geology 163, 25–42. https://doi.org/10.1016/S0009-2541(99)00132-1

Bhattacharya, S.S., Kim, K.-H., Das, S., Uchimiya, M., Jeon, B.H., Kwon, E., Szulejko, J.E., 2016. A review on the role of organic inputs in maintaining the soil carbon pool of the terrestrial ecosystem. Journal of Environmental Management 167, 214–227. https://doi.org/10.1016/j.jenvman.2015.09.042

Bhogal, A., Williams, J.R., Nicholson, F.A., Chadwick, D.R., Chambers, K.H., Chambers, B.J., 2016. Mineralization of organic nitrogen from farm manure applications. Soil Use and Management 32, 32–43. https://doi.org/10.1111/sum.12263

Blanc-Betes, E., Kantola, I.B., Gomez-Casanovas, N., Hartman, M.D., Parton, W.J., Lewis, A.L., Beerling, D.J., DeLucia, E.H., 2021. In silico assessment of the potential of basalt amendments to reduce N_2O emissions from bioenergy crops. GCB Bioenergy 13, 224–241. https://doi.org/10.1111/gcbb.12757

Borges, C.S., Ribeiro, B.T., Costa, E.T.D.S., Curi, N., Wendling, B., 2019. Effects of phosphate, carbonate, and silicate anions on CO_2 emission in a typical oxisol from cerrado region. Biosci. J. 35. https://doi.org/10.14393/BJ-v35n4a2019-42239

Bouwman, A.F., Boumans, L.J.M., Batjes, N.H., 2002. Emissions of N_2 O and NO from fertilized fields: Summary of available measurement data. Global Biogeochemical Cycles 16. https://doi.org/10.1029/2001GB001811

Brad, A., Schneider, E., 2023. Carbon dioxide removal and mitigation deterrence in EU climate policy: Towards a research approach. Environmental Science & Policy 150, 103591. https://doi.org/10.1016/j.envsci.2023.103591

Brenzinger, K., Drost, S.M., Korthals, G., Bodelier, P.L.E., 2018. Organic Residue Amendments to Modulate Greenhouse Gas Emissions From Agricultural Soils. Front. Microbiol. 9. https://doi.org/10.3389/fmicb.2018.03035

Buss, W., Hasemer, H., Ferguson, S., Borevitz, J., 2024. Stabilisation of soil organic matter with rock dust partially counteracted by plants. Global Change Biology 30, e17052. https://doi.org/10.1111/gcb.17052

Calusinska, M., Goux, X., Fossépré, M., Muller, E.E.L., Wilmes, P., Delfosse, P., 2018. A year of monitoring 20 mesophilic full-scale bioreactors reveals the existence of stable but different core microbiomes in bio-waste and wastewater anaerobic digestion systems. Biotechnology for Biofuels 11, 196. https://doi.org/10.1186/s13068-018-1195-8

Calvin, K., Dasgupta, D., Krinner, G., Mukherji, A., Thorne, P.W., Trisos, C., Romero, J., Aldunce, P., Barrett, K., Blanco, G., Cheung, W.W.L., Connors, S., Denton, F., Diongue-Niang, A., Dodman, D., Garschagen, M., Geden, O., Hayward, B., Jones, C., Jotzo, F., Krug, T., Lasco, R., Lee, Y.-Y., Masson-Delmotte, V., Meinshausen, M., Mintenbeck, K., Mokssit, A., Otto, F.E.L., Pathak, M., Pirani, A., Poloczanska, E., Pörtner, H.-O., Revi, A., Roberts, D.C., Roy, J., Ruane, A.C., Skea, J., Shukla, P.R., Slade, R., Slangen, A., Sokona, Y., Sörensson, A.A., Tignor, M., Van Vuuren, D., Wei, Y.-M., Winkler, H., Zhai, P., Zommers, Z., Hourcade, J.-C., Johnson, F.X., Pachauri, S., Simpson, N.P., Singh, C., Thomas, A., Totin, E., Arias, P., Bustamante, M., Elgizouli, I., Flato, G., Howden, M., Méndez-Vallejo, C., Pereira, J.J., Pichs-Madruga, R., Rose, S.K., Saheb, Y., Sánchez Rodríguez, R., Ürge-Vorsatz, D., Xiao, C., Yassaa, N., Alegría, A., Armour, K., Bednar-Friedl, B., Blok, K., Cissé, G., Dentener, F., Eriksen, S., Fischer, E., Garner, G., Guivarch, C., Haasnoot, M., Hansen, G., Hauser, M., Hawkins, E., Hermans, T., Kopp, R., Leprince-Ringuet, N., Lewis, J., Ley, D., Ludden, C., Niamir, L., Nicholls, Z., Some, S., Szopa, S., Trewin, B., Van Der Wijst, K.-I., Winter, G., Witting, M., Birt, A., Ha, M., Romero, J., Kim, J., Haites, E.F., Jung, Y., Stavins, R., Birt, A., Ha, M., Orendain, D.J.A., Ignon, L., Park, S., Park, Y., Reisinger, A., Cammaramo, D., Fischlin, A., Fuglestvedt, J.S., Hansen, G., Ludden, C., Masson-Delmotte, V., Matthews, J.B.R., Mintenbeck, K., Pirani, A., Poloczanska, E., Leprince-Ringuet, N., Péan, C., 2023. IPCC, 2023: Climate Change 2023: Synthesis Report. Contribution of Working Groups I, II and III to the Sixth Assessment Report of the Intergovernmental Panel on Climate Change [Core Writing Team, H. Lee and J. Romero (eds.)]. IPCC, Geneva, Switzerland. Intergovernmental Panel on Climate Change (IPCC). https://doi.org/10.59327/IPCC/AR6-9789291691647

Carvalhais, L.C., Dennis, P.G., Fedoseyenko, D., Hajirezaei, M., Borriss, R., Von Wirén, N., 2011. Root exudation of sugars, amino acids, and organic acids by maize as affected by nitrogen, phosphorus, potassium, and iron deficiency. Z. Pflanzenernähr. Bodenk. 174, 3–11. https://doi.org/10.1002/jpln.201000085

Cervarich, M., Shu, S., Jain, A.K., Arneth, A., Canadell, J., Friedlingstein, P., Houghton, R.A., Kato, E., Koven, C., Patra, P., Poulter, B., Sitch, S., Stocker, B., Viovy, N., Wiltshire, A., Zeng, N., 2016. The terrestrial carbon budget of South and Southeast Asia. Environ. Res. Lett. 11, 105006. https://doi.org/10.1088/1748-9326/11/10/105006

César Izaurralde, R., Rosenberg, N.J., Lal, R., 2001. Mitigation of climatic change by soil carbon sequestration: Issues of science, monitoring, and degraded lands, in: Advances in Agronomy. Academic Press, pp. 1–75. https://doi.org/10.1016/S0065-2113(01)70003-X

Chen, H., Shang, Z., Cai, H., Zhu, Y., 2019. Irrigation Combined with Aeration Promoted Soil Respiration through Increasing Soil Microbes, Enzymes, and Crop Growth in Tomato Fields. Catalysts 9, 945. https://doi.org/10.3390/catal9110945

Chen, Q., Zhang, P., Hu, Z., Li, S., Zhang, Y., Hu, L., Zhou, L., Lin, B., Li, X., 2022. Soil Organic Carbon and Geochemical Characteristics on Different Rocks and Their Significance for Carbon Cycles. Front. Environ. Sci. 9. https://doi.org/10.3389/fenvs.2021.784868

Chen, R., Senbayram, M., Blagodatsky, S., Myachina, O., Dittert, K., Lin, X., Blagodatskaya, E., Kuzyakov, Y., 2014. Soil C and N availability determine the priming effect: microbial N mining and stoichiometric decomposition theories. Global Change Biology 20, 2356–2367. https://doi.org/10.1111/gcb.12475

Chen, Xinli, Chen, H.Y.H., Chen, Xin, Wang, J., Chen, B., Wang, D., Guan, Q., 2016. Soil labile organic carbon and carbon-cycle enzyme activities under different thinning intensities in Chinese fir plantations. Applied Soil Ecology 107, 162–169. https://doi.org/10.1016/j.apsoil.2016.05.016

Chen, Z., Xu, Y., He, Y., Zhou, X., Fan, J., Yu, H., Ding, W., 2018. Nitrogen fertilization stimulated soil heterotrophic but not autotrophic respiration in cropland soils: A greater role of organic over inorganic fertilizer. Soil Biology and Biochemistry 116, 253–264. https://doi.org/10.1016/j.soilbio.2017.10.029

Chirinda, N., Olesen, J.E., Porter, J.R., Schjønning, P., 2010a. Soil properties, crop production and greenhouse gas emissions from organic and inorganic fertilizer-based arable cropping systems. Agriculture, Ecosystems & Environment 139, 584–594. https://doi.org/10.1016/j.agee.2010.10.001

Chirinda, N., Olesen, J.E., Porter, J.R., Schjønning, P., 2010b. Soil properties, crop production and greenhouse gas emissions from organic and inorganic fertilizer-based arable cropping systems. Agriculture, Ecosystems & Environment 139, 584–594. https://doi.org/10.1016/j.agee.2010.10.001

Cole-Dai, J., 2010. Volcanoes and climate. Wiley Interdisciplinary Reviews: Climate Change 1, 824–839. https://doi.org/10.1002/wcc.76

Conant, R.T., Ryan, M.G., Ågren, G.I., Birge, H.E., Davidson, E.A., Eliasson, P.E., Evans, S.E., Frey, S.D., Giardina, C.P., Hopkins, F.M., Hyvönen, R., Kirschbaum, M.U.F., Lavallee, J.M., Leifeld, J., Parton, W.J., Megan Steinweg, J., Wallenstein, M.D., Martin Wetterstedt, J.Å., Bradford, M.A., 2011. Temperature and soil organic matter decomposition rates – synthesis of current knowledge and a way forward. Global Change Biology 17, 3392–3404. https://doi.org/10.1111/j.1365-2486.2011.02496.x

Cowie, A.L., Smith, P., Johnson, D., 2006. Does Soil Carbon Loss in Biomass Production Systems Negate the Greenhouse Benefits of Bioenergy? Mitig Adapt Strat Glob Change 11, 979–1002. https://doi.org/10.1007/s11027-006-9030-0

Czubaszek, R., Wysocka-Czubaszek, A., 2018. Emissions of carbon dioxide and methane from fields fertilized with digestate from an agricultural biogas plant. International Agrophysics 32, 29–37. https://doi.org/10.1515/intag-2016-0087

Dang, C., Kong, F., Li, Y., Jiang, Z., Xi, M., 2022. Soil inorganic carbon dynamic change mediated by anthropogenic activities: An integrated study using meta-analysis and random forest model. Science of The Total Environment 835, 155463. https://doi.org/10.1016/j.scitotenv.2022.155463

de Oliveira Garcia, W., Amann, T., Hartmann, J., Karstens, K., Popp, A., Boysen, L.R., Smith, P., Goll, D., 2020. Impacts of enhanced weathering on biomass production for negative emission technologies and soil hydrology. Biogeosciences 17, 2107–2133. https://doi.org/10.5194/bg-17-2107-2020

Deng, Q., Cheng, X., Hui, D., Zhang, Qian, Li, M., Zhang, Quanfa, 2016. Soil microbial community and its interaction with soil carbon and nitrogen dynamics following afforestation in central China. Science of The Total Environment 541, 230–237. https://doi.org/10.1016/j.scitotenv.2015.09.080

Diacono, M., Montemurro, F., 2010. Long-term effects of organic amendments on soil fertility. A review. Agronomy for Sustainable Development 30, 401–422. https://doi.org/10.1051/agro/2009040

Dietzen, C., Harrison, R., Michelsen-Correa, S., 2018a. Effectiveness of enhanced mineral weathering as a carbon sequestration tool and alternative to agricultural lime: An incubation experiment. International Journal of Greenhouse Gas Control 74, 251–258. https://doi.org/10.1016/j.ijggc.2018.05.007

Dietzen, C., Harrison, R., Michelsen-Correa, S., 2018b. Effectiveness of enhanced mineral weathering as a carbon sequestration tool and alternative to agricultural lime: An incubation experiment. International Journal of Greenhouse Gas Control 74, 251–258. https://doi.org/10.1016/j.ijggc.2018.05.007

Dijkstra, F.A., Cheng, W., 2007. Moisture modulates rhizosphere effects on C decomposition in two different soil types. Soil Biology and Biochemistry 39, 2264–2274. https://doi.org/10.1016/j.soilbio.2007.03.026

Dijkstra, F.A., Keitel, C., 2024. Maximising carbon sequestration through mixing compost in moist soil. Soil Biology and Biochemistry 191, 109330. https://doi.org/10.1016/j.soilbio.2024.109330

Ding, S., Zhou, D., Wei, H., Wu, S., Xie, B., 2021. Alleviating soil degradation caused by watermelon continuous cropping obstacle: Application of urban waste compost. Chemosphere 262, 128387. https://doi.org/10.1016/j.chemosphere.2020.128387

Dowell, N.M., Reiner, D.M., Haszeldine, R.S., 2022. Comparing approaches for carbon dioxide removal. Joule 6, 2233–2239. https://doi.org/10.1016/j.joule.2022.09.005

Drigo, B., Kowalchuk, G.A., Knapp, B.A., Pijl, A.S., Boschker, H.T.S., van Veen, J.A., 2013. Impacts of 3 years of elevated atmospheric CO_2 on rhizosphere carbon flow and microbial community dynamics. Global Change Biology 19, 621–636. https://doi.org/10.1111/gcb.12045

Duan, Y., Li, D., Li, Z., Luo, J., Sun, X., Zhang, H., Li, Y., Liu, F., Zhang, K., Hu, Y., Zhang, X., Zhu, Z., 2024. Enhancing phosphorus bioavailability in lateritic red soil: Combining Bacillus subtilis inoculated microbial organic fertilizer with reduced chemical input. Soil Use and Management 40, e12987. https://doi.org/10.1111/sum.12987

Edwards, D.P., Lim, F., James, R.H., Pearce, C.R., Scholes, J., Freckleton, R.P., Beerling, D.J., 2017. Climate change mitigation: potential benefits and pitfalls of enhanced rock weathering in tropical agriculture. Biol. Lett. 13, 20160715. https://doi.org/10.1098/rsbl.2016.0715

Egene, C.E., Regelink, I., Sigurnjak, I., Adani, F., Tack, F.M.G., Meers, E., 2022. Greenhouse gas emissions from a sandy loam soil amended with digestate-derived biobased fertilisers – A microcosm study. Applied Soil Ecology 178, 104577. https://doi.org/10.1016/j.apsoil.2022.104577

Elisa, A.A., Ninomiya, S., Shamshuddin, J., Roslan, I., 2016. Alleviating aluminum toxicity in an acid sulfate soil from Peninsular Malaysia by calcium silicate application. Solid Earth 7, 367–374. https://doi.org/10.5194/se-7-367-2016

Flanagan, L.B., Johnson, B.G., 2005. Interacting effects of temperature, soil moisture and plant biomass production on ecosystem respiration in a northern temperate grassland. Agricultural and Forest Meteorology 130, 237–253. https://doi.org/10.1016/j.agrformet.2005.04.002

Foereid, B., Szocs, J., Patinvoh, R.J., Horváth, I.S., 2021. Effect of anaerobic digestion of manure before application to soil – benefitsfor nitrogen utilisation? International Journal of Recycling of Organic Waste in Agriculture 10. https://doi.org/10.30486/ijrowa.2020.1897538.1055

Foroud, N., Mündel, H.-H., Saindon, G., Entz, T., 1993. Effect of level and timing of moisture stress on soybean plant development and yield components. Irrig Sci 13, 149–155. https://doi.org/10.1007/BF00190029

Freibauer, A., Rounsevell, M.D.A., Smith, P., Verhagen, J., 2004. Carbon sequestration in the agricultural soils of Europe. Geoderma 122, 1–23. https://doi.org/10.1016/j.geoderma.2004.01.021

Fu, L., Yan, Y., Li, X., Liu, Y., Lu, X., 2022. Rhizosphere soil microbial community and its response to different utilization patterns in the semi-arid alpine grassland of northern Tibet. Front. Microbiol. 13. https://doi.org/10.3389/fmicb.2022.931795

Fuss, S., Lamb, W.F., Callaghan, M.W., Hilaire, J., Creutzig, F., Amann, T., Beringer, T., Garcia, W. de O., Hartmann, J., Khanna, T., Luderer, G., Nemet, G.F., Rogelj, J., Smith, P., Vicente, J.L.V., Wilcox, J., Dominguez, M. del M.Z., Minx, J.C., 2018. Negative emissions—Part 2: Costs, potentials and side effects. Environ. Res. Lett. 13, 063002. https://doi.org/10.1088/1748-9326/aabf9f

Gabriel, J.L., Quemada, M., 2011. Replacing bare fallow with cover crops in a maize cropping system: Yield, N uptake and fertiliser fate. European Journal of Agronomy 34, 133–143. https://doi.org/10.1016/j.eja.2010.11.006

Galamini, G., Ferretti, G., Rosinger, C., Huber, S., Mentler, A., Diaz–Pines, E., Faccini, B., Keiblinger, K.M., 2025. Potential for agricultural recycling of struvite and zeolites to improve soil microbial physiology and mitigate CO2 emissions. Geoderma 453, 117149. https://doi.org/10.1016/j.geoderma.2024.117149

Golicz, K., Hallett, S.H., Sakrabani, R., Pan, G., 2019. The potential for using smartphones as portable soil nutrient analyzers on suburban farms in central East China. Sci Rep 9, 16424. https://doi.org/10.1038/s41598-019-52702-8

Gore, S., Renforth, P., Perkins, R., 2019. The potential environmental response to increasing oceanalkalinity for negative emissions. Mitig Adapt Strateg Glob Change 24, 1191–1211. https://doi.org/10.1007/s11027-018-9830-z

Graven, H., Keeling, R.F., Rogelj, J., 2020. Changes to Carbon Isotopes in Atmospheric CO_2 Over the Industrial Era and Into the Future. Global Biogeochemical Cycles 34, e2019GB006170. https://doi.org/10.1029/2019GB006170

Guo, F., Sun, H., Yang, J., Zhang, L., Mu, Y., Wang, Y., Wu, F., 2023a. Improving food security and farmland carbon sequestration in China through enhanced rock weathering: Field evidence and potential assessment in different humid regions. Science of The Total Environment 903, 166118. https://doi.org/10.1016/j.scitotenv.2023.166118

Guo, F., Wang, Y., Zhu, H., Zhang, C., Sun, H., Fang, Z., Yang, J., Zhang, L., Mu, Y., Man, Y.B., Wu, F., 2023b. Crop productivity and soil inorganic carbon change mediated by enhanced rock weathering in farmland: A comparative field analysis of multi-agroclimatic regions in central China. Agricultural Systems 210, 103691. https://doi.org/10.1016/j.agsy.2023.103691

Guo, Z., Wang, Y., Wan, Z., Zuo, Y., He, L., Li, D., Yuan, F., Wang, N., Liu, J., Song, Y., Song, C., Xu, X., 2020. Soil dissolved organic carbon in terrestrial ecosystems: Global budget, spatial distribution and controls. Global Ecology and Biogeography 29, 2159–2175. https://doi.org/10.1111/geb.13186

Han, H., Teng, Y., Yang, H., Li, J., 2017. Effects of Long-Term Use of Compost on N2O and CO2 Fluxes in Greenhouse Vegetable Systems. Compost Science & Utilization 25, S61–S69. https://doi.org/10.1080/1065657X.2016.1238786

Han, W.-Y., Xu, J.-M., Wei, K., Shi, R.-Z., Ma, L.-F., 2013. Soil carbon sequestration, plant nutrients and biological activities affected by organic farming system in tea (Camellia sinensis (L.) O. Kuntze) fields. Soil Science and Plant Nutrition 59, 727–739. https://doi.org/10.1080/00380768.2013.833857

Haque, F., Santos, R.M., Chiang, Y.W., 2020. CO2 sequestration by wollastonite-amended agricultural soils – An Ontario field study. International Journal of Greenhouse Gas Control 97, 103017. https://doi.org/10.1016/j.ijggc.2020.103017

Harrington, K.J., Hilton, R.G., Henderson, G.M., 2023. Implications of the Riverine Response to Enhanced Weathering for CO_2 removal in the UK. Applied Geochemistry 152, 105643. https://doi.org/10.1016/j.apgeochem.2023.105643

Hartmann, J., West, A.J., Renforth, P., Köhler, P., De La Rocha, C.L., Wolf-Gladrow, D.A., Dürr, H.H., Scheffran, J., 2013. Enhanced chemical weathering as a geoengineering strategy to reduce atmospheric carbon dioxide, supply nutrients, and mitigate ocean acidification. Reviews of Geophysics 51, 113–149. https://doi.org/10.1002/rog.20004

He, X., Chi, Q., Cai, Z., Cheng, Y., Zhang, J., Müller, C., 2020. 15N tracing studies including plant N uptake processes provide new insights on gross N transformations in soil-plant systems. Soil Biology and Biochemistry 141, 107666. https://doi.org/10.1016/j.soilbio.2019.107666

He, Z., Ding, B., Pei, S., Cao, H., Liang, J., Li, Z., 2023. The impact of organic fertilizer replacement on greenhouse gas emissions and its influencing factors. Science of The Total Environment 905, 166917. https://doi.org/10.1016/j.scitotenv.2023.166917

Hendricks, S., Zechmeister-Boltenstern, S., Kandeler, E., Sandén, T., Diaz-Pines, E., Schnecker, J., Alber, O., Miloczki, J., Spiegel, H., 2022. Agricultural management affects active carbon and nitrogen mineralisation potential in soils. Journal of Plant Nutrition and Soil Science 185, 513–528. https://doi.org/10.1002/jpln.202100130

Hicks, A., Dholabhai, P., Ali, A., Santos, R.M., 2022. Nutrient-doped synthetic silicates for enhanced weathering, remineralization and fertilization on agricultural lands of global cold regions – A perspective on the research ahead. iScience 25, 105556. https://doi.org/10.1016/j.isci.2022.105556

Hinsinger, P., Bengough, A.G., Vetterlein, D., Young, I.M., 2009. Rhizosphere: biophysics, biogeochemistry and ecological relevance. Plant Soil 321, 117–152. https://doi.org/10.1007/s11104-008-9885-9

Holatko, J., Hammerschmiedt, T., Mustafa, A., Kintl, A., Radziemska, M., Baltazar, T., Jaskulska, I., Malicek, O., Latal, O., Brtnicky, M., 2022. Carbon-enriched organic amendments differently affect the soil chemical, biological properties and plant biomass in a cultivation time-dependent manner. Chem. Biol. Technol. Agric. 9, 52. https://doi.org/10.1186/s40538-022-00319-x

Holden, F.J., Davies, K., Bird, M.I., Hume, R., Green, H., Beerling, D.J., Nelson, P.N., 2024. In-field carbon dioxide removal via weathering of crushed basalt applied to acidic tropical agricultural soil. Science of The Total Environment 955, 176568. https://doi.org/10.1016/j.scitotenv.2024.176568

Holland, J.E., Fornara, D., Gordon, A., Boughton, C.J., 2024. Effects of nutrient fertilization and soil tillage on soil CO2 emissions in a long-term grassland experiment. Soil and Tillage Research 244, 106232. https://doi.org/10.1016/j.still.2024.106232

Hseu, Z.-Y., 2004. Evaluating heavy metal contents in nine composts using four digestion methods. Bioresource Technology 95, 53–59. https://doi.org/10.1016/j.biortech.2004.02.008

Huang, X., Jia, Z., Guo, J., Li, T., Sun, D., Meng, H., Yu, G., He, X., Ran, W., Zhang, S., Hong, J., Shen, Q., 2019. Ten-year long-term organic fertilization enhances carbon sequestration and calcium-mediated stabilization of aggregate-associated organic carbon in a reclaimed Cambisol. Geoderma 355, 113880. https://doi.org/10.1016/j.geoderma.2019.113880

Immovilli, A., Fabbri, C., Valli, L., 2008. Odour and ammonia emissions from cattle slurry treated with anaerobic digestion. Chem. Eng. Trans 15, 247–254.

Impraim, R., Weatherley, A., Chen, D., Suter, H., 2022. Effect of lignite amendment on carbon and nitrogen mineralization from raw and composted manure during incubation with soil. Pedosphere 32, 785–795. https://doi.org/10.1016/j.pedsph.2022.06.003

IPCC, 2023. Climate Change 2022 – Impacts, Adaptation and Vulnerability: Working Group II Contribution to the Sixth Assessment Report of the Intergovernmental Panel on Climate Change, 1st ed. Cambridge University Press. https://doi.org/10.1017/9781009325844

IPCC, 2018. Global Warming of 1.5 ºC —. URL https://www.ipcc.ch/sr15/ (accessed 12.23.24).

IPCC, 2005. Carbon Dioxide Capture and Storage — IPCC. URL https://www.ipcc.ch/report/carbon-dioxide-capture-and-storage/ (accessed 12.23.24).

IUSS Working Group WRB, 2006. World reference base for soil resources 2006 - A framework for international classification, correlation and communication [WWW

Document]. EPIC3Rome, Food and Agriculture Organization of the United Nations. URL https://epic.awi.de/id/eprint/35324/ (accessed 10.31.21).

Jariwala, H., Haque, F., Vanderburgt, S., Santos, R.M., Chiang, Y.W., 2022. Mineral–Soil–Plant–Nutrient Synergisms of Enhanced Weathering for Agriculture: Short-Term Investigations Using Fast-Weathering Wollastonite Skarn. Front. Plant Sci. 13. https://doi.org/10.3389/fpls.2022.929457

Jin, L., Wei, D., Yin, D., Zou, G., Li, Y., Zhang, Y., Ding, J., Wang, L., Liang, L., Sun, L., Wang, W., Shen, H., Wang, Y., Xu, J., 2023. Prediction of Soil Water-Soluble Organic Matter by Continuous Use of Corn Biochar Using Three-Dimensional Fluorescence Spectra and Deep Learning. Comput Intell Neurosci 2023, 7535594. https://doi.org/10.1155/2023/7535594

Jing, H., Wang, J., Wang, G., Liu, G., Cheng, Y., 2023. Enzyme activities of rhizosphere soil with different root diameters had varied responses to N deposition in *Pinus tabuliformis* forest. Forest Ecology and Management 548, 121396. https://doi.org/10.1016/j.foreco.2023.121396

Jones, D.L., Cooledge, E.C., Hoyle, F.C., Griffiths, R.I., Murphy, D.V., 2019. pH and exchangeable aluminum are major regulators of microbial energy flow and carbon use efficiency in soil microbial communities. Soil Biology and Biochemistry 138, 107584. https://doi.org/Malik

Joseph, R.A., Van Hai, T., Lambert, J., 1976. Effect of ammonium concentration on growth and nitrogen accumulation by soybean grown in nutrient solution. Biol Plant 18, 339–343. https://doi.org/10.1007/BF02922459

Kantola, I.B., Blanc-Betes, E., Masters, M.D., Chang, E., Marklein, A., Moore, C.E., von Haden, A., Bernacchi, C.J., Wolf, A., Epihov, D.Z., Beerling, D.J., DeLucia, E.H., 2023. Improved net carbon budgets in the US Midwest through direct measured impacts of enhanced weathering. Global Change Biology 29, 7012–7028. https://doi.org/10.1111/gcb.16903

Keel, S.G., Anken, T., Büchi, L., Chervet, A., Fliessbach, A., Flisch, R., Huguenin-Elie, O., Mäder, P., Mayer, J., Sinaj, S., Sturny, W., Wüst-Galley, C., Zihlmann, U., Leifeld, J., 2019. Loss of soil organic carbon in Swiss long-term agricultural experiments over a wide range of management practices. Agriculture, Ecosystems & Environment 286, 106654. https://doi.org/10.1016/j.agee.2019.106654

Kelland, M.E., Wade, P.W., Lewis, A.L., Taylor, L.L., Sarkar, B., Andrews, M.G., Lomas, M.R., Cotton, T.E.A., Kemp, S.J., James, R.H., Pearce, C.R., Hartley, S.E., Hodson, M.E., Leake, J.R., Banwart, S.A., Beerling, D.J., 2020. Increased yield and CO_2 sequestration potential with the C4 cereal Sorghum bicolor cultivated in basaltic rock dust-amended agricultural soil. Global Change Biology 26, 3658–3676. https://doi.org/10.1111/gcb.15089

Keuper, F., Wild, B., Kummu, M., Beer, C., Blume-Werry, G., Fontaine, S., Gavazov, K., Gentsch, N., Guggenberger, G., Hugelius, G., Jalava, M., Koven, C., Krab, E.J., Kuhry, P., Monteux, S., Richter, A., Shahzad, T., Weedon, J.T., Dorrepaal, E., 2020. Carbon loss from northern circumpolar permafrost soils amplified by rhizosphere priming. Nat. Geosci. 13, 560–565. https://doi.org/10.1038/s41561-020-0607-0

Khalsa, S.D.S., Smart, D.R., Muhammad, S., Armstrong, C.M., Sanden, B.L., Houlton, B.Z., Brown, P.H., 2020. Intensive fertilizer use increases orchard N cycling and lowers net global warming potential. Science of The Total Environment 722, 137889. https://doi.org/10.1016/j.scitotenv.2020.137889

Kindler, R., Siemens, J., Kaiser, K., Walmsley, D.C., Bernhofer, C., Buchmann, N., Cellier, P., Eugster, W., Gleixner, G., Grũnwald, T., Heim, A., Ibrom, A., Jones, S.K., Jones, M., Klumpp, K., Kutsch, W., Larsen, K.S., Lehuger, S., Loubet, B., Mckenzie, R., Moors, E., Osborne, B., Pilegaard, K., Rebmann, C., Saunders, M., Schmidt, M.W.I., Schrumpf, M., Seyfferth, J., Skiba, U., Soussana, J.-F., Sutton, M.A., Tefs, C., Vowinckel, B., Zeeman, M.J., Kaupenjohann, M., 2011. Dissolved carbon leaching from soil is a crucial component of the net ecosystem carbon balance. Global Change Biology 17, 1167–1185. https://doi.org/10.1111/j.1365-2486.2010.02282.x

Kirschbaum, M.U.F., 2000. Will changes in soil organic carbon act as a positive or negative feedback on global warming? Biogeochemistry 48, 21–51. https://doi.org/10.1023/A:1006238902976

Kitamura, R., Sugiyama, C., Yasuda, K., Nagatake, A., Yuan, Y., Du, J., Yamaki, N., Taira, K., Kawai, M., Hatano, R., 2021. Effects of Three Types of Organic Fertilizers on Greenhouse Gas Emissions in a Grassland on Andosol in Southern Hokkaido, Japan. Front. Sustain. Food Syst. 5. https://doi.org/10.3389/fsufs.2021.649613

Kleber, M., 2010. What is recalcitrant soil organic matter? Environ. Chem. 7, 320–332. https://doi.org/10.1071/EN10006

Klotz, F., Horst, W.J., 1988. Effect of ammonium- and nitrate-nitrogen nutrition on aluminium tolerance of soybean (Glycine max L.). Plant Soil 111, 59–65. https://doi.org/10.1007/BF02182037

Knowles, J.F., Blanken, P.D., Williams, M.W., 2015. Soil respiration variability across a soil moisture and vegetation community gradient within a snow-scoured alpine meadow. Biogeochemistry 125, 185–202. https://doi.org/10.1007/s10533-015-0122-3

Kobierski, M., Kondratowicz-Maciejewska, K., Banach-Szott, M., Wojewódzki, P., Peñas Castejón, J.M., 2018. Humic substances and aggregate stability in rhizospheric and non-rhizospheric soil. J Soils Sediments 18, 2777–2789. https://doi.org/10.1007/s11368-018-1935-1

Kosslak, R.M., Chamberlin, M.A., Palmer, R.G., Bowen, B.A., 1997. Programmed cell death in the root cortex of soybean root necrosis mutants. The Plant Journal 11, 729–745. https://doi.org/10.1046/j.1365-313X.1997.11040729.x

Lal, R., 2004. Soil carbon sequestration to mitigate climate change. Geoderma 123, 1–22. https://doi.org/10.1016/j.geoderma.2004.01.032

Lamolinara, B., Pérez-Martínez, A., Guardado-Yordi, E., Guillén Fiallos, C., Diéguez-Santana, K., Ruiz-Mercado, G.J., 2022. Anaerobic digestate management, environmental impacts, and techno-economic challenges. Waste Management 140, 14–30. https://doi.org/10.1016/j.wasman.2021.12.035

Lan, T., Hao, L., Lu, J., Yin, Y., Chen, X., Fan, Y., Zhao, W., Hou, Y., 2021. Geochemical Behavior of Different Chemical Elements during Weathering of the Basalts in Changbai Mountain, Northeast China. Sustainability 13, 12796. https://doi.org/10.3390/su132212796

Lark, R.M., Ferguson, R.B., 2004. Mapping risk of soil nutrient deficiency or excess by disjunctive and indicator kriging. Geoderma 118, 39–53. https://doi.org/10.1016/S0016-7061(03)00168-X

Lawrence, C., Harden, J., Maher, K., 2014. Modeling the influence of organic acids on soil weathering. Geochimica et Cosmochimica Acta 139, 487–507. https://doi.org/10.1016/j.gca.2014.05.003

Lazcano, C., Gómez-Brandón, M., Revilla, P., Domínguez, J., 2013. Short-term effects of organic and inorganic fertilizers on soil microbial community structure and function. Biol Fertil Soils 49, 723–733. https://doi.org/10.1007/s00374-012-0761-7

Lean, J.L., 2010. Cycles and trends in solar irradiance and climate. WIREs Climate Change 1, 111–122. https://doi.org/10.1002/wcc.18

Lefebvre, D., Goglio, P., Williams, A., Manning, D.A.C., de Azevedo, A.C., Bergmann, M., Meersmans, J., Smith, P., 2019. Assessing the potential of soil carbonation and enhanced weathering through Life Cycle Assessment: A case study for Sao Paulo State, Brazil. Journal of Cleaner Production 233, 468–481. https://doi.org/10.1016/j.jclepro.2019.06.099

Lehmann, J., Gaunt, J., Rondon, M., 2006. Bio-char Sequestration in Terrestrial Ecosystems – A Review. Mitig Adapt Strat Glob Change 11, 403–427. https://doi.org/10.1007/s11027-005-9006-5

Leroux, L., Faye, N.F., Jahel, C., Falconnier, G.N., Diouf, A.A., Ndao, B., Tiaw, I., Senghor, Y., Kanfany, G., Balde, A., Dieye, M., Sirdey, N., Alobo Loison, S., Corbeels, M., Baudron, F., Bouquet, E., 2022. Exploring the agricultural landscape diversity-food security nexus: an analysis in two contrasted parklands of Central Senegal. Agricultural Systems 196, 103312. https://doi.org/10.1016/j.agsy.2021.103312

Leuning, R., Etheridge, D., Luhar, A., Dunse, B., 2008. Atmospheric monitoring and verification technologies for CO2 geosequestration. International Journal of Greenhouse

Gas Control, EGU General Assembly 2007: Advances in CO2 Storage in Geological Systems 2, 401–414. https://doi.org/10.1016/j.ijggc.2008.01.002

Lewis, A.L., Sarkar, B., Wade, P., Kemp, S.J., Hodson, M.E., Taylor, L.L., Yeong, K.L., Davies, K., Nelson, P.N., Bird, M.I., Kantola, I.B., Masters, M.D., DeLucia, E., Leake, J.R., Banwart, S.A., Beerling, D.J., 2021. Effects of mineralogy, chemistry and physical properties of basalts on carbon capture potential and plant-nutrient element release via enhanced weathering. Applied Geochemistry 132, 105023. https://doi.org/10.1016/j.apgeochem.2021.105023

Li, C., Ma, Shou-chen, Shao, Y., Ma, Shou-tian, Zhang, L., 2018. Effects of long-term organic fertilization on soil microbiologic characteristics, yield and sustainable production of winter wheat. Journal of Integrative Agriculture 17, 210–219. https://doi.org/10.1016/S2095-3119(17)61740-4

Li, Gaojun, Hartmann, J., Derry, L.A., West, A.J., You, C.-F., Long, X., Zhan, T., Li, L., Li, Gen, Qiu, W., Li, T., Liu, L., Chen, Y., Ji, J., Zhao, L., Chen, J., 2016. Temperature dependence of basalt weathering. Earth and Planetary Science Letters 443, 59–69. https://doi.org/10.1016/j.epsl.2016.03.015

Li, M., Shimizu, M., Hatano, R., 2015. Evaluation of N2O and CO2 hot moments in managed grassland and cornfield, southern Hokkaido, Japan. CATENA 133, 1–13. https://doi.org/10.1016/j.catena.2015.04.014

Li, Z., Wei, B., Wang, X., Zhang, Y., Zhang, A., 2018. Response of soil organic carbon fractions and CO_2 emissions to exogenous composted manure and calcium carbonate. J Soils Sediments 18, 1832–1843. https://doi.org/10.1007/s11368-018-1946-y

Liang, C., Hao, X., Schoenau, J., Ma, B.-L., Zhang, T., MacDonald, J.D., Chantigny, M., Dyck, M., Smith, W.N., Malhi, S.S., Thiagarajan, A., Lafond, J., Angers, D., 2021. Manure-induced carbon retention measured from long-term field studies in Canada. Agriculture, Ecosystems & Environment 321, 107619. https://doi.org/10.1016/j.agee.2021.107619

Liang, C., Piñeros, M.A., Tian, J., Yao, Z., Sun, L., Liu, J., Shaff, J., Coluccio, A., Kochian, L.V., Liao, H., 2013. Low pH, Aluminum, and Phosphorus Coordinately Regulate Malate Exudation through GmALMT1 to Improve Soybean Adaptation to Acid Soils. Plant Physiology 161, 1347–1361. https://doi.org/10.1104/pp.112.208934

Liang, Y., Al-Kaisi, M., Yuan, J., Liu, J., Zhang, H., Wang, L., Cai, H., Ren, J., 2021. Effect of chemical fertilizer and straw-derived organic amendments on continuous maize yield, soil carbon sequestration and soil quality in a Chinese Mollisol. Agriculture, Ecosystems & Environment 314, 107403. https://doi.org/10.1016/j.agee.2021.107403

Liu, H., Li, D., Huang, Y., Lin, Q., Huang, L., Cheng, S., Sun, S., Zhu, Z., 2023. Addition of bacterial consortium produced high-quality sugarcane bagasse compost as an environmental-friendly fertilizer: Optimizing arecanut (*Areca catechu* L.) production, soil fertility and microbial community structure. Applied Soil Ecology 188, 104920. https://doi.org/10.1016/j.apsoil.2023.104920

Liu, L., Greaver, T.L., 2010. A global perspective on belowground carbon dynamics under nitrogen enrichment. Ecology Letters 13, 819–828. https://doi.org/10.1111/j.1461-0248.2010.01482.x

Liu, S., Lin, F., Wu, S., Ji, C., Sun, Y., Jin, Y., Li, S., Li, Z., Zou, J., 2017. A meta-analysis of fertilizer-induced soil NO and combined NO+N2O emissions. Global Change Biology 23, 2520–2532. https://doi.org/10.1111/gcb.13485

Liu, X., Herbert, S.J., Hashemi, A.M., Zhang, X., Ding, G., 2006. Effects of agricultural management on soil organic matter and carbon transformation - a review. Plant, Soil and Environment 52, 531–543. https://doi.org/10.17221/3544-PSE

Liyanage, L.R.M.C., Sulaiman, M.F., Ismail, R., Gunaratne, G.P., Dharmakeerthi, R.S., Rupasinghe, M.G.N., Mayakaduwa, A.P., Hanafi, M.M., 2021. Carbon Mineralization Dynamics of Organic Materials and Their Usage in the Restoration of Degraded Tropical Tea-Growing Soil. Agronomy 11, 1191. https://doi.org/10.3390/agronomy11061191

Long, G.-Q., Jiang, Y.-J., Sun, B., 2015. Seasonal and inter-annual variation of leaching of dissolved organic carbon and nitrogen under long-term manure application in an acidic clay soil in subtropical China. Soil and Tillage Research 146, 270–278. https://doi.org/10.1016/j.still.2014.09.020

Lorenz, K., Lal, R., 2016. Environmental Impact of Organic Agriculture, in: Advances in Agronomy. Elsevier, pp. 99–152. https://doi.org/10.1016/bs.agron.2016.05.003

Loubet, B., Laville, P., Lehuger, S., Larmanou, E., Fléchard, C., Mascher, N., Genermont, S., Roche, R., Ferrara, R.M., Stella, P., Personne, E., Durand, B., Decuq, C., Flura, D., Masson, S., Fanucci, O., Rampon, J.-N., Siemens, J., Kindler, R., Gabrielle, B., Schrumpf, M., Cellier, P., 2011. Carbon, nitrogen and Greenhouse gases budgets over a four years crop rotation in northern France. Plant Soil 343, 109–137. https://doi.org/10.1007/s11104-011-0751-9

Lu, T., Wang, X., Zhang, W., 2020. Total and dissolved soil organic and inorganic carbon and their relationships in typical loess cropland of Fengu Basin. Geoscience Letters 7, 17. https://doi.org/10.1186/s40562-020-00167-3

Luan, H., Gao, W., Huang, S., Tang, J., Li, M., Zhang, H., Chen, X., Masiliūnas, D., 2020. Organic amendment increases soil respiration in a greenhouse vegetable production system through decreasing soil organic carbon recalcitrance and increasing carbon-degrading microbial activity. J Soils Sediments 20, 2877–2892. https://doi.org/10.1007/s11368-020-02625-z

Luchese, A.V., Pivetta, L.A., Batista, M.A., Steiner, F., Giaretta, A.P. da S., Curtis, J.C.D., 2021. Agronomic feasibility of using basalt powder as soil nutrient remineralizer. AJAR 17, 487–497. https://doi.org/10.5897/AJAR2020.15234

Luo, K., Ma, J., Wang, Z., Zhu, G., Zeng, T., Wei, G., 2024. Fractionation Mechanism and Flux Estimation of Strontium Isotopes During Basalt Weathering. Geochemistry, Geophysics, Geosystems 25, e2023GC011215. https://doi.org/10.1029/2023GC011215

Lv, B., Zhang, D., Cui, Y., Yin, F., 2018. Effects of C/N ratio and earthworms on greenhouse gas emissions during vermicomposting of sewage sludge. Bioresource Technology 268, 408–414. https://doi.org/10.1016/j.biortech.2018.08.004

M. San-Emeterio, L., De la Rosa, J.M., Knicker, H., López-Núñez, R., González-Pérez, J.A., 2023. Evolution of Maize Compost in a Mediterranean Agricultural Soil: Implications for Carbon Sequestration. Agronomy 13, 769. https://doi.org/10.3390/agronomy13030769

Maillard, É., Angers, D.A., 2014. Animal manure application and soil organic carbon stocks: a meta-analysis. Global Change Biology 20, 666–679. https://doi.org/10.1111/gcb.12438

Malik, A.A., Puissant, J., Buckeridge, K.M., Goodall, T., Jehmlich, N., Chowdhury, S., Gweon, H.S., Peyton, J.M., Mason, K.E., van Agtmaal, M., Blaud, A., Clark, I.M., Whitaker, J., Pywell, R.F., Ostle, N., Gleixner, G., Griffiths, R.I., 2018. Land use driven change in soil pH affects microbial carbon cycling processes. Nat Commun 9, 3591. https://doi.org/10.1038/s41467-018-05980-1

McDaniel, M.D., Middleton, T.A., 2024. Putting the soil health principles to the test in Iowa. Soil Science Society of America Journal 88, 2238–2253. https://doi.org/10.1002/saj2.20761

Medeiros, F. de P., Carvalho, A.M.X. de, Gindri Ramos, C., Dotto, G.L., Cardoso, I.M., Theodoro, S.H., 2024. Rock Powder Enhances Soil Nutrition and Coffee Quality in Agroforestry Systems. Sustainability 16, 354. https://doi.org/10.3390/su16010354

Meng, F., Qiao, Y., Wu, W., Smith, P., Scott, S., 2017. Environmental impacts and production performances of organic agriculture in China: A monetary valuation. Journal of Environmental Management 188, 49–57. https://doi.org/10.1016/j.jenvman.2016.11.080

Mi, N., Wang, S., Liu, J., Yu, G., Zhang, W., Jobbágy, E., 2008. Soil inorganic carbon storage pattern in China. Global Change Biology 14, 2380–2387. https://doi.org/10.1111/j.1365-2486.2008.01642.x

Miao, Y., Niu, Y., Luo, R., Li, Y., Zheng, H., Kuzyakov, Y., Chen, Z., Liu, D., Ding, W., 2021. Lower microbial carbon use efficiency reduces cellulose-derived carbon retention in soils amended with compost versus mineral fertilizers. Soil Biology and Biochemistry 156, 108227. https://doi.org/10.1016/j.soilbio.2021.108227

Milkereit, J., Burger, M., Hodson, A.K., 2025. Influence of recycled organic waste amendments on carbon pools, greenhouse gas emissions, and nematode indicators of soil health. Applied Soil Ecology 208, 105967. https://doi.org/10.1016/j.apsoil.2025.105967

Miller, S.B., Heuberger, A.L., Broeckling, C.D., Jahn, C.E., 2019. Non-Targeted Metabolomics Reveals Sorghum Rhizosphere-Associated Exudates are Influenced by the Belowground Interaction of Substrate and Sorghum Genotype. International Journal of Molecular Sciences 20, 431. https://doi.org/10.3390/ijms20020431

Miura, T., Okuno, R., 1993. Detailed Description of Calculation of Potential Evapotranspiration Using the Penman Equation. Transactions of The Japanese Society of Irrigation, Drainage and Reclamation Engineering 1993, 157-163,a3. https://doi.org/10.11408/jsidre1965.1993.164_157

Mustapha, A.A., Abdu, N., Oyinlola, E.Y., Nuhu, A.A., 2023. Evaluating Different Methods of Organic Carbon Estimation on Nigerian Savannah Soils. J Soil Sci Plant Nutr 23, 790–800. https://doi.org/10.1007/s42729-022-01082-6

Nazir, M.J., Hussain, M.M., Albasher, G., Iqbal, B., Khan, K.A., Rahim, R., Li, G., Du, D., 2024. Glucose input profit soil organic carbon mineralization and nitrogen dynamics in relation to nitrogen amended soils. Journal of Environmental Management 351, 119715. https://doi.org/10.1016/j.jenvman.2023.119715

NOAA, 2024. Climate Change: Atmospheric Carbon Dioxide | NOAA Climate.gov [WWW Document]. URL http://www.climate.gov/news-features/understanding-climate/climate-change-atmospheric-carbon-dioxide (accessed 12.23.24).

Ofosu-Budu, K.G., Fujita, K., Ogata, S., 1990. Excretion of ureide and other nitrogenous compounds by the root system of soybean at different growth stages. Plant Soil 128, 135–142. https://doi.org/10.1007/BF00011102

Ögren, E., Evans, J.R., 1993. Photosynthetic light-response curves. Planta 189, 182–190. https://doi.org/10.1007/BF00195075

Parson, E.A., Buck, H.J., 2020. Large-Scale Carbon Dioxide Removal: The Problem of Phasedown. Global Environmental Politics 20, 70–92. https://doi.org/10.1162/glep_a_00575

Patrícia Vieira da Cunha, K., Williams Araújo do Nascimento, C., José da Silva, A., 2008. Silicon alleviates the toxicity of cadmium and zinc for maize (Zea mays L.) grown on a contaminated soil. Journal of Plant Nutrition and Soil Science 171, 849–853. https://doi.org/10.1002/jpln.200800147

Paustian, K., Lehmann, J., Ogle, S., Reay, D., Robertson, G.P., Smith, P., 2016. Climate-smart soils. Nature 532, 49–57. https://doi.org/10.1038/nature17174

Peachey, D., Roberts, J.L., Scot-Baker, J., 1973. Rapid colorimetric determination of phosphorus in geochemical survey samples. Journal of Geochemical Exploration 2, 115–120. https://doi.org/10.1016/0375-6742(73)90010-1

Powlson, D.S., Gregory, P.J., Whalley, W.R., Quinton, J.N., Hopkins, D.W., Whitmore, A.P., Hirsch, P.R., Goulding, K.W.T., 2011. Soil management in relation to sustainable agriculture and ecosystem services. Food Policy, The challenge of global food sustainability 36, S72–S87. https://doi.org/10.1016/j.foodpol.2010.11.025

Prescher, A.-K., Grünwald, T., Bernhofer, C., 2010. Land use regulates carbon budgets in eastern Germany: From NEE to NBP. Agricultural and Forest Meteorology 150, 1016–1025. https://doi.org/10.1016/j.agrformet.2010.03.008

Ramos, C.G., Querol, X., Oliveira, M.L.S., Pires, K., Kautzmann, R.M., Oliveira, L.F.S., 2015. A preliminary evaluation of volcanic rock powder for application in agriculture as soil a remineralizer. Science of The Total Environment 512–513, 371–380. https://doi.org/10.1016/j.scitotenv.2014.12.070

Ramteke, P., Gabhane, V., Kadu, P., Kharche, V., Jadhao, S., Turkhede, A., Gajjala, R.C., 2024. Long-term nutrient management effects on organic carbon fractions and carbon sequestration in Typic Haplusterts soils of Central India. Soil Use and Management 40, e12950. https://doi.org/10.1111/sum.12950

Rau, G.H., Caldeira, K., 1999. Enhanced carbonate dissolution: a means of sequestering waste CO_2 as ocean bicarbonate. Energy Conversion.

Raza, S., Miao, N., Wang, P., Ju, X., Chen, Z., Zhou, J., Kuzyakov, Y., 2020. Dramatic loss of inorganic carbon by nitrogen-induced soil acidification in Chinese croplands. Global Change Biology 26, 3738–3751. https://doi.org/10.1111/gcb.15101

Reifschneider, L., Eichinger, V.F., Pihlap, E., Garcia-Franco, N., Kühnel, A., Bucka, F., Kögel-Knabner, I., Vidal, A., 2021. Can we improve soil properties and plant biomass using rock powder as soil amendment? (No. EGU21-4512). Presented at the EGU21, Copernicus Meetings. https://doi.org/10.5194/egusphere-egu21-4512

Ren, J., Liu, X., Yang, W., Yang, X., Li, W., Xia, Q., Li, J., Gao, Z., Yang, Z., 2021. Rhizosphere soil properties, microbial community, and enzyme activities: Short-term responses to partial substitution of chemical fertilizer with organic manure. Journal of

Environmental Management 299, 113650. https://doi.org/10.1016/j.jenvman.2021.113650

Rennert, T., Herrmann, L., 2022. Thermal-gradient analysis of soil organic matter using an elemental analyser – A tool for qualitative characterization? Geoderma 425, 116085. https://doi.org/10.1016/j.geoderma.2022.116085

Revelle, R., Suess, H.E., 1957. Carbon Dioxide Exchange Between Atmosphere and Ocean and the Question of an Increase of Atmospheric CO_2 during the Past Decades. Tellus 9, 18–27. https://doi.org/10.1111/j.2153-3490.1957.tb01849.x

Ribeiro, I.D.A., Volpiano, C.G., Vargas, L.K., Granada, C.E., Lisboa, B.B., Passaglia, L.M.P., 2020. Use of Mineral Weathering Bacteria to Enhance Nutrient Availability in Crops: A Review. Front. Plant Sci. 11, 590774. https://doi.org/10.3389/fpls.2020.590774

Rühlemann, L., Schmidtke, K., 2015. Evaluation of monocropped and intercropped grain legumes for cover cropping in no-tillage and reduced tillage organic agriculture. European Journal of Agronomy 65, 83–94. https://doi.org/10.1016/j.eja.2015.01.006

Saia, S., Rappa, V., Ruisi, P., Abenavoli, M.R., Sunseri, F., Giambalvo, D., Frenda, A.S., Martinelli, F., 2015. Soil inoculation with symbiotic microorganisms promotes plant growth and nutrient transporter genes expression in durum wheat. Front. Plant Sci. 6. https://doi.org/10.3389/fpls.2015.00815

Santos, C., Fonseca, J., Coutinho, J., Trindade, H., Jensen, L.S., 2021. Chemical properties of agro-waste compost affect greenhouse gas emission from soils through changed C and N mineralisation. Biol Fertil Soils 57, 781–792. https://doi.org/10.1007/s00374-021-01560-6

Sapkota, S., Ghimire, R., Bista, P., Hartmann, D., Rahman, T., Adhikari, S., 2024. Greenhouse gas mitigation and soil carbon stabilization potential of forest biochar varied with biochar type and characteristics. Science of The Total Environment 931, 172942. https://doi.org/10.1016/j.scitotenv.2024.172942

Scheiner, D., 1976. Determination of ammonia and Kjeldahl nitrogen by indophenol method. Water Research 10, 31–36. https://doi.org/10.1016/0043-1354(76)90154-8

Schlesinger, W.H., Andrews, J.A., 2000. Soil respiration and the global carbon cycle. Biogeochemistry 48, 7–20. https://doi.org/10.1023/A:1006247623877

Sheng, Y., Zhan, Y., Zhu, L., 2016. Reduced carbon sequestration potential of biochar in acidic soil. Science of The Total Environment 572, 129–137. https://doi.org/10.1016/j.scitotenv.2016.07.140

Shi, J., Song, M., Yang, L., Zhao, F., Wu, J., Li, J., Yu, Z., Li, A., Shangguan, Z., Deng, L., 2023. Recalcitrant organic carbon plays a key role in soil carbon sequestration along a long-term vegetation succession on the Loess Plateau. CATENA 233, 107528. https://doi.org/10.1016/j.catena.2023.107528

Shimizu, M., Limin, A., Desyatkin, A.R., Jin, T., Mano, M., Ono, K., Miyata, A., Hata, H., Hatano, R., 2015. Effect of manure application on seasonal carbon fluxes in a temperate managed grassland in Southern Hokkaido, Japan. CATENA 133, 474–485. https://doi.org/10.1016/j.catena.2015.05.011

Shimizu, M., Marutani, S., Desyatkin, A.R., Jin, T., Hata, H., Hatano, R., 2009. The effect of manure application on carbon dynamics and budgets in a managed grassland of Southern Hokkaido, Japan. Agriculture, Ecosystems & Environment 130, 31–40. https://doi.org/10.1016/j.agee.2008.11.013

Singla, A., Inubushi, K., 2014. Effect of Biogas Digested Liquid on CH4 and N2O Flux in Paddy Ecosystem. Journal of Integrative Agriculture 13, 635–640. https://doi.org/10.1016/S2095-3119(13)60721-2

Smith, P., Bhogal, A., Edgington, P., Black, H., Lilly, A., Barraclough, D., Worrall, F., Hillier, J., Merrington, G., 2010. Consequences of feasible future agricultural land-use change on soil organic carbon stocks and greenhouse gas emissions in Great Britain. Soil Use and Management 26, 381–398. https://doi.org/10.1111/j.1475-2743.2010.00283.x

Song, C., Li, M., Wei, Z., Jia, X., Xi, B., Liu, D., Zhu, C., Pan, H., 2016. Effect of inoculation with multiple composite microorganisms on characteristics of humic fractions and bacterial community structure during biogas residue and livestock manure co-composting. Journal of Chemical Technology & Biotechnology 91, 155–164. https://doi.org/10.1002/jctb.4554

Stockmann, U., Adams, M.A., Crawford, J.W., Field, D.J., Henakaarchchi, N., Jenkins, M., Minasny, B., McBratney, A.B., Courcelles, V. de R. de, Singh, K., Wheeler, I., Abbott, L., Angers, D.A., Baldock, J., Bird, M., Brookes, P.C., Chenu, C., Jastrow, J.D., Lal, R., Lehmann, J., O'Donnell, A.G., Parton, W.J., Whitehead, D., Zimmermann, M., 2013. The knowns, known unknowns and unknowns of sequestration of soil organic carbon. Agriculture, Ecosystems & Environment 164, 80–99. https://doi.org/10.1016/j.agee.2012.10.001

Strefler, J., Amann, T., Bauer, N., Kriegler, E., Hartmann, J., 2018. Potential and costs of carbon dioxide removal by enhanced weathering of rocks. Environ. Res. Lett. 13, 034010. https://doi.org/10.1088/1748-9326/aaa9c4

Suseela, V., Conant, R.T., Wallenstein, M.D., Dukes, J.S., 2012. Effects of soil moisture on the temperature sensitivity of heterotrophic respiration vary seasonally in an old-field climate change experiment. Global Change Biology 18, 336–348. https://doi.org/10.1111/j.1365-2486.2011.02516.x

Tampio, E., Marttinen, S., Rintala, J., 2016. Liquid fertilizer products from anaerobic digestion of food waste: mass, nutrient and energy balance of four digestate liquid treatment systems. Journal of Cleaner Production 125, 22–32. https://doi.org/10.1016/j.jclepro.2016.03.127

Tang, S., Guo, J., Li, S., Li, J., Xie, S., Zhai, X., Wang, C., Zhang, Y., Wang, K., 2019. Synthesis of soil carbon losses in response to conversion of grassland to agriculture land. Soil and Tillage Research 185, 29–35. https://doi.org/10.1016/j.still.2018.08.011

Tao, S., Lin, B., 2000. Water soluble organic carbon and its measurement in soil and sediment. Water Research 34, 1751–1755. https://doi.org/10.1016/S0043-1354(99)00324-3

Thomsen, I.K., Olesen, J.E., Møller, H.B., Sørensen, P., Christensen, B.T., 2013. Carbon dynamics and retention in soil after anaerobic digestion of dairy cattle feed and faeces. Soil Biology and Biochemistry 58, 82–87. https://doi.org/10.1016/j.soilbio.2012.11.006

Tian, S., Zhu, B., Yin, R., Wang, M., Jiang, Y., Zhang, C., Li, D., Chen, X., Kardol, P., Liu, M., 2022. Organic fertilization promotes crop productivity through changes in soil aggregation. Soil Biology and Biochemistry 165, 108533. https://doi.org/10.1016/j.soilbio.2021.108533

Tirol-Padre, A., Ladha, J.K., 2004. Assessing the Reliability of Permanganate-Oxidizable Carbon as an Index of Soil Labile Carbon. Soil Science Society of America Journal 68, 969–978. https://doi.org/10.2136/sssaj2004.9690

Tong, Y., Liu, J., Li, X., Sun, J., Herzberger, A., Wei, D., Zhang, W., Dou, Z., Zhang, F., 2017. Cropping System Conversion led to Organic Carbon Change in China's Mollisols Regions. Sci Rep 7, 18064. https://doi.org/10.1038/s41598-017-18270-5

Tsuno, Y., Fujimatsu, T., Endo, K., Sugiyama, A., Yazaki, K., 2018. Soyasaponins: A New Class of Root Exudates in Soybean (Glycine max). Plant and Cell Physiology 59, 366–375. https://doi.org/10.1093/pcp/pcx192

van Midden, C., Harris, J., Shaw, L., Sizmur, T., Morgan, H., Pawlett, M., 2024. Immobilisation of anaerobic digestate supplied nitrogen into soil microbial biomass is dependent on lability of high organic carbon materials additives. Front. Sustain. Food Syst. 8. https://doi.org/10.3389/fsufs.2024.1356469

Vance, E.D., Brookes, P.C., Jenkinson, D.S., 1987. An extraction method for measuring soil microbial biomass C. Soil Biology and Biochemistry 19, 703–707. https://doi.org/10.1016/0038-0717(87)90052-6

Velthof, G.L., Mosquera, J., 2011. The impact of slurry application technique on nitrous oxide emission from agricultural soils. Agriculture, Ecosystems & Environment 140, 298–308. https://doi.org/10.1016/j.agee.2010.12.017

Verma, B.C., Pramanik, P., Bhaduri, D., 2020a. Organic Fertilizers for Sustainable Soil and Environmental Management, in: Meena, R.S. (Ed.), Nutrient Dynamics for Sustainable Crop Production. Springer, Singapore, pp. 289–313. https://doi.org/10.1007/978-981-13-8660-2_10

Verma, B.C., Pramanik, P., Bhaduri, D., 2020b. Organic Fertilizers for Sustainable Soil and Environmental Management, in: Meena, R.S. (Ed.), Nutrient Dynamics for Sustainable Crop Production. Springer, Singapore, pp. 289–313. https://doi.org/10.1007/978-981-13-8660-2_10

Vienne, A., Poblador, S., Portillo-Estrada, M., Hartmann, J., Ijiehon, S., Wade, P., Vicca, S., 2022. Enhanced Weathering Using Basalt Rock Powder: Carbon Sequestration, Co-benefits and Risks in a Mesocosm Study With Solanum tuberosum. Front. Clim. 4. https://doi.org/10.3389/fclim.2022.869456

Villarino, S.H., McDaniel, M.D., Blauwet, M.J., Sievers, B., Sievers, L., Schulte, L.A., Miguez, F.E., 2025. Adding anaerobic digestate to commercial farm fields increases soil organic carbon. Journal of Agriculture and Food Research 21, 101942. https://doi.org/10.1016/j.jafr.2025.101942

Villarino, S. H., Potter, S.W., Hall, S.J., Blauwet, M., Miguez, F.E., McDaniel, M.D., 2025. Carbon and nutrient release from anaerobic digestate solids applied as a soil amendment. Soil Science Society of America Journal 89, e70063. https://doi.org/10.1002/saj2.70063

Walling, E., Vaneeckhaute, C., 2020. Greenhouse gas emissions from inorganic and organic fertilizer production and use: A review of emission factors and their variability. Journal of Environmental Management 276, 111211. https://doi.org/10.1016/j.jenvman.2020.111211

Wang, F.L., Alva, A.K., 1999. Transport of soluble organic and inorganic carbon in sandy soils under nitrogen fertilization. Can. J. Soil. Sci. 79, 303–310. https://doi.org/10.4141/S97-074

Wang, Y., Ge, L., Chendi, S., Wang, H., Han, J., Guo, Z., Lu, Y., 2020. Analysis on hydraulic characteristics of improved sandy soil with soft rock. PLOS ONE 15, e0227957. https://doi.org/10.1371/journal.pone.0227957

Wei, W., Yan, Y., Cao, J., Christie, P., Zhang, F., Fan, M., 2016. Effects of combined application of organic amendments and fertilizers on crop yield and soil organic matter: An integrated analysis of long-term experiments. Agriculture, Ecosystems & Environment 225, 86–92. https://doi.org/10.1016/j.agee.2016.04.004

Wei, Z., Xi, B., Zhao, Y., Wang, S., Liu, H., Jiang, Y., 2007. Effect of inoculating microbes in municipal solid waste composting on characteristics of humic acid. Chemosphere 68, 368–374. https://doi.org/10.1016/j.chemosphere.2006.12.067

Weyers, S.L., Spokas, K.A., 2011. Impact of Biochar on Earthworm Populations: A Review. Applied and Environmental Soil Science 2011, 541592. https://doi.org/10.1155/2011/541592

Wiesmeier, M., Poeplau, C., Sierra, C.A., Maier, H., Frühauf, C., Hübner, R., Kühnel, A., Spörlein, P., Geuß, U., Hangen, E., Schilling, B., von Lützow, M., Kögel-Knabner, I., 2016. Projected loss of soil organic carbon in temperate agricultural soils in the 21st century: effects of climate change and carbon input trends. Sci Rep 6, 32525. https://doi.org/10.1038/srep32525

Wijewardana, C., Reddy, K.R., Alsajri, F.A., Irby, J.T., Krutz, J., Golden, B., 2018. Quantifying soil moisture deficit effects on soybean yield and yield component distribution patterns. Irrig Sci 36, 241–255. https://doi.org/10.1007/s00271-018-0580-1

Wu, H., Zhang, S., Zhou, J., Cong, H., Feng, S., Sun, F., 2024. Relative Contribution of Fungal Communities to Carbon Loss and Humification Process in Algal Sludge Aerobic Composting. Water 16, 1084. https://doi.org/10.3390/w16081084

Wu, J., Joergensen, R.G., Pommerening, B., Chaussod, R., Brookes, P.C., 1990. Measurement of soil microbial biomass C by fumigation-extraction—an automated procedure. Soil Biology and Biochemistry 22, 1167–1169. https://doi.org/10.1016/0038-0717(90)90046-3

Wu, X., Liu, J., Sun, W., Liu, Y., Michalski, J., Tan, W., Qin, X., Zou, Y., 2024. Quantifying the chemical composition of weathering products of Hainan basalts with reflectance spectroscopy and its implications for Mars. Earth Planet. Phys. https://doi.org/10.26464/epp2024011

Wu, Z., Chen, X., Lu, X., Zhu, Y., Han, X., Yan, J., Yan, L., Zou, W., 2025. Impact of combined organic amendments and chemical fertilizers on soil microbial limitations, soil quality, and soybean yield. Plant Soil 507, 317–334. https://doi.org/10.1007/s11104-024-06733-4

Xia, H., Riaz, M., Zhang, M., Liu, B., El-Desouki, Z., Jiang, C., 2020. Biochar increases nitrogen use efficiency of maize by relieving aluminum toxicity and improving soil quality in acidic soil. Ecotoxicology and Environmental Safety 196, 110531. https://doi.org/10.1016/j.ecoenv.2020.110531

Xu, M., Lou, Y., Sun, X., Wang, W., Baniyamuddin, M., Zhao, K., 2011. Soil organic carbon active fractions as early indicators for total carbon change under straw incorporation. Biol Fertil Soils 47, 745. https://doi.org/10.1007/s00374-011-0579-8

Xu, Y., Sheng, J., Zhang, L., Sun, G., Zheng, J., 2025. Organic fertilizer substitution increased soil organic carbon through the association of microbial necromass C with iron oxides. Soil and Tillage Research 248, 106402. https://doi.org/10.1016/j.still.2024.106402

Xu, Y., Sheng, J., Zhang, Y., Zhang, L., Kan, Z.-R., Sun, G., Zheng, J., 2024. The effect on the carbon footprint of the rice-wheat system of substituting chemical fertilizers by pig manure: The results of a field experiment. Sustainable Production and Consumption 49, 1–11. https://doi.org/10.1016/j.spc.2024.06.003

Yan, X., Gong, W., 2010. The role of chemical and organic fertilizers on yield, yield variability and carbon sequestration— results of a 19-year experiment. Plant Soil 331, 471–480. https://doi.org/10.1007/s11104-009-0268-7

Yang, Q., Zhang, M., 2023. Effect of bio-organic fertilizers partially substituting chemical fertilizers on labile organic carbon and bacterial community of citrus orchard soils. Plant Soil 483, 255–272. https://doi.org/10.1007/s11104-022-05735-4

Yang, Y., Kosaka, G., Uchibayashi, H., Zhu, Y., Kuramochi, K., Shinano, T., Watanabe, T., Maruyama, H., Hamamoto, S., Nakao, A., Toma, Y., 2025. Enhanced CO2 removal and improved carbon budget by enhanced rock weathering: a field experiment in Hokkaido, Japan. Nutr Cycl Agroecosyst. https://doi.org/10.1007/s10705-025-10414-8

Yang, Y., Liu, H., Dai, Y., Tian, H., Zhou, W., Lv, J., 2021. Soil organic carbon transformation and dynamics of microorganisms under different organic amendments. Science of The Total Environment 750, 141719. https://doi.org/10.1016/j.scitotenv.2020.141719

Yu, H., Han, M., Cai, C., Lv, F., Teng, Y., Zou, L., Ding, G., Bai, X., Yao, J., Ni, K., Zhu, C., 2023. Soil organic carbon stability and exogenous nitrogen fertilizer influence the priming effect of paddy soil under long-term exposure to elevated atmospheric CO2. Environ Sci Pollut Res 30, 102313–102322. https://doi.org/10.1007/s11356-023-29485-7

Zhang, L.H., Chen, Y.N., Zhao, R.F., Li, W.H., 2010. Significance of temperature and soil water content on soil respiration in three desert ecosystems in Northwest China. Journal of Arid Environments 74, 1200–1211. https://doi.org/10.1016/j.jaridenv.2010.05.031

Zhao, H.-T., Li, T.-P., Zhang, Y., Hu, J., Bai, Y.-C., Shan, Y.-H., Ke, F., 2017. Effects of vermicompost amendment as a basal fertilizer on soil properties and cucumber yield and quality under continuous cropping conditions in a greenhouse. J Soils Sediments 17, 2718–2730. https://doi.org/10.1007/s11368-017-1744-y

Zhao, L., Hong, H., Fang, Q., Hei, H., Algeo, T.J., 2023. Hydrologic regulation of clay-mineral transformations in a redoximorphic soil of subtropical monsoonal China. American Mineralogist 108, 1881–1896. https://doi.org/10.2138/am-2022-8706

Zhao, Y., Hao, Y., Liu, Z., Yang, F., 2024. Effect of soil management practice on soil phosphorus dynamics: A meta-analysis. Soil Use and Management 40, e12986. https://doi.org/10.1111/sum.12986

Zhong, W., Gu, T., Wang, W., Zhang, B., Lin, X., Huang, Q., Shen, W., 2010. The effects of mineral fertilizer and organic manure on soil microbial community and diversity. Plant Soil 326, 511–522. https://doi.org/10.1007/s11104-009-9988-y

Zhong, W., Zhang, Z., Luo, Y., Sun, S., Qiao, W., Xiao, M., 2011. Effect of biological pretreatments in enhancing corn straw biogas production. Bioresource Technology 102, 11177–11182. https://doi.org/10.1016/j.biortech.2011.09.077

Zhong, Y., Li, J., Xiong, H., 2021. Effect of deficit irrigation on soil CO_2 and N_2O emissions and winter wheat yield. Journal of Cleaner Production 279, 123718. https://doi.org/10.1016/j.jclepro.2020.123718

Zhou, X., Gao, T., Pang, Y., Mahan, H., Li, X., Zheng, N., Suyker, A.E., Awada, T., Zhu, J., 2021. Based on Atmospheric Physics and Ecological Principle to Assess the Accuracies of Field CO_2/H_2O Measurements From Infrared Gas Analyzers in Closed-Path Eddy-Covariance Systems. Earth and Space Science 8, e2021EA001763. https://doi.org/10.1029/2021EA001763

Zhou, Y., Selvam, A., Wong, J.W.C., 2014. Evaluation of humic substances during co-composting of food waste, sawdust and Chinese medicinal herbal residues. Bioresource Technology, Special Issue on Advance Biological Treatment Technologies for Sustainable Waste Management (ICSWHK2013) 168, 229–234. https://doi.org/10.1016/j.biortech.2014.05.070

Zhou, Z., Zhang, G., Hua, J., Xue, J., Yu, C., 2024. Tree species selection for optimizing soil carbon storage: Insights from litter decomposition and bacterial community analysis in coastal ecosystems. Journal of Environmental Management 370, 122984. https://doi.org/10.1016/j.jenvman.2024.122984

Zilio, M., Pigoli, A., Rizzi, B., Goglio, A., Tambone, F., Giordano, A., Maretto, L., Squartini, A., Stevanato, P., Meers, E., Schoumans, O., Adani, F., 2023. Nitrogen dynamics in soils fertilized with digestate and mineral fertilizers: A full field approach.

Science of The Total Environment 868, 161500. https://doi.org/10.1016/j.scitotenv.2023.161500